Copyright

by

Yeonjeong Ha

2014

The Dissertation Committee for Yeonjeong Ha Certifies that this is the approved version of the following dissertation:

BIOAVAILABILITY OF FULLERENE NANOPARTICLES: FACTORS AFFECTING MEMBRANE PARTITIONING AND CELLULAR UPTAKE

Committee:

Howard M. Liljestrand, Co-Supervisor

Lynn E. Katz, Co-Supervisor

Kerry A. Kinney

Jennifer A. Maynard

Jung-Hwan Kwon

BIOAVAILABILITY OF FULLERENE NANOPARTICLES: FACTORS AFFECTING MEMBRANE PARTITIONING AND CELLULAR UPTAKE

by

Yeonjeong Ha, B.S.; M.City.Plan.

Dissertation

Presented to the Faculty of the Graduate School of

The University of Texas at Austin

in Partial Fulfillment

of the Requirements

for the Degree of

Doctor of Philosophy

The University of Texas at Austin

December 2014

Dedication

To all my families and relatives in Korea

Acknowledgements

I would like to express my deep appreciation and gratitude to my advisors, Dr. Howard Liljestrand and Dr. Lynn Katz, for their support, advice, and patience throughout my doctoral study. Dr. Liljestrand always encouraged me to pursue the topic that I am interested in, and I sincerely appreciate the wisdom and advice that he provided. Also, thanks to him, I had over four years of teaching experience, and I learned to have a great attitude as a lecturer from him. Dr. Katz inspired me to do creative thinking and helped me to solve research problems when I encountered difficulties. Her enthusiasm and support encouraged me to push myself towards higher quality work. I am truly fortunate to have great advisors.

I would also like to thank my committee members, Dr. Kerry Kinney, Dr. Jennifer Maynard, and Dr. Jung-Hwan Kwon, for their guidance and comments on my dissertation. Dr. Kinney's comments helped me to broaden my ideas to solve real environmental problems. With Dr. Maynard's help, I was able to conduct the cellular uptake experiments. I sincerely thank Dr. Kwon for his support and help when I worked as a researcher in Ajou University in Korea. Many other EWRE faculty also encouraged me in various ways, especially Dr. Desmond Lawler, and Dr. Navid Saleh.

Special thanks go to Xianzhe Wang and Dr. Maynard's research group members who helped me to learn cellular uptake experiments from beginning to end. Previous and current members of Dr. Katz's research group, Amanda, Aurore, Celina, Changmin, Cameron, Ellison, Felipe, Fernando, Jerry, Justin, Jinyong, Joon Kyoung, Katie, Lee, Ling, Michael, and Seunghwan helped me when I conducted experiments in the lab. I also thank to many other EWRE friends, Amad, Anne, Bryant, Dai Go, Dr. Lu,

Katherine, Sarah, Sedat, Shahana, and Tongren. Also thanks to the Korean students in EWRE, Dr. Bae, Chanhoo, Gihye, Kyoungseok, Kyunghwa, Sungmin, Taegyu, Soyoon, and Yongsik. With great friends, I enjoyed my life as a graduate student. I also thank Charlie Perego for his support.

I sincerely thank my parents' deepest love. They are my role models wherever I am. Also thanks go to my younger sister, Yeonho, for her love and support. I especially thank my parents-in-law for their love and prayers. I truly appreciate all the support from my family members and relatives.

Finally, my deepest love and thank go to my husband, Ijung, who always lead me in a better way. He is my best friend, a great supporter, and a person who has a true love. My little one, Sunyul! Thank you for being my daughter!

BIOAVAILABILITY OF FULLERENE NANOPARTICLES: FACTORS AFFECTING MEMBRANE PARTITIONING AND CELLULAR UPTAKE

Yeonjeong Ha, Ph.D.

The University of Texas at Austin, 2014

Co-Supervisors: Howard M. Liljestrand, Lynn E. Katz

Interactions of engineered nanomaterials (ENMs) with environmental interfaces have become a critical aspect of environmental health and safety evaluations. Carbon fullerene (C_{60}) has emerged at the forefront of nanoscale research and applications due to its unique properties. Although there are concerns associated with the harmful effects of fullerene towards living organisms, the mechanisms of fullerene toxicity are still under debate. A first step toward assessing these mechanisms requires evaluation of the bio-accumulation and bio-uptake of fullerene through lipid membranes which serve as biological barriers in cells. In this dissertation, partitioning of fullerene between water and lipid membranes and cellular uptake of fullerene were investigated to assess bioavailability of this nanoparticle.

Traditional methods to estimate the equilibrium partitioning of molecular level chemicals between water and lipid membranes (K_{lipw}) cannot be applied to measure K_{lipw} of nanoparticles due to the large size of nanoparticle aggregates. In this study, we developed an *in vitro* method to estimate K_{lipw} of fullerene using solid supported lipid membranes (SSLMs) with various membrane compositions. K_{lipw} of fullerene increased with increasing acyl chain length and K_{lipw} values were higher after creating phase

separation in ternary lipid membranes compared to pre-phase separation. In addition, the partitioning values (K_{lipw}) were found to depend on the lipid head charges. These results suggest that the lipid membrane composition can be a critical factor for assessing bioaccumulation of fullerene. Evaluation of the partitioning thermodynamics of fullerene demonstrated that the partitioning mechanism of fullerene is different from that of molecular level chemicals. It is generally acknowledged that molecular level chemicals partition into the hydrophobic center of lipid membranes (i.e., absorption), however, the partitioning mechanism of fullerene is a combination of adsorption on the lipid membrane surface and absorption.

Caco-2 cellular uptake of fullerene nanoparticles was investigated using an *in vitro* method developed in this study to distinguish between active and passive transport across cell membranes. Energy dependent endocytosis is hypothesized to be the main cellular transport mechanism based on an observed temperature dependence of cellular uptake and evidence for saturation of the active sites of transport during cellular uptake of fullerene. Metabolic inhibitors decreased the mass of fullerene taken up by the cells, which supports an active transport mechanism of fullerene through the cell membranes.

To evaluate bioavilability of fullerene under environmentally relevant conditions, the effects of humic acid and fetal bovine serum (FBS) on the lipid accumulation and cellular uptake were also investigated. Humic acid and FBS changed the surface characteristics of fullerene. The presence of FBS significantly decreased lipid accumulation of fullerene presumably due to higher steric hinderance of FBS coated fullerene as well as the changes in surface energy, water solubility, and lipid solubility of charged FBS coated fullerene relative to that of bare fullerene. Both humic acid and FBS also effectively lowered the cellular uptake of fullerene. These results imply that natural

organic matter and biomolecules in natural aquatic and biological environments have significant effects on the bioavilability of fullerene nanoparticles.

Table of Contents

List of Tables

List of Figures

Chapter 1: Introduction

1.1. Problem Statement

The release of nanoparticles into the environment has been a forseeable consequence of the dramatic increase in the innovative use of engineered nanomaterials (ENMs) over past decades. Based on current production volumes, prominence in health and safety research, and potential widespread usage in applications ranging from sunscreens and cosmetics to paint pigments and antimicrobial agents (Hendren et al. 2011), nanosilver (nano-Ag), carbon based nanomaterials (e.g., carbon nanotube and fullerene), cerium oxide (CeO_2), and nano titanium dioxide (nano-TiO_2) are of greatest concern with respect to their release to the environment and potential health concerns. Carbon fullerene (C_{60}) has emerged at the center of nanoscale research and applications. Due to its unique properties (e.g., electron-rich cage structure, high reactivity, and ability to accept and release electrons), fullerene has been incorporated into numerous commercial (e.g., batteries, fuel cells, photovoltaics, and face creams) and medical applications (e.g., drug carriers, antioxidants, biosensor, and biomedical imaging). Indeed, estimated industrial production of fullerene has already approached approximately 10 tons per year in 2007 (Frontier Carbon Corporation, 2012) and the estimated global market for fullerene reached $1,312 million in 2011 with an expected 70 % annual growth rate, which could approach $4.7 billion by 2016 (BCC Research, 2006). As the production of fullerene increases rapidly, the release of fullerene from manufacturing facilities into the environment can occur. Thus, concerns related to the possible harmful effects of fullerene towards humans and the environment have grown.

There are several critical reasons why potential biological and environmental effects of fullerene have raised considerable concern. First, fullerene is strongly

hydrophobic; its potential for partitioning to organic matter is greater than polycyclic aromatic hydrocarbons (PAHs) or polychlorinated biphenyls (PCBs). Due to its hydrophobic properties, fullerene can associate strongly with cell membranes and may easily penetrate and accumulate in lipid cell membranes. Second, although a single fullerene molecule exhibits low solubility in water, it is generally acknowledged that fullerene can form highly stable, negatively charged colloidal aggregates (nC_{60}) when exposed to water. This change in solubility has critical implications for fullerene transport in the environment and its biological effects. Third, predicted fullerene concentrations in the environment are relatively high compared to other nanomaterials; predicted fullerene concentrations in water of 0.31 μg/L are greater than values reported for nanosilver, carbon nanotubes, and cerium oxides of 0.010-0.03 μg/L, 0.0005-0.0008 μg/L, and < 0.0001 μg/L, respectively (Pérez 2009). The reactivity of fullerene including virus inactivation, cell toxicity, and lipid peroxidation of brain and gill cells in fish have been reported at concentrations less than 1 mg/L (Kasermann and Kempf 1997, Oberdörster 2004, Sayes 2004). Thus, environmental concentrations in the high hundreds of micrograms per liter range are of concern.

Fullerene dispersions in water have been reported to exhibit toxicity toward living organisms in aquatic environments (Cho et al. 2009b, Lovern and Klaper 2006, Lyon et al. 2006, Sayes et al. 2005), but the mechanism of fullerene toxicity toward living organisms is still under debate. A first step toward assessing the mechanisms associated with fullerene toxicity requires evaluation of the bio-accumulation and bio-uptake of aqueous fullerene dispersions through lipid membranes which serve as biological barriers to target or reactive sites in cells. Transport of fullerene nanoparticles from aquatic environments to an organism occurs via lipid membranes. Storage and accumulation of fullerene within the lipid membranes of cells are also expected. In addition, it is generally

acknowledged that lipids affect the health of organisms (e.g., fish) by affecting growth, reproduction behavior, and immune response (Arts et al. 2009). Thus, understanding accumulation and uptake through lipid membranes is of critical importance for assessing environmental effects as well as potential toxicity of fullerene. Unfortunately, to date, only a few studies have addressed the lipid accumulation of fullerene using *in vitro* lipid membranes (Hou et al. 2011). Moreover, little to no research has been conducted to assess the impact of lipid head charges, hydrophobicity of the lipid (e.g., acyl chain length), and lipid surface structure (e.g., the height mismatch between unsaturated and saturated lipids in ternary lipid mixtures) on fullerene membrane diffusion in lipid membranes. With respect to uptake within cells, a number of studies have focused on quantitative estimation of cellular uptake of engineered nanoparticles (Cho et al. 2009a, Guarnieri et al. 2011, Lesniak et al. 2012) . However, no research has quantitatively evaluated cellular uptake of fullerene due to the difficulties associated with measuring fullerene concentrations in solutions containing biomolecules. In addition, although nanoparticle surface characteristics can be altered under environmentally relevant conditions (e.g., in the presence of natural organic matter and biological macromolecules), only a few studies have investigated the effects of environmentally relevant matrices on bioavailability of fullerene (Chen et al. 2014). Addressing these deficiencies in the scientific literature is the major focus of this research.

1.2. RESEARCH OBJECTIVES, HYPOTHESES AND APPROACH

The primary objectives of this research were to evaluate the bioavailability of aqueous fullerene dispersions by developing a more complete understanding of 1) partitioning of fullerene in lipid/water systems and, 2) the cellular uptake of fullerene. While a conceptual image of fullerene partitioning and transport through lipid

membranes is beginning to emerge (Figure 1.1), the importance of lipid membrane composition on partitioning and identification of the dominant transport mechanism are critical first steps toward prediction of fullerene partitioning in aquatic organisms and the bioavailability of fullerene in aquatic environments.

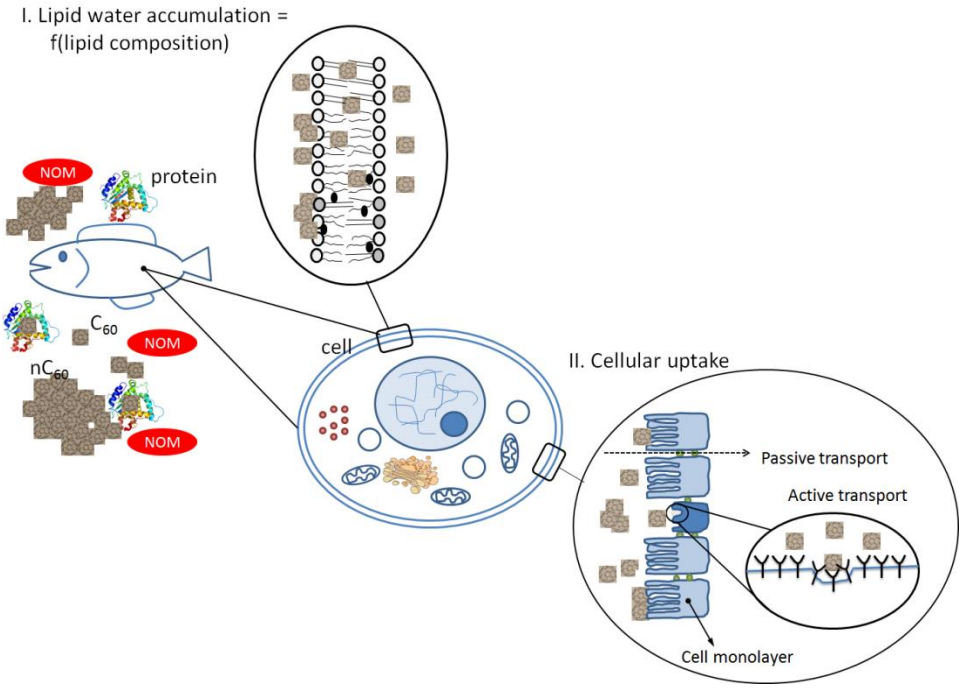

Figure 1.1: System description of this study

This dissertation addressed these objectives by testing four specific hypotheses that enabled us to develop a better screening tool and theoretical model for estimating the lipid water partition coefficient of fullerene and to elucidate the mechanisms of lipid membrane transport. The four main hypotheses of this study summarized in Table 1.1.

Table 1.1: Research hypotheses

Hypotheses	Related tasks
Hypothesis I: The lipid water partitioning coefficient (K_{lipw}) of fullerene is affected by lipid composition.	Task 1, 2
Hypothesis II: The lipid water partitioning mechanism of fullerene is different from that of molecular level chemicals and these differences can be explained by partitioning thermodynamics.	Task 1, 3
Hypothesis III: Fullerene can be transported into the cell membrane via active transport.	Task 4
Hypothesis IV: Lipid accumulation and cellular uptake of fullerene are affected by the presence of natural organic matter and biological macromolecules in environmentally relevant conditions.	Task 5

Five specific tasks were performed to address these hypotheses as shown in Table 1.1 and outlined below:

1. To develop an *in vitro* method for quantifying partition coefficients for fullerene between water and lipid membranes of varying composition
2. To elucidate the effects of lipid membrane composition (e.g., acyl chain length, lipid head charge, height mismatch in ternary lipid membrane) on lipid water partitioning of fullerene

3. To estimate thermodynamic parameters that describe lipid water partitioning of fullerene that supports the conceptual understanding plausible partitioning mechanism
4. To develop a quantitative *in vitro* method to elucidate the cellular uptake mechanism of fullerene
5. To evaluate the effects of environmentally relevant matrices (e.g., natural organic matter and biological macromolecule) on the lipid accumulation and cellular uptake of fullerene

The first three tasks address hypotheses I and II by evaluating fullerene partitioning to lipid membranes of varying composition. The methods of Hou et al., (Hou et al. 2011) and methods previously developed by Liljestrand and co-workers (Kwon et al. 2006, Kwon et al. 2007, Yamamoto and Liljestrand 2004, Yamamoto et al. 2004) were modified to account for the significantly larger hydrodynamic diameter of fullerene relative to molecular chemicals. Specifically, solid supported lipid membranes (SSLMs) of varying lipid composition (e.g., different head charges and acyl chain lengths, and ternary lipid membranes before and after phase separation) were prepared and used to estimate K_{lipw} partitioning coefficients of fullerene. In addition, partitioning thermodynamics were investigated by determining K_{lipw} values as a function of temperature to help elucidate the relative impact of enthalpic and entropic contributions to the thermodynamics of the partitioning process (Hypothesis II). Comparisons to previous work (Ávila and Martínez 2003, Go and Ngiam 1997, Kwon et al. 2007, Seelig and Ganz 1991) with hydrophobic and ionic chemicals allowed us to distinguish partitioning of nanoparticles from more traditional molecular level contaminants.

With regard to hypothesis III, an *in vitro* model using the Caco-2 cell line was employed to describe membrane transport of fullerene in Task 4. Caco-2 cells, a human colon adenocarcinoma cell line, have been successfully used to demonstrate the membrane transport mechanism of drugs and molecular level chemicals (Buesen et al. 2003, Hidalgo and Borchardt 1990, Sugano et al. 2010, Vasiluk et al. 2007). In addition, recent studies in pharmaceutical fields have reported that the main transport mechanism of nanosize particles is active transport using Caco-2 cell (Lin et al. 2012, Ma and Lim 2003, Mao et al. 2005, Win and Feng 2005). Therefore, the *in vitro* method using Caco-2 cells can be a realistic model for determining the mechanism of membrane transport of engineered nanomaterials as well.

One of the unique features of this study is the assessment of the effects of environmentally relevant matrices on the bioavailability of fullerene (Hypothesis IV). Humic acid and fetal bovine serum (FBS) were selected as representative natural organic matter in the aquatic environment and biological macromolecules, respectively. To investigate the bioavailability of fullerene under environmentally relevant conditions, lipid accumulation and cellular uptake tests were employed in Task 5. The *in vitro* methods developed in Tasks 1 and 4 were modified as necessary to compare humic acid and FBS coated fullerene partitioning and cellular uptake to that of bare fullerene.

1.3. STRUCTURE OF THIS DISSERTATION

In this dissertation, a research overview is provided in Chapter 2 which includes the physicochemical properties and known toxicity data for fullerene and a brief review of literature assessing the bioavilability of fullerene based on octanol water partitioning coefficient (K_{ow}), lipid water distribution coefficients (K_{lipw}) and cellular uptake studies of fullerene and its derivatives. Chapter 3 presents the details of the *in vitro* method

developed for estimating lipid water partitioning coefficients (K_{lipw}) of fullerene for various lipid membrane compositions. Chapter 4 focuses on the influence of lipid membrane composition on the K_{lipw} values. Partitioning thermodynamics are used to support the proposed partitioning mechanism of fullerene between water and lipid membranes. Chapter 5 describes cellular uptake of fullerene in Caco-2 cells and elucidates the dominant mechanisms of membrane transport in these systems. Chapter 6 examines the bioavailability of fullerene nanoparticles in the presence of environmentally relevant materials. Chapters 3 through Chapter 6 are drafts of papers to be submitted for peer-reviewed publications. Therefore, some introductory material and method development are repeated from previous chapters. In Chapter 7, major conclusions of each results chapter (Chapters 3 to 6) are summarized and suggestions for future research are presented.

1.4. REFERENCES

Arts, M.T., Brett, M.T. and Kainz, M.J. (2009) Lipids in aquatic ecosystems, Springer, Dordrecht ; New York.

Ávila, C.M. and Martínez, F. (2003) Thermodynamics of partitioning of benzocaine in some organic solvent/buffer and liposome systems. Chem Pharm Bull (Tokyo) 51(3), 237-240.

BCC Research. (2006) Accessed on http://www.bccresearch.com/.

Buesen, R., Mock, M., Nau, H., Seidel, A., Jacob, J. and Lampen, A. (2003) Human intestinal Caco-2 cells display active transport of benzo[a]pyrene metabolites. Chem Biol Interact 142(3), 201-221.

Chen, Q., Yin, D., Li, J. and Hu, X. (2014) The effects of humic acid on the uptake and depuration of fullerene aqueous suspensions in two aquatic organisms. Environ Toxicol Chem 33(5), 1090-1097.

Cho, E.C., Xie, J., Wurm, P.A. and Xia, Y. (2009a) Understanding the role of surface charges in cellular adsorption versus internalization by selectively removing gold nanoparticles on the cell surface with a I_2/KI etchant. Nano Lett 9(3), 1080-1084.

Cho, M., Fortner, J.D., Hughes, J.B. and Kim, J.H. (2009b) *Escherichia coli* inactivation by water-soluble, ozonated C_{60} derivative: kinetics and mechanisms. Environ Sci Technol 43(19), 7410-7415.

Frontier Carbon Corporation. (2012) Accessed on http://www.f-carbon.com/eng/.

Go, M.L. and Ngiam, T.L. (1997) Thermodynamics of partitioning of the antimalarial drug mefloquine in phospholipid bilayers and bulk solvents. Chem Pharm Bull (Tokyo) 45(12), 2055-2060.

Guarnieri, D., Guaccio, A., Fusco, S. and Netti, P.A. (2011) Effect of serum proteins on polystyrene nanoparticle uptake and intracellular trafficking in endothelial cells. Journal of Nanoparticle Research 13(9), 4295-4309.

Hendren, C.O., Mesnard, X., Droge, J. and Wiesner, M.R. (2011) Estimating production data for five engineered nanomaterials as a basis for exposure assessment. Environ Sci Technol 45(7), 2562-2569.

Hidalgo, I.J. and Borchardt, R.T. (1990) Transport of a large neutral amino acid (phenylalanine) in a human intestinal epithelial cell line: Caco-2. Biochim Biophys Acta 1028(1), 25-30.

Hou, W.C., Moghadam, B.Y., Westerhoff, P. and Posner, J.D. (2011) Distribution of fullerene nanomaterials between water and model biological membranes. Langmuir 27(19), 11899-11905.

Käsermann, F. and Kempf, C. (1997) Photodynamic inactivation of enveloped viruses by buckminsterfullerene. Antiviral Res 34(1), 65-70.

Kwon, J.H., Liljestrand, H.M. and Katz, L.E. (2006) Partitioning of moderately hydrophobic endocrine disruptors between water and synthetic membrane vesicles. Environ Toxicol Chem 25(8), 1984-1992.

Kwon, J.H., Liljestrand, H.M., Katz, L.E. and Yamamoto, H. (2007) Partitioning thermodynamics of selected endocrine disruptors between water and synthetic membrane vesicles: effects of membrane compositions. Environ Sci Technol 41(11), 4011-4018.

Lesniak, A., Fenaroli, F., Monopoli, M.P., Aberg, C., Dawson, K.A. and Salvati, A. (2012) Effects of the presence or absence of a protein corona on silica nanoparticle uptake and impact on cells. ACS Nano 6(7), 5845-5857.

Lin, I.C., Liang, M., Liu, T.Y., Monteiro, M.J. and Toth, I. (2012) Cellular transport pathways of polymer coated gold nanoparticles. Nanomedicine 8(1), 8-11.

Lovern, S.B. and Klaper, R. (2006) *Daphnia magna* mortality when exposed to titanium dioxide and fullerene (C_{60}) nanoparticles. Environ Toxicol Chem 25(4), 1132-1137.

Lyon, D.Y., Adams, L.K., Falkner, J.C. and Alvarezt, P.J. (2006) Antibacterial activity of fullerene water suspensions: effects of preparation method and particle size. Environ Sci Technol 40(14), 4360-4366.

Ma, Z. and Lim, L.Y. (2003) Uptake of chitosan and associated insulin in Caco-2 cell monolayers: a comparison between chitosan molecules and chitosan nanoparticles. Pharm Res 20(11), 1812-1819.

Mao, S., Germershaus, O., Fischer, D., Linn, T., Schnepf, R. and Kissel, T. (2005) Uptake and transport of PEG-graft-trimethyl-chitosan copolymer-insulin nanocomplexes by epithelial cells. Pharm Res 22(12), 2058-2068.

Oberdörster, E. (2004) Manufactured nanomaterials (fullerenes, C_{60}) induce oxidative stress in the brain of juvenile largemouth bass. Environ Health Perspect 112(10), 1058-1062.

Pérez, S.F., M.; Barceló, D (2009) Analysis, behavior and ecotoxicity of carbon-based nanomaterials in the aquatic environment. Trends in Analytical Chemistry 28(6), 820-832.

Sayes, C.M., Gobin, A.M., Ausman, K.D., Mendez, J., West, J.L. and Colvin, V.L. (2005) Nano-C60 cytotoxicity is due to lipid peroxidation. Biomaterials 26(36), 7587-7595.

Sayes, C.M.F., J.D.; Guo, W.; Lyon, D.; Boyd, A.M.; Ausman, K.D.; Tao, Y.J.; Sitharaman, B.; Wilson, L.J.; Hughes, J.B.; West, J.L.; Colvin, V.L. (2004) The differential cytotoxicity of water-soluble fullerenes. Nano Lett 4, 1881-1887.

Seelig, J. and Ganz, P. (1991) Nonclassical hydrophobic effect in membrane binding equilibria. Biochemistry 30(38), 9354-9359.

Sugano, K., Kansy, M., Artursson, P., Avdeef, A., Bendels, S., Di, L., Ecker, G.F., Faller, B., Fischer, H., Gerebtzoff, G., Lennernaes, H. and Senner, F. (2010) Coexistence of passive and carrier-mediated processes in drug transport. Nat Rev Drug Discov 9(8), 597-614.

Vasiluk, L., Pinto, L.J., Walji, Z.A., Tsang, W.S., Gobas, F.A., Eickhoff, C. and Moore, M.M. (2007) Benzo[a]pyrene bioavailability from pristine soil and contaminated sediment assessed using two in vitro models. Environ Toxicol Chem 26(3), 387-393.

Win, K.Y. and Feng, S.S. (2005) Effects of particle size and surface coating on cellular uptake of polymeric nanoparticles for oral delivery of anticancer drugs. Biomaterials 26(15), 2713-2722.

Yamamoto, H. and Liljestrand, H.M. (2004) Partitioning of selected estrogenic compounds between synthetic membrane vesicles and water: effects of lipid components. Environ Sci Technol 38(4), 1139-1147.

Yamamoto, H., Liljestrand, H.M. and Shimizu, Y. (2004) Effects of dissolved organic matter surrogates on the partitioning of 17beta-estradiol and p-nonylphenol between synthetic membrane vesicles and water. Environ Sci Technol 38(8), 2351-2358.

Chapter 2: Literature Review

2.1. INTRODUCTION

In this dissertation, bioavailability of fullerene was investigated by determining the characteristics of fullerene accumulation in lipid membranes and cellular uptake in Caco-2 cells. As part of this research, a thorough literature review was conducted to assess the current state of knowledge regarding fullerene properties, partitioning and uptake. In section 2.2, the general characteristics of fullerene were reviewed, including its physicochemical properties, expected environmental fate and transport, and reported toxicity towards living organisms. In section 2.3, a brief review of prior research examining interactions of fullerene with model biological phases (e.g., octanol, synthetic lipid membranes, and cells) is provided. Finally, section 2.4 provides a review of the influence of environmentally relevant matrices on fullerene properties.

2.2. CARBON FULLERENE (C_{60})

2.2.1. Physicochemical properties

Carbon fullerene (C_{60}, Buckminsterfullerene) has a sp^2 hybridized cage-like structure which consists of twenty hexagons and twelve pentagons of carbon. Fullerene was discovered by Kroto, Curl, Smalley and others (Kroto et al. 1985) and in the 1990s, production of large quantities of fullerene using condensation of vaporized graphite was possible (Isaacson et al. 2009).

Representative physicochemical properties of fullerene molecules were summarized in Dresselhaus et al. ((Dresselhaus et al. 1996) and are reproduced in Table 2.1. The molecular diameter of fullerene is approximately 7 Å, and it can easily accept electrons due to the high electron affinity (Table 2.1) associated with its structure.

Table 2.1: Physicochemical constants of the fullerene molecule (Dresselhaus et al. 1996)

Quantity	Value	Quantity	Value
Average C-C distance	1.44 Å	Bonding energy per atom	7.40 eV
C-C bond length on a pentagon	1.46 Å	Heat of formation (per g C atom)	10.16 kcal
C-C bond length on a hexagon	1.40 Å	Electron affinity	2.65 ± 0.05 eV
C_{60} mean ball diameter	7.10 Å	Cohesive energy per C atom	1.4 eV/atom
C_{60} ball outer diameter	10.34 Å	First ionization potential	7.58 eV
Volume per C_{60}	$1.87 \times 10^{-23}/cm^3$	Second ionization potential	11.5 eV

Fullerene's electron rich cage structure results from the C=C double bonds (fullerene can be classified as an alkene) that are arranged in hexagonal rings (Dresselhaus et al. 1996). It undergoes redox reactions such as hydrogenation, alkylation, halogenation, and bridging reactions. It is generally acknowledged that in most cases, the carbon double bonds are the reactive sites in fullerene and the reactivity is strongly photosensitive and oxygen sensitive (Dresselhaus et al. 1996).

Fullerene is a highly stable and hydrophobic molecule. Experimentally, fullerene molecule is thermally stable up to 1700 K (Eletskii and Smirnov 1995) and due to its strong hydrophobicity, fullerene has negligible solubility in water and polar H-bonding in solvents such as acetone, methanol and ethanol (Ruoff et al. 1993). Therefore, synthesizing water soluble fullerene derivatives for use in biomedical applications is challenging. However, fullerene is soluble in nonpolar solvents, especially aromatic solvents and solubility increases with increasing aromatic ring size (Ruoff et al. 1993).

2.2.2. Environmental fate and transport

Carbon fullerene can be produced by both natural and anthropogenic processes (Figure 2.1). Naturally occurring fullerene has been found in meteors and many geologic

samples (Becker et al. 1994, Pizzarello et al. 2001). As anthropogenic production of fullerene has increased, fullerene can be released into the environment from both point sources (e.g., production plants, and wastewater treatment) and nonpoint sources (e.g., non-intentional release during fullerene containing products) (Petosa et al. 2010).

It is important to estimate fullerene concentrations in the various environmental compartments (e.g. soil, air, water) to perform risk assessment studies. However, only a few studies have reported the predicted environmental concentrations of fullerene using models (Boxall et al. 2008, Gottschalk et al. 2009) or through direct sampling and measurement (Farré et al. 2010). The estimated fullerene concentrations in environmental media are summarized in Table 2.2 which highlights the fact that there is not only a lack of data but also inconsistency in the limited amount of data available. Therefore, developing a standard method to estimate and measure fullerene concentrations in environmental media is of critical importance.

Table 2.2: Estimated fullerene concentrations in environmental media

	Air (ng/m^3)	Soil ($\Delta ng/kg/y$)	Water (ng/L)	Sediment ($\Delta ng/kg/y$)	Wastewater effluent (ng/L)	ref
Europe	<0.005	0.057-0.605	0.015-0.12	6.22-530	4.23-26.4	
U.S.	<0.005	0.024-0.292	0.0024-0.021	1.05-91.3	4.49-32.66	(Gottschalk et al. 2009)[a]
Switzerland	<0.005	0.016-0.058	0.018-0.19	8.2-787	3.69-25.1	
UK	-	13.2 (μg/kg)	310			(Boxall et al. 2008)
Spain					0.5-19,100	(Farré et al. 2010)

[a] For air, soil, water and wastewater effluent, simulation results show fullerene concentrations in 2008, and for soil and sediment, the annual increase of the fullerene concentrations were reported.

Recent studies have reported that fullerene characteristics can change during transport in the environment. First of all, although molecular fullerene has strong hydrophobicity, many previous studies have suggested that fullerene can form highly stable, negatively charged colloidal aggregates (nC_{60}) when it is exposed to water (Andrievsky et al. 1995, Deguchi et al. 2001, Fortner et al. 2005). This change in solubility has critical implications for fullerene transport in the environment and its biological effects. Second, fullerene can form different size aggregates and the degree of dispersion depends on the presence and character of natural organic matter (Xie et al. 2008), surfactants (Zhang et al. 2009a), and the ionic strength of the background water (Brant et al. 2005). Third, because fullerene is a very strong photosensitizing agent, photochemical transformation of fullerene can occur under sunlight (Hou and Jafvert 2009b). Previous studies have demonstrated that this transformation produces reactive oxygen species (ROS) which can be responsible for cytotoxicity of fullerene (Cho et al. 2011, Hou and Jafvert 2009a). In addition, UV irradiation (e.g. sunlight) can produce water soluble derivatives of fullerene (Hou et al. 2010) and decrease fullerene aggregate size in the aqueous phase (Cho et al. 2011).

2.2.3. Toxicity

A number of previous studies have reported that fullerene dispersions exhibit toxicity towards human cell lines (Sayes et al. 2005), bacteria (Cho et al. 2009b, Lyon et al. 2006), and aquatic organisms (Lovern and Klaper 2006, Oberdörster 2006). These studies have suggested potential mechanisms of fullerene toxicity towards living organisms including production of reactive oxygen species (ROS) and lipid peroxidation (Sayes et al. 2005), however, the operative mechanism is still under debate. The reactivity of fullerene including virus inactivation, cell toxicity, and lipid peroxidation of

brain and gill cells in fish have been reported at concentrations less than 1 mg/L (Kasermann and Kempf 1997, Oberdörster 2004, Sayes et al. 2005). Due to the heterogeneity of fullerene dispersions in water, previous studies have demonstrated that results from both *in vivo* and *in vitro* tests of fullerene toxicity depends on the particular physicochemical properties of the fullerene suspension (e.g., particle size and surface charge) as well as the preparation method of the fullerene dispersions in water (e.g., solvent exchange method *vs*. sonication method) (Chae et al. 2010, Lyon et al. 2006). Thus, it is imperative to develop standard methods for assessing toxicity of fullerene nanoparticles in aquatic environments. Table 2.3 summarizes the biological effects of fullerene reported in previous studies.

Table 2.3: Biological effects of fullerene nanoparticles

C_{60} preparation method	C_{60} concentration (ppm)	Biological effects	Reference
Sonicated C_{60}	-	• C_{60} illuminating with visible light inactivates virus • In the presence of bovine serum albumin decreases the inactivation kinetics	(Kasermann and Kempf 1997)
Solvent exchange method (THF/C_{60})	0.5 - 1	• C_{60} suspensions in water induce lipid peroxidation and glutathione (GSH) depletion in an aquatic organisms *in vivo* • C_{60} suspensions locate in cell membranes *in vitro*	(Oberdörster 2004)
Solvent exchange method (THF/C_{60})	0 - 2.4	• Human cell cytotoxicity of C_{60} occurs by lipid peroxidation and resultant membrane damage	(Sayes et al. 2005)
Solvent exchange method (THF/C_{60})	0.04 - 0.88	• C_{60} shows high toxicity to *Daphnia Magna* at low concentration (THF/C_{60} :100 mortality at 0.88 ppm, mortality is not applicable with sonicated C_{60})	(Lovern and Klaper 2006)
Sonicated C_{60}	0 - 9		
Four preparation methods (THF/C_{60}, sonicated/C_{60}, aq/C_{60}, and PVP/C_{60})	2 - 15	• C_{60} shows strong antibacterial activity • Antibacterial activity is affected by C_{60} preparation method and particle size	(Lyon et al. 2006)
Ozonated C_{60}	0 - 10	• C_{60} suspensions in water inactivate *E.coli* in the presence of light and oxygen • Ozonated C_{60} inactivates *E.coli* faster than parent C_{60} • Ozonated C_{60} penetrates cell and induces oxidative damage to the cell cytoplasmic membrane	(Cho et al. 2009b)

2.3. PARTITIONING OF FULLERENE BETWEEN MODEL BIOLOGICAL PHASES AND WATER

2.3.1. The octanol-water partition coefficient (K_{ow})

The octanol-water partition coefficient (K_{ow}) has been widely used to estimate the bioaccumulation of chemicals. Octanol is used frequently as a surrogate for fat tissue, natural organic phases such as humic acid, and lipid membranes of living organisms

(Schwarzenbach et al. 2003). To date, only one study has measured K_{ow} values of fullerene using a cosolvent method, and from their measurement, the log K_{ow} of fullerene is 6.67 (Jafvert and Kulkarni 2008). This reported K_{ow} of fullerene is higher than many endocrine disrupting chemicals (EDCs), and in the range of strongly hydrophobic polycyclic aromatic hydrocarbons (PAHs) such as dibenzo[a,c]anthraces (6.17), benzo[a]pyrene (6.35), and benzo[ghi]perylene (6.90). This implies that molecular fullerene has strong hydrophobicity and can be strongly associated with lipid membranes as well as natural organic materials in the environment.

Even though K_{ow} values for nonpolar contaminants have been successfully used to evaluate the bioaccumulation of these chemicals, previous research has demonstrated that partitioning thermodynamics between water and 1-octanol are significantly different than that between water and aquatic organisms (Kwon et al. 2006, Opperhuizen et al. 1988). In contrast to a solution of bulky 1-octanol molecules, living organisms have highly organized lipid membranes. This structural difference between 1-octanol and lipid membranes is responsible for disparities between the partitioning thermodynamics in octanol/water and living organism/water systems. Equilibrium partition coefficients between water and lipid membranes (K_{lipw}) are more appropriate for estimating the potential for bioconcentration of various contaminants.

2.3.2. The lipid-water distribution coefficient (K_{lipw})

As with other molecular hydrophobic chemicals, fullerene accumulation in lipid membranes can also be investigated by determining partition coefficients of fullerene between water and lipid phases (K_{lipw}). For molecular scale contaminants, K_{lipw} values have been successfully determined using an equilibrium dialysis technique (Kwon et al.

2006, Yamamoto and Liljestrand 2004). A schematic diagram depicting the equilibrium dialysis technique is presented in Figure 2.1. In this technique, molecular level chemicals (placed in the donor cell) and liposome solutions (placed in the acceptor cell) are separated by a dialysis membrane which allows chemical diffusion but not liposome diffusion. However, the equilibrium dialysis technique cannot be applied for estimating K_{lipw} values of nanomaterials because nanoparticle aggregates cannot freely diffuse through the dialysis membrane due to their large size relative to the pore size of the dialysis membrane. Therefore, developing a new technique to measure K_{lipw} values of nanomaterials was of critical importance in this research.

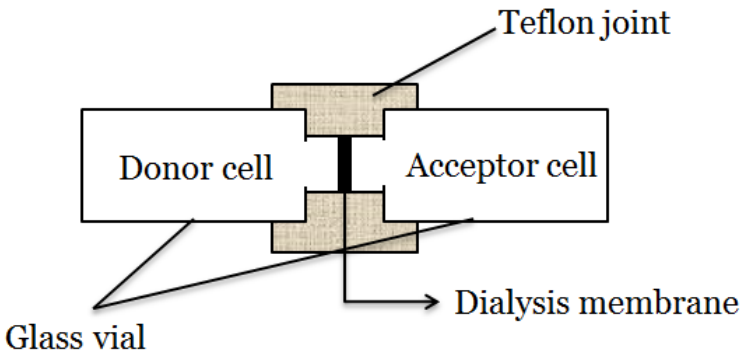

Figure 2.1: Schematic diagram of the equilibrium dialysis technique

A few recent studies have examined lipid water partitioning of engineered nanomaterials. Hou et al.(Hou et al. 2011) first developed a quantitative method for studying lipid water association coefficients (K_{lipw}) of fullerene and fullerol using solid supported lipid membranes (SSLMs). They also applied SSLMs to gold nanoparticles (Hou et al. 2012b). SSLMs are solids (e.g., silica microspheres) that are uniformly coated with lipid bilayers (Figure 2.2). Employing SSLMs to investigate partitioning of nanomaterials between water and lipid membranes is novel and relevant for two reasons:

1) SSLMs are stable (Bayerl and Bloom 1990) and preserve fluidity of the lipid membranes (Baksh et al. 2004), and 2) SSLMs easily settle, which allows free nanoparticles in water to be separated from the SSLMs. The estimated values of log K_{lipw} of fullerene and fullerol determined by Hou et al.(2011) were 2.99-3.05, and 2.42-2.45, respectively (the equilibrium fullerene concentration in water was 10 mg/L and the pH was 7.4).

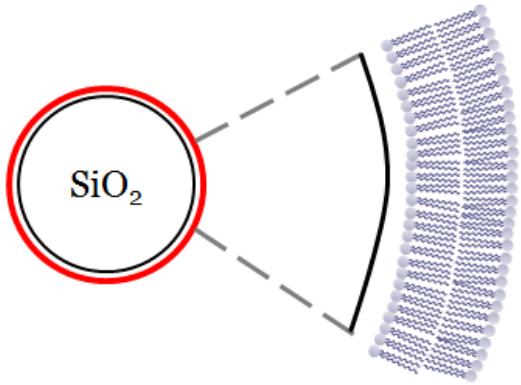

Figure 2.2: Structure of solid supported lipid membranes (SSLMs) (Baksh et al. 2004)

Although these previous studies sucessfully applied SSLMs to estimate lipid water partitioning of nanomaterials, they utilized a commercial SSLM which provided only one lipid membrane composition, egg phospholipid, as a model membrane. However, actual lipid membranes consist of various components such as unsaturated lipids, saturated lipids, and cholesterol, and many previous studies revealed that partitioning values of molecular hydrophobic chemicals can be significantly affected by lipid membrane composition (Kwon et al. 2007, Yamamoto and Liljestrand 2004). Thus, it is imperative to investigate the effects of lipid composition on the partitioning of nanoparticles between water and lipids.

Thermodynamic parameters (enthalpy change (ΔH) and entropy change (ΔS)) describing molecular chemical partitioning have been estimated. Kwon et al. (Kwon et al. 2007) demonstrated that for a series of endocrine disruptors, introduction of a solute into lipid bilayers leads to creation of a cavity in the membrane, which increases the enthalpy and entropy changes. However, partitioning processes of fullerene nanoparticles may be different from dissolved molecules due to their unique physicochemical properties and larger size relative to most dissolved molecules. Comparison of enthalpy and entropy values for partitioning of moleculer level chemicals and fullerene will help to elucidate these differences.

2.3.3. Computational simulations used to elucidate the fullerene transport mechanism through lipid membranes

Computational simulations have shown that pristine fullerene can easily diffuse into lipid bilayers and translocate into the membrane (Bedrov et al. 2008, Qiao et al. 2007). In particular, Qiao et al. (Qiao et al. 2007) demonstrated that pristine fullerene (nC_{60}) can easily diffuse into a dipalmitoylphosphatidylcholine (DPPC) membrane bilayer and translocate the membrane in a few milliseconds, while fullerol ($C_{60}(OH)_{20}$) did not significantly diffuse into the bilayer. Atomistic molecular dynamics simulations also suggested that fullerene can freely penetrate into the membrane (Bedrov et al. 2008).

Wong-Ekkabut et al. (Wong-Ekkabut et al. 2008) also indicated that passive permeation through lipid membranes is the main mechanism for transport of small aggregated fullerene (< 10 molecules); when aggregated fullerenes are located close to the lipid head groups, only small clusters form and rapidly penetrate into the bilayer.

Although these molecular dynamics studies provide insight into the behavior of fullerene, the focus of their research was only on molecular fullerene or small clusters.

Also, they only employed one lipid membrane composition and did not consider the possible interactions of fullerene with other membrane components such as other lipid rafts, proteins, and carbohydrates which can be responsible for active transport of chemicals through lipid membranes. Thus, further research should address the membrane transport mechanism of larger fullerene aggregates that exist in water. In addition, future studies must consider transport of fullerene through cell membranes which have membrane compositions that mimic organisms.

2.3.4. Cellular uptake

Visulalization techniques have been employed to locate fullerene or fullerene derivatives inside cells (Foley et al. 2002, Porter et al. 2007, Porter et al. 2006, Rouse et al. 2006). For quantitave measurements of fullerene nanoparticle uptake by cells, radioactive or fluorescent labled fullerene has been used to easily detect the fullerene particles in bio-matrices (Cagle et al. 1999, Gulson and Wong 2006). A summary of methods and major conclusions from these cellular uptake studies is presented in Table 2.4. The main focus of these experiments was to confirm that fullerene accumulates inside cells.

Other recent studies have demonstrated that nanoparticles (e.g., carbon nanotubes, gold nanoparticles, and polymeric nanoparticles) are transported through cell membranes via active transport (Chithrani et al. 2006, Ma and Lim 2003, Mao et al. 2005, Win and Feng 2005, Yaron et al. 2011). To date, there is no study which investigates the cellular transport mechanism of bare fullerene due to the difficulties associated with detecting bare fullerene taken up by cells. Only one quantitative study has suggested that a malonic acid fullerene derivative ($C_{60}(C(COOH)_2)_3$) is transported through cell membranes via active transport (Li et al. 2008). While the physicochemical properties of fulllerene

derivatives may differ from that of bare fullerene, and hence the transport mechanisms may be different, evidence for active transport of any fullerene molecule provides support for further investigation of the transport mechanism of bare fullerene molecules .

Table 2.4: Summary of cellular uptake studies of fullerene and fullerene derivatives

Fullerene (C_{60}) species	Fullerene dimensions (nm)	Cell line	Dose, incubation time	Methods	Conclusions	Reference
C_{60} dissolved in tetrahydrofuran (THF)	Individual particles: 60-270 Clusters: 420-1300	Human monocyte macrophages (HMMs)	0.16 – 10 µg/ml, over 48 hr	1) Energy-filtered transmission electron microscopy (EFTEM) 2) Scanning TEM (STEM)-based electron tomography	• Significant toxicity was not observed • C_{60} can accumulate inside cellular compartments (e.g., cell membranes, lysosome, and nucleus)	(Porter et al. 2006)
Aqueous suspensions of micronized C_{60}[a]	7 % : 1000 < d < 1650 43% : 500 < d< 1000 28 % : 250 < d < 450 22 % : d < 200 nm	Rat liver cell	0.5 g/kg of body weight, up to 21 days	1) HPLC with diode-array detection 2) SEM	• C_{60} can accumulate inside the liver cells, and an average size of C_{60} aggregates is less than 50 nm	(Gharbi et al. 2005)
Fullerol $C_{60}OH_{20-24}$)	Average diameter : 218 nm	Murine macrophage cell line (RAW 264.7)	-	TEM	• Fullerol taken by RAW 264 cell line was revealed by Electron microscopy	(Xia et al. 2006a)
Fullerol	Fullerol in 70 µM HBSS buffer: 695 ±50 nm Fullerol incubated with α crystalline : 23 ±2 nm, 356 ±35 nm	Human lens epithelial cell line (HLE B-3)	~50 µM, ~ 15 hr	1) Phase contrast illumination 2) Spectrometric determination (using fullerol absorbance at 405 nm)	• Fullerol was uptake by the cells and it accumulates in the cells	(Roberts et al. 2008)
Radiolabeling fullerol	In H_2O : 20 nm In 10 % FBS-DMEM : 81.7 nm (12 hr) In DMEM : 230.9 nm (71.5 %)	CHO cell lines	50 µg/ml, up to 3 hrs	Radio-tracer technique	• Radiolabeling fullerol taken by CHO cell reached saturation in 3 hr • Uptake of fullerol incubated in serum-free media is higher than in serum containing medium	(Su et al. 2010)
Fullerene-based amino acid	-	Human epidermal keratinocytes(HEK)	0.004, 0.04, and 0.4 mg/mL, up to 48 hrs	TEM	• TEM confirmed that 0.04 and 0.4 mg/mL fullerene-based amino acid localized inside the cell	(Rouse et al. 2006)

[a]Fullerene added to distilled water containing 0.02 % of Tween 60, 0.9 DS carboxymethyl cellulose(CMC), and NaCl

2.4. FULLERENE UNDER THE PRESENCE OF ENVIRONMENTALLY RELEVANT MATRICES

2.4.1. Natural organic matter (NOM)

Natural organic matter (NOM), which is ubiquitous in natural water, consists of a hydrophobic backbone and various hydrophilic functional groups such as phenolic and carboxylic groups (Xie et al. 2008). Previous studies have revealed that NOM readily adsorbs onto colloidal particles and stabilizes those particles (Buffle and Leppard 1995, Jermann et al. 2008). NOM also has been reported to prevent the aggregation of many engineered nanomaterials (e.g., ZnO, TiO_2, SiO_2, and Al_2O_3), enhancing the stability of those nanoparticles in natural aquatic environments (Bian et al. 2011, Ghosh et al. 2010, Zhang et al. 2009b).

As with other colloidal and engineered particles, NOM can interact with fullerene and affect its characteristics. NOM has been reported to increase the stability and mobility of fullerene nanoparticles (Chen and Elimelech 2007, 2008, Singh and Lillard 2009, Xie et al. 2008). Major conclusions in previous research which concern the effects of NOM on the characteristics of fullerene are summarized in Table 2.5.

Increasing stability and changing characteristics of fullerene in the presence of NOM can significantly affect the bioavailability of fullerene. To date, only one study has investigated the impact of humic acid on fullerene cellular uptake, and it was shown that humic acid effectively decreased the uptake of fullerene in two aquatic organisms: *Daphnia magna* and *zebrafish* (Chen et al. 2014). The authors proposed that the main reason for the reduction in fullerene uptake by the organisms in the presence of humic acid was the polarity change due to the surface modification of fullerene by the humic acid.

Table 2.5: Summary of the effects of NOM on fullerene characteristics and stability

C_{60} preparation method	C_{60} concentration (mg/L)	NOM type [a] (concentration)	NOM effects on fullerene characteristics and stability	Reference
Stirred method (aq/C_{60})	0.31, 0.35	SRHA II (20 mg/L) SRFA I (20 mg/L)	• Presence of NOM significantly increase fullerene dispersion kinetics	(Singh and Lillard 2009)
Solvent exchange method and stirred method (toluene/C_{60}, THF/C_{60}, and aq/C_{60})	3	SRHA II (5-20 mg/L) SRFA I (5-20 mg/L)	• Fullerene particle distributions are smaller in the presence of NOM • As SRFA concentration increased, negative surface charge density of fullerene increased	(Xie et al. 2008)
Solvent exchange method using ethanol	5.8	SRHA II (1 mg/L as TOC)	• Humic acid effectively decreases the deposition of fullerene on silica surfaces	(Chen and Elimelech 2008)
Solvent exchange method (toluene/C_{60})	5.92	SRHA II (1 mg/L and 5 mg/L as TOC)	• Nanoparticle suspensions are significantly stabilized in the presence of humic acid • At higher $CaCl_2$ concentrations, humic acid aggregations were created, resulting in fullerene aggregations	(Chen and Elimelech 2007)

[a] SRHA II: Suwannee river humic acid standard II, SRFA I: Suwannee river fulvic acid standard I. Both SRHA and SRFA were obtained from International Humic Substances Society (IHSS, St.Paul, MNO)

2.4.2. Biological macromolecules

One of the most promising uses of fullerene is in biological applications such as the use of fullerene as an inhibitor of the HIV protease (Friedman et al. 1993), as a drug carrier (Friedman et al. 1993), and as an anti-cancer drug (Fan et al. 2013). When fullerene nanoparticles are released into biological fluids in living organisms, the surface of fullerene can be covered by biological macromolecules (e.g., proteins and lipids). Indeed, it is generally accepted that proteins immediately adsorb and cover the surface of nanoparticles, resulting in surface modification of the nanomaterials (Lynch and Dawson 2008). In addition, this surface modification can affect interactions of nanoparticles with living systems as well as possible toxicity towards them (Ehrenberg et al. 2009, Fabrega et al. 2009, Giri et al. 2014, Guarnieri et al. 2011, Lesniak et al. 2012).

Previous research has reported that surface modification of nanoparticles (e.g., fullerene, carbon nanotubes, and polystyrene particles) by protein effectively prevented particle aggregation and increased stability of those materials (Casey et al. 2007, Deguchi et al. 2007, Ehrenberg et al. 2009, Saleh et al. 2010, Zhu et al. 2009). These changes in surface characteristics resulting from protein-coating can affect the nanoparticle's interaction within biological systems. For example, many studies have demonstrated that in the presence of protein, cellular uptake of nanoparticles was significantly reduced due to the decrease in surface energy of the protein coated nanoparticles compared to bare particles (Guarnieri et al. 2011, Lesniak et al. 2012, Zhu et al. 2009). However, to our knowledge, no study has reported the effect of biological macromolecules on the bioavailability of fullerene nanoparticles.

2.5. REFERENCES

Andrievsky, G.V., Kosevich, M.V., Vovk, O.M., Shelkovsky, V.S. and Vashchenko, L.A. (1995) On the production of an aqueous colloidal solution of fullerenes. J Chem Soc Chem Commun (12), 1281-1282.

Baksh, M.M., Jaros, M. and Groves, J.T. (2004) Detection of molecular interactions at membrane surfaces through colloid phase transitions. Nature 427(6970), 139-141.

Bayerl, T.M. and Bloom, M. (1990) Physical properties of single phospholipid bilayers adsorbed to micro glass beads. A new vesicular model system studied by ^{2}H-nuclear magnetic resonance. Biophys J 58(2), 357-362.

Becker, L., Bada, J.L., Winans, R.E. and Bunch, T.E. (1994) Fullerenes in Allende meteorite. Nature 372(6506), 507.

Bedrov, D., Smith, G.D., Davande, H. and Li, L. (2008) Passive transport of C_{60} fullerenes through a lipid membrane: a molecular dynamics simulation study. J Phys Chem B 112(7), 2078-2084.

Bian, S.W., Mudunkotuwa, I.A., Rupasinghe, T. and Grassian, V.H. (2011) Aggregation and dissolution of 4 nm ZnO nanoparticles in aqueous environments: influence of pH, ionic strength, size, and adsorption of humic acid. Langmuir 27(10), 6059-6068.

Boxall, A.B.A., Chaudhry, Q., Jones, A., Jefferson, B. and Watts, C.D. (2008) Current and future predicted environmental exposure to engineered nanoparticles, Central Science Laboratory, Sand Hutton, UK.

Brant, J., Lecoanet, H. and Wiesner, M.R. (2005) Aggretagion and deposition characteristics of fullerene nanoparticles in aqueous systems. Journal of Nanoparticle Research 7, 545-553.

Buffle, J. and Leppard, G.G. (1995) Characterization of aquatic colloids and macromolecules. 1. Structure and behavior of colloidal material. Environ Sci Technol 29(9), 2169-2175.

Cagle, D.W., Kennel, S.J., Mirzadeh, S., Alford, J.M. and Wilson, L.J. (1999) *In vivo* studies of fullerene-based materials using endohedral metallofullerene radiotracers. Proc Natl Acad Sci U S A 96(9), 5182-5187.

Casey, A., Davoren, M., Herzog, E., Lyng, F.M., Byrne, H.J. and Chambers, G. (2007) Probing the interaction of single walled carbon nanotubes within cell culture medium as a precursor to toxicity testing. Carbon 45(1), 34-40.

Chae, S.R., Badireddy, A.R., Farner Budarz, J., Lin, S., Xiao, Y., Therezien, M. and Wiesner, M.R. (2010) Heterogeneities in fullerene nanoparticle aggregates affecting reactivity, bioactivity, and transport. ACS Nano 4(9), 5011-5018.

Chen, K.L. and Elimelech, M. (2007) Influence of humic acid on the aggregation kinetics of fullerene (C_{60}) nanoparticles in monovalent and divalent electrolyte solutions. J Colloid Interface Sci 309(1), 126-134.

Chen, K.L. and Elimelech, M. (2008) Interaction of fullerene (C_{60}) nanoparticles with humic acid and alginate coated silica surfaces: measurements, mechanisms, and environmental implications. Environ Sci Technol 42(20), 7607-7614.

Chen, Q., Yin, D., Li, J. and Hu, X. (2014) The effects of humic acid on the uptake and depuration of fullerene aqueous suspensions in two aquatic organisms. Environ Toxicol Chem 33(5), 1090-1097.

Chithrani, B.D., Ghazani, A.A. and Chan, W.C. (2006) Determining the size and shape dependence of gold nanoparticle uptake into mammalian cells. Nano Lett 6(4), 662-668.

Cho, M., Fortner, J.D., Hughes, J.B. and Kim, J.H. (2009) Escherichia coli inactivation by water-soluble, ozonated C_{60} derivative: kinetics and mechanisms. Environ Sci Technol 43(19), 7410-7415.

Cho, M., Snow, S.D., Hughes, J.B. and Kim, J.H. (2011) *Escherichia coli* Inactivation by UVC-Irradiated C_{60}: kinetics and mechanisms. Environ Sci Technol 45(22), 9627-9633.

Deguchi, S., Alargova, R.G. and GTsujii, K. (2001) Stable dispersions of fullerenes, C_{60} and C_{70} in water. Preparation and characterization. Langmuir 17, 6013-6017.

Deguchi, S., Yamazaki, T., Mukai, S.A., Usami, R. and Horikoshi, K. (2007) Stabilization of C_{60} nanoparticles by protein adsorption and its implications for toxicity studies. Chem Res Toxicol 20(6), 854-858.

Dresselhaus, M.S., Dresselhaus, G. and Eklund, P.C. (1996) Science of fullerenes and carbon nanotubes, Academic Press, San Diego.

Duclos, S.J., Brister, K., Haddon, R.C., Kortan, A.R. and Thiel, F.A. (1991) Effects of Pressure and Stress on C_{60} Fullerite to 20 Gpa. Nature 351(6325), 380-382.

Ehrenberg, M.S., Friedman, A.E., Finkelstein, J.N., Oberdörster, G. and McGrath, J.L. (2009) The influence of protein adsorption on nanoparticle association with cultured endothelial cells. Biomaterials 30(4), 603-610.

Eletskii, A.V. and Smirnov, B.M. (1995) Fullerenes and carbon structures. Physics-Uspekhi 38(9), 935-964.

Fabrega, J., Fawcett, S.R., Renshaw, J.C. and Lead, J.R. (2009) Silver nanoparticle impact on bacterial growth: effect of pH, concentration, and organic matter. Environ Sci Technol 43(19), 7285-7290.

Fan, J.Q., Fang, G., Zeng, F., Wang, X.D. and Wu, S.Z. (2013) Water-dispersible fullerene aggregates as a targeted anticancer prodrug with both chemo- and photodynamic therapeutic actions. Small 9(4), 613-621.

Farré, M., Pérez, S., Gajda-Schrantz, K., Osorio, V., Kantiani, L., Ginerbreda, A. and Barceló, D. (2010) First determination of C_{60} an C_{70} fullerenes and N-methylfulleropyrrolidine C60 on the suspended materaisl of wastwater effluents by liquid chromatography hybrid quadrupole linear ion trap tandem mass spectrometry. Journal of Hydrology 383, 44-51.

Foley, S., Crowley, C., Smaihi, M., Bonfils, C., Erlanger, B.F., Seta, P. and Larroque, C. (2002) Cellular localisation of a water-soluble fullerene derivative. Biochem Biophys Res Commun 294(1), 116-119.

Fortner, J.D., Lyon, D.Y., Sayes, C.M., Boyd, A.M., Falkner, J.C., Hotze, E.M., Alemany, L.B., Tao, Y.J., Guo, W., Ausman, K.D., Colvin, V.L. and Hughes, J.B. (2005) C_{60} in water: nanocrystal formation and microbial response. Environ Sci Technol 39(11), 4307-4316.

Friedman, S.H., Decamp, D.L., Sijbesma, R.P., Srdanov, G., Wudl, F. and Kenyon, G.L. (1993) Inhibition of the Hiv-1 Protease by Fullerene Derivatives - Model-Building Studies and Experimental-Verification. Journal of the American Chemical Society 115(15), 6506-6509.

Gharbi, N., Pressac, M., Hadchouel, M., Szwarc, H., Wilson, S.R. and Moussa, F. (2005) [60]fullerene is a powerful antioxidant in vivo with no acute or subacute toxicity. Nano Lett 5(12), 2578-2585.

Ghosh, S., Mashayekhi, H., Bhowmik, P. and Xing, B. (2010) Colloidal stability of Al_2O_3 nanoparticles as affected by coating of structurally different humic acids. Langmuir 26(2), 873-879.

Giri, K., Shameer, K., Zimmermann, M.T., Saha, S., Chakraborty, P.K., Sharma, A., Arvizo, R.R., Madden, B.J., McCormick, D.J., Kocher, J.P., Bhattacharya, R. and Mukherjee, P. (2014) Understanding protein-nanoparticle interaction: a new gateway to disease therapeutics. Bioconjug Chem 25(6), 1078-1090.

Gottschalk, F., Sonderer, T., Scholz, R.W. and Nowack, B. (2009) Modeled environmental concentrations of engineered nanomaterials (TiO_2, ZnO, Ag, CNT, Fullerenes) for different regions. Environ Sci Technol 43(24), 9216-9222.

Guarnieri, D., Guaccio, A., Fusco, S. and Netti, P.A. (2011) Effect of serum proteins on polystyrene nanoparticle uptake and intracellular trafficking in endothelial cells. Journal of Nanoparticle Research 13(9), 4295-4309.

Gulson, B. and Wong, H. (2006) Stable isotopic tracing-a way forward for nanotechnology. Environ Health Perspect 114(10), 1486-1488.

Hou, W.C. and Jafvert, C.T. (2009a) Photochemical transformation of aqueous C_{60} clusters in sunlight. Environ Sci Technol 43(2), 362-367.

Hou, W.C. and Jafvert, C.T. (2009b) Photochemistry of aqueous C_{60} clusters: evidence of $^1O_2$ formation and its role in mediating C_{60} phototransformation. Environ Sci Technol 43(14), 5257-5262.

Hou, W.C., Kong, L., Wepasnick, K.A., Zepp, R.G., Fairbrother, D.H. and Jafvert, C.T. (2010) Photochemistry of aqueous C_{60} clusters: wavelength dependency and product characterization. Environ Sci Technol 44(21), 8121-8127.

Hou, W.C., Moghadam, B.Y., Corredor, C., Westerhoff, P. and Posner, J.D. (2012) Distribution of functionalized gold nanoparticles between water and lipid bilayers as model cell membranes. Environ Sci Technol 46(3), 1869-1876.

Hou, W.C., Moghadam, B.Y., Westerhoff, P. and Posner, J.D. (2011) Distribution of fullerene nanomaterials between water and model biological membranes. Langmuir 27(19), 11899-11905.

Isaacson, C.W., Kleber, M. and Field, J.A. (2009) Quantitative analysis of fullerene nanomaterials in environmental systems: a critical review. Environ Sci Technol 43(17), 6463-6474.

Jafvert, C.T. and Kulkarni, P.P. (2008) Buckminsterfullerene's (C_{60}) octanol-water partition coefficient (K_{ow}) and aqueous solubility. Environ Sci Technol 42(16), 5945-5950.

Jermann, D., Pronk, W. and Boller, M. (2008) Mutual influences between natural organic matter and inorganic particles and their combined effect on ultrafiltration membrane fouling. Environ Sci Technol 42(24), 9129-9136.

Käsermann, F. and Kempf, C. (1997) Photodynamic inactivation of enveloped viruses by buckminsterfullerene. Antiviral Res 34(1), 65-70.

Kroto, H.W., Heath, J.R., Obrien, S.C., Curl, R.F. and Smalley, R.E. (1985) C_{60}: Buckminsterfullerene. Nature 318(6042), 162-163.

Kwon, J.H., Liljestrand, H.M. and Katz, L.E. (2006) Partitioning of moderately hydrophobic endocrine disruptors between water and synthetic membrane vesicles. Environ Toxicol Chem 25(8), 1984-1992.

Kwon, J.H., Liljestrand, H.M., Katz, L.E. and Yamamoto, H. (2007) Partitioning thermodynamics of selected endocrine disruptors between water and synthetic membrane vesicles: effects of membrane compositions. Environ Sci Technol 41(11), 4011-4018.

Lesniak, A., Fenaroli, F., Monopoli, M.P., Aberg, C., Dawson, K.A. and Salvati, A. (2012) Effects of the presence or absence of a protein corona on silica nanoparticle uptake and impact on cells. ACS Nano 6(7), 5845-5857.

Li, Q., Xie, B., Hwang, Y.S. and Xu, Y. (2009) Kinetics of C_{60} fullerene dispersion in water enhanced by natural organic matter and sunlight. Environ Sci Technol 43(10), 3574-3579.

Li, W., Chen, C., Ye, C., Wei, T., Zhao, Y., Lao, F., Chen, Z., Meng, H., Gao, Y., Yuan, H., Xing, G., Zhao, F., Chai, Z., Zhang, X., Yang, F., Han, D., Tang, X. and Zhang, Y. (2008) The translocation of fullerenic nanoparticles into lysosome via the pathway of clathrin-mediated endocytosis. Nanotechnology 19(14), 145102.

Lovern, S.B. and Klaper, R. (2006) *Daphnia magna* mortality when exposed to titanium dioxide and fullerene (C_{60}) nanoparticles. Environ Toxicol Chem 25(4), 1132-1137.

Lynch, I. and Dawson, K.A. (2008) Protein-nanoparticle interactions. Nano Today 3(1-2), 40-47.

Lyon, D.Y., Adams, L.K., Falkner, J.C. and Alvarezt, P.J. (2006) Antibacterial activity of fullerene water suspensions: effects of preparation method and particle size. Environ Sci Technol 40(14), 4360-4366.

Ma, Z. and Lim, L.Y. (2003) Uptake of chitosan and associated insulin in Caco-2 cell monolayers: a comparison between chitosan molecules and chitosan nanoparticles. Pharm Res 20(11), 1812-1819.

Mao, S., Germershaus, O., Fischer, D., Linn, T., Schnepf, R. and Kissel, T. (2005) Uptake and transport of PEG-graft-trimethyl-chitosan copolymer-insulin nanocomplexes by epithelial cells. Pharm Res 22(12), 2058-2068.

Oberdörster, E. (2004) Manufactured nanomaterials (fullerenes, C_{60}) induce oxidative stress in the brain of juvenile largemouth bass. Environ Health Perspect 112(10), 1058-1062.

Oberdörster, E.Z., S.; Blickley, M.; Mcglellan-Green, P.; Haasch, M.L. (2006) Ecotoxicology of carbon-based engineered nanoparticles: Effects of fullerene (C60) on aquatic organisms. Carbon 44, 1112-1120.

Opperhuizen, A., Serne, P. and Van der Steen, J.M. (1988) Thermodynamics of fish/water and octan-1-ol/water partitioning of some chlorinated benzenes. Environ Sci Technol 22(3), 286-292.

Pérez, S., Farré, M.I. and Bàrceló, D. (2009) Anlaysis, behavior and ecotoxicity of carbon-based nanomaterials in the aquatic environment. Trends in Analytical Chemistry 28(6), 820-832.

Petosa, A.R., Jaisi, D.P., Quevedo, I.R., Elimelech, M. and Tufenkji, N. (2010) Aggregation and deposition of engineered nanomaterials in aquatic environments: role of physicochemical interactions. Environ Sci Technol 44(17), 6532-6549.

Pizzarello, S., Huang, Y., Becker, L., Poreda, R.J., Nieman, R.A., Cooper, G. and Williams, M. (2001) The organic content of the Tagish Lake meteorite. Science 293(5538), 2236-2239.

Porter, A.E., Gass, M., Muller, K., Skepper, J.N., Midgley, P. and Welland, M. (2007) Visualizing the uptake of C_{60} to the cytoplasm and nucleus of human monocyte-derived macrophage cells using energy-filtered transmission electron microscopy and electron tomography. Environ Sci Technol 41(8), 3012-3017.

Porter, A.E., Muller, K., Skepper, J., Midgley, P. and Welland, M. (2006) Uptake of C_{60} by human monocyte macrophages, its localization and implications for toxicity: studied by high resolution electron microscopy and electron tomography. Acta Biomater 2(4), 409-419.

Qiao, R., Roberts, A.P., Mount, A.S., Klaine, S.J. and Ke, P.C. (2007) Translocation of C_{60} and its derivatives across a lipid bilayer. Nano Lett 7(3), 614-619.

Roberts, J.E., Wielgus, A.R., Boyes, W.K., Andley, U. and Chignell, C.F. (2008) Phototoxicity and cytotoxicity of fullerol in human lens epithelial cells. Toxicol Appl Pharmacol 228(1), 49-58.

Rouse, J.G., Yang, J., Barron, A.R. and Monteiro-Riviere, N.A. (2006) Fullerene-based amino acid nanoparticle interactions with human epidermal keratinocytes. Toxicol In Vitro 20(8), 1313-1320.

Ruoff, R.S., Tse, D.S., Malhotra, R. and Lorents, D.C. (1993) Solubility of C_{60} in a Variety of Solvents. Journal of Physical Chemistry 97(13), 3379-3383.

Saleh, N.B., Pfefferle, L.D. and Elimelech, M. (2010) Influence of biomacromolecules and humic acid on the aggregation kinetics of single-walled carbon nanotubes. Environ Sci Technol 44(7), 2412-2418.

Sayes, C.M., Gobin, A.M., Ausman, K.D., Mendez, J., West, J.L. and Colvin, V.L. (2005) Nano-C_{60} cytotoxicity is due to lipid peroxidation. Biomaterials 26(36), 7587-7595.

Schwarzenbach, R.P., Gschwend, P.M. and Imboden, D.M. (2003) Environmental organic chemistry, Wiley, Hoboken, N.J.

Su, Y., Xu, J.Y., Shen, P., Li, J., Wang, L., Li, Q., Li, W., Xu, G.T., Fan, C. and Huang, Q. (2010) Cellular uptake and cytotoxic evaluation of fullerenol in different cell lines. Toxicology 269(2-3), 155-159.

Win, K.Y. and Feng, S.S. (2005) Effects of particle size and surface coating on cellular uptake of polymeric nanoparticles for oral delivery of anticancer drugs. Biomaterials 26(15), 2713-2722.

Wong-Ekkabut, J., Baoukina, S., Triampo, W., Tang, I.M., Tieleman, D.P. and Monticelli, L. (2008) Computer simulation study of fullerene translocation through lipid membranes. Nat Nanotechnol 3(6), 363-368.

Xia, T., Kovochich, M., Brant, J., Hotze, M., Sempf, J., Oberley, T., Sioutas, C., Yeh, J.I., Wiesner, M.R. and Nel, A.E. (2006) Comparison of the abilities of ambient and manufactured nanoparticles to induce cellular toxicity according to an oxidative stress paradigm. Nano Lett 6(8), 1794-1807.

Xie, B., Xu, Z., Guo, W. and Li, Q. (2008) Impact of natural organic matter on the physicochemical properties of aqueous C_{60} nanoparticles. Environ Sci Technol 42(8), 2853-2859.

Yamamoto, H. and Liljestrand, H.M. (2004) Partitioning of selected estrogenic compounds between synthetic membrane vesicles and water: effects of lipid components. Environ Sci Technol 38(4), 1139-1147.

Yaron, P.N., Holt, B.D., Short, P.A., Losche, M., Islam, M.F. and Dahl, K.N. (2011) Single wall carbon nanotubes enter cells by endocytosis and not membrane penetration. J Nanobiotechnology 9, 45.

Zhang, B., Cho, M., Hughes, J.B. and Kim, J.H. (2009a) Translocation of C_{60} from aqueous stable colloidal aggregates into surfactant micelles. Environ Sci Technol 43(24), 9124-9129.

Zhang, Y., Chen, Y., Westerhoff, P. and Crittenden, J. (2009b) Impact of natural organic matter and divalent cations on the stability of aqueous nanoparticles. Water Res 43(17), 4249-4257.

Zhu, Y., Li, W.X., Li, Q.N., Li, Y.G., Li, Y.F., Zhang, X.Y. and Huang, Q. (2009) Effects of serum proteins on intracellular uptake and cytotoxicity of carbon nanoparticles. Carbon 47(5), 1351-1358.

Chapter 3: An *in vitro* method to estimate partitioning of fullerene between water and lipid membranes of varying composition[1]

ABSTRACT

An *in vitro* method for quantitative measurement of fullerene partition coefficients (K_{lipw}) between water and solid supported lipid membranes was developed in this chapter. K_{lipw} values of fullerene were determined for membranes comprised of three different unsaturated lipids over a range of temperatures. The log K_{lipw} (L/kg) values for fullerene, which range from 3.1 to 5.3, were generally consistent with lipid-water association parameters and bioconcentration factors of fullerene reported in previous studies. Partition coefficients were found to increase with increasing temperature, increasing acyl chain length of the unsaturated lipids. The results indicate that lipid composition is a critical factor for bioconcentration of fullerene.

Keywords

fullerene, unsaturated lipid membranes, partitioning

3.1. INTRODUCTION

The release of engineered nanomaterials (ENMs) into the environment has significantly increased over the past decade. Carbon fullerene (C_{60}), which is at the forefront of ENMs, has been used in applications ranging from electronic devices to cosmetics due to its unique properties (e.g., electron-rich cage structure, high reactivity, and ability to serve as an electron donor and acceptor). As the production of fullerene rapidly increases, concerns associated with the unknown risks of this nanoparticle towards humans and the environment have grown.

---

[1] Part of this chapter was published in Water Science and Technology at 2013 (Yeonjeong Ha, Howard M. Liljestrand, Lynn E. Katz, 2013, Effects of lipid composition on partitioning of fullerene between water and lipid membranes, *Water Science and Technology* 68(2) 290-295). This paper was supervised by Dr. Howard Liljestrand and Dr. Lynn Katz.

A number of previous studies have reported that fullerene aggregates (nC_{60}) in water exhibit toxicity toward aquatic organisms (Lovern and Klaper 2006, Oberdörster 2004), however, the mechanisms of fullerene toxicity are still under debate (Wiesner et al. 2008). A first step toward investigating the mechanisms of fullerene toxicity requires evaluation of the bioaccumulation of aqueous fullerene dispersions (nC_{60}) through lipid membranes which act as biological barriers to target or reactive sites in cells. Previous studies suggested that fullerene can associate strongly with cell membranes because of its strong hydrophobicity (Wang et al. 1999), and accumulation of fullerene in lipid membranes in biological systems is one of the important routes controlling the fate of fullerene in water (Zhang et al. 2009a). Therefore, understanding lipid accumulation of fullerene is essential not only to evaluate toxicity, but also to assess its fate and transport in water.

For hydrophobic chemicals such as estrogenic compounds and phthalates, lipid membrane accumulation has been investigated by determining partition coefficients between well-defined lipids and water (K_{lipw}) using an equilibrium dialysis technique (Kwon et al. 2006, Yamamoto and Liljestrand 2004) . However, this method is less useful for fullerene because diffusion of the nanoparticles through the dialysis membrane may be limited by nanoparticle aggregation.

Recently, Hou et al. (Hou et al. 2011) developed a novel method to determine lipid-water partitioning coefficients (K_{lipw}) of fullerene using solid supported lipid membranes (SSLMs). However, because they purchased their SSLMs, their study focused on partitioning values with only one type of lipid, chicken egg phosphatidylcholine, as a model membrane. Actual lipid membranes consist of various lipid components, and previous studies indicate lipid-water partitioning values of organic chemicals can be affected significantly by the lipid membrane composition (Kwon et al.

2007, Yamamoto and Liljestrand 2004). Therefore, further research investigating the effects of lipid composition on partitioning of nanoparticles between lipids and water is necessary to assess the fate and transport of these potentially toxic substances.

In this chapter, an *in vitro* method for determining lipid-water partition coefficients (K_{lipw}) of fullerene was developed for membranes of varying composition using SSLMs. We synthesized the SSLMs in our lab. Nonporous silica beads were chosen as the solid support, and coatings of various composition were used to investigate the effects of lipid composition on the partitioning behavior of fullerene between water and lipids.

3.2. MATERIALS AND METHODS

Chemicals. Carbon fullerene (C_{60}, 99.5+ %) was obtained from SES Research (Houston, TX). Three unsaturated phospholipids, 1,2-dimyristoleoyl-sn-glycero-3-phosphocholine (DMoPC, C 14:1, 14:1), 1,2-dioleoyl-sn-glycero-3-phosphocholine (DOPC, C 18:1, 18:1), and 1,2-dierucoyl-sn-glycero-3-phosphocholine (DEruPC, C 22:1, 22:1) were selected as representative lipid membrane phases. Various types of lipid components in chloroform were obtained from Avanti Polar Lipids (Albaster, AL). To make SSLMs, non-functionalized silica microspheres (mean diameter of 5.2 μm, 100 % solid content) were purchased from Bangs Laboratories, Inc. (Fisher, IN). To take a fluorescence image of the SSLMs, N-(6-tetramethylrhodaminethiocarbamoyl)-1,2-dihexadecanoyl-sn-glycero-3-phosphoethanolamine (TRITC-DHPE) was purchased from Molecular Probes (Eugene, OR).

Preparation of aqueous fullerene suspension (nC_{60}). Aqueous fullerene solutions (nC_{60}) were prepared using the SON/nC_{60} sonication method described in Brant et al. (Brant et al. 2006). In short, fullerenes were dissolved in toluene, and then the

solution was mixed with a large volume of deionized water. After the removal of the toluene under ultrasonic treatment, a yellowish fullerene aqueous solution remained. This fullerene suspension was filtered through a 0.8 μm membrane filter to remove any large aggregates.

Preparation of solid supported lipid membranes (SSLMs). Liposome suspensions containing the selected lipid components were prepared using the thin film hydration technique followed by the rapid extrusion process as described previously (Kwon et al. 2006). Briefly, the lipid solution in chloroform was evaporated using a gentle nitrogen stream and the thin residue film was dissolved in deionized water and stored overnight at 4 °C. The resulting lipid suspensions were extruded through the 0.8 μm polycarbonate membranes more than 10 times to reduce vesicle polydiversity. The silica beads were washed with 1 M nitric acid followed by extensive mixing with methanol and water. Then, synthetic vesicle dispersions were vigorously mixed with the silica beads for 60 seconds using a vortex mixer, and gently mixed in a shaker for 2 hrs. After mixing, excess vesicles that were not adsorbed onto the silica beads were removed by centrifugation which separated the silica beads from the supernatant. The mass of lipids adsorbed onto the silica beads was determined by measuring differences between initial lipid concentration and supernatant concentration. A total organic carbon analyzer (Tekmar Dohrmann Apollo 9000, Cincinnati, OH) was used to measure lipid concentration.

Determination of K_{lipw} of fullerene. The aqueous fullerene solution and SSLMs were placed into 1.8 mL amber vials with polytetrafluroethylene/silicon septa. The reactors were incubated for 80 hrs, and the SSLMs and fullerene dispersions were completely mixed at different temperatures (4, 11, 25 °C) using custom-made tumbling devices or shakers (30, 50 °C). For each temperature, one vial which contained fullerene

solution without SSLMs was prepared as a control to evaluate the potential for fullerene adsorption onto the vial in each experimental setup. The free fullerene concentration that does not interact with SSLMs did not change after 72 hrs based on preliminary experiments. Thus, we chose an apparent equilibrium time of 80 hrs for conducting the experiments. After equilibration, the solid supported bilayers were allowed to settle, and the supernatant contained only free fullerene without lipid. Fullerene was destabilized with 0.1 M $Mg(ClO_4)_2$, extracted with toluene and analyzed using a Waters 2690 high performance liquid chromatography system equipped with a Waters 996 photodiode array detector (Milford, MA). A YMC ODS-A column (5 μm, 6.0 × 150 mm, YMA America Inc. Allentown, PA) was used in the HPLC analysis. The lipid-water partition coefficient was determined from a mass balance, as follows:

$$K_{lipw}(L/kg-lipid)=\frac{C_{lip}}{C_w m}=\frac{C_0-C_w}{C_w m} \qquad (3\text{-}1)$$

where C_{lip} is the concentration of fullerene on the lipid side determined from the difference between the initial or control C_{60} concentration (C_0) and the fullerene concentration in the supernatant (C_w). The variable m is the lipid concentration (kg-lipid/L).

3.3. Results And Discussion

Characterization of materials. Aqueous fullerene suspensions (nC_{60}) prepared by the SON/nC_{60} method were characterized using dynamic light scattering (Malvern Zetasizer nano ZS, Malvern, England) to assess the size range and particle charge. The diameter and zeta potential of the prepared nC_{60} (1-8 mg/L) ranged from 120 to 130 nm and -35 to -50 mV, respectively. These values are generally consistent with measurements made in previous studies that used similar procedures to prepare fullerene dispersions in water (Brant et al. 2006, Chen et al. 2008). Figure 3.1 shows the effective

particle diameters and zeta potentials of fullerene suspensions used in this research. These data were collected after the experiment for each of the five different temperatures. As shown in Figure 3.1, neither size nor zeta potential of fullerenes changed significantly as a function of temperature. Preliminary experiments also showed that the values remained constant throughout the duration of the experiments.

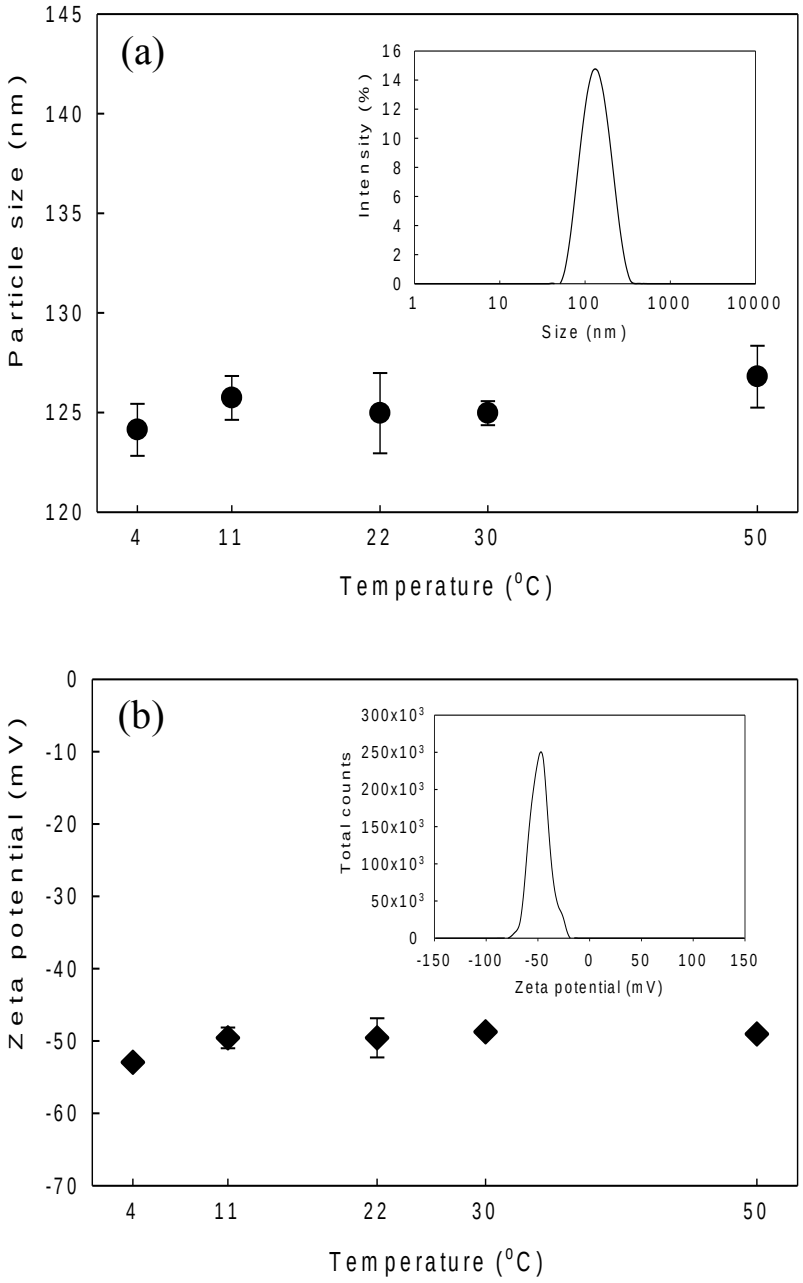

Figure 3.1: (a) Effective particle sizes and (b) zeta potentials of fullerene dispersions in water (nC_{60} = 1.7 mg/L, pH = 6.3 ± 0.1) at different temperatures after 80 hrs. Insets of Figure 3.1(a) and 1(b) are size distributions and zeta potentials of nC_{60} saved at 11°C, respectively. The error bars indicate standard deviations of triplicate analyses (not shown when the error bars are smaller than the symbol).

The SSLMs described schematically in Figure 3.2(a) are selected phospholipid membranes assembled on nonporous silica microspheres with an average hydrodynamic diameter of 5.2 μm. Uniform coating of the micro silica beads used in this study was confirmed by taking a confocal fluorescence microscope image with the aid of 0.1 mol% of TRITC-DHPE phospholipids that were labeled at the head group with bright, red-orange fluorescent tetramethylrhodamine dye (Figure 3.2(b)). The known thickness of the outer lipid bilayer is approximately 4-5 nm (Baksh et al. 2004). Previous studies have reported that SSLMs have mechanical stability and retain the fluidity of their lipid membranes (Baksh et al. 2004, Bayerl and Bloom 1990). The lipid concentrations used in this study ranged from 2 to 12 mg-lipid/L.

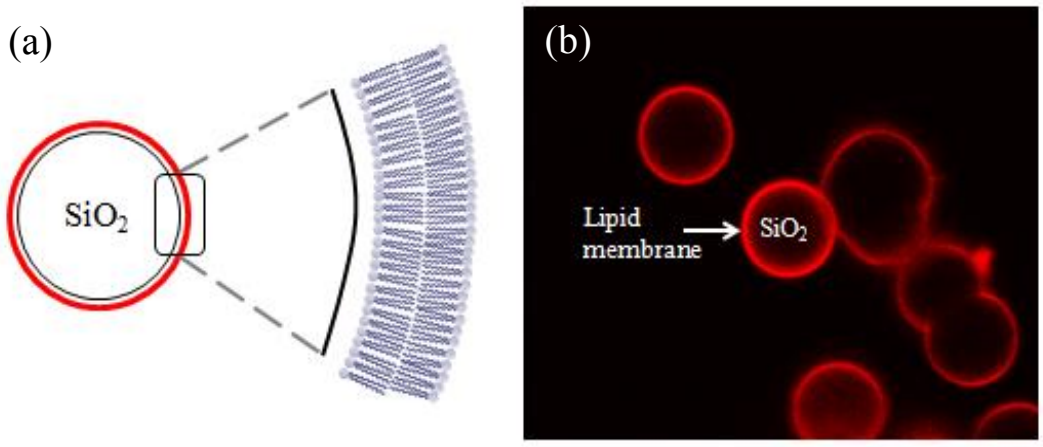

Figure 3.2: (a) Schematic diagram of a solid supported lipid membranes (SSLMs, modified from Baksh et al., (2004)). (b) confocal fluorescence image of SSLMs using DEruPC and 0.1 mol% TRITC-DHPE, a fluorescently labeled lipid

Mass balance recovery from reactors. Fullerene mass recovered from reactors was carefully measured at 4 °C and 50 °C, which were the lowest and highest temperatures used in this study. To perform the mass balance, supernatants that contain free fullerene were first moved to new vials. Then, SSLMs were re-suspended with DI water and carefully transferred to new vials. Free fullerene in supernatant and fullerene that interacted with the lipid membranes were extracted with 0.1 M $Mg(ClO_4)_2$ and toluene. Finally, to calculate the fullerene mass adsorbed onto the vials, original vials were washed with DI water and dried under nitrogen purging, and nC_{60} was extracted with toluene by gently rotating the vials. As shown in Figure 3.3, total mass recovered from the reactors reached more than 98 %, and less than 10 % of the total nC_{60} adsorbed onto vials. To consider possible adsorption of fullerene onto vials, one control vial which contained only fullerene suspensions in water was prepared at each temperature. We used C_0 (eq 3-1) as the initial fullerene concentration since the difference between the concentration in the control vial and the initial concentration was negligible (less than 2 %).

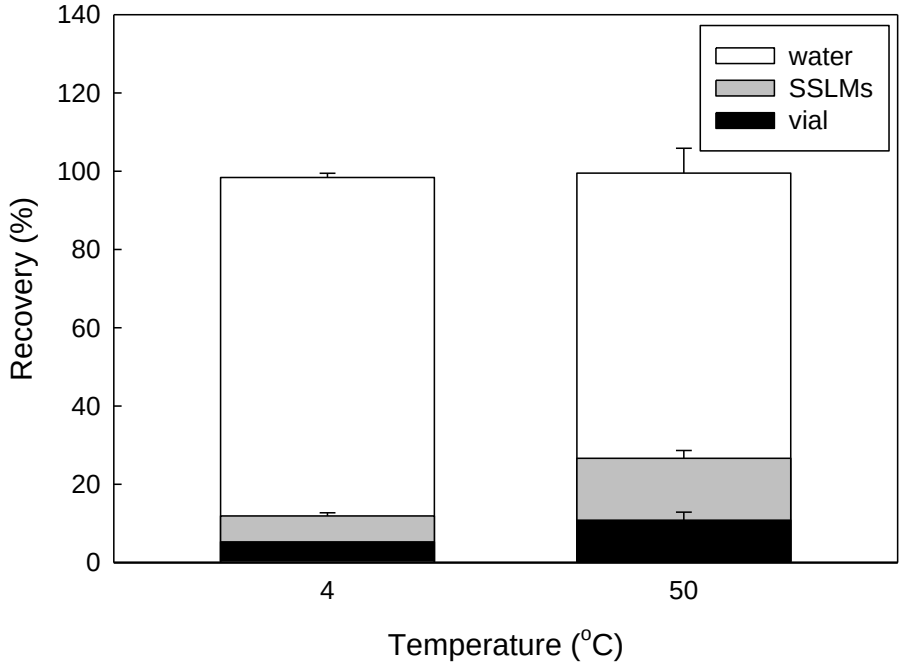

Figure 3.3: nC_{60} mass recovered from reactors at 4 °C and 50 °C. White bars indicate free nC_{60} remaining in the supernatants, gray bars indicate nC_{60} interacted with the solid supported lipid membranes (SSLMs), and black bars represent nC_{60} adsorbed onto the vials. The error bars indicate standard deviations of triplicate analyses.

Lipie-water partition coefficients (K_{lipw}). K_{lipw} values of fullerene for the SSLM prepared from three different unsaturated lipids, DMoPC, DOPC, and DEruPC at five different temperatures are summarized in Table 3.1. Log K_{lipw} (L/kg) values range from 3.1 to 5.3 which are similar to partitioning values of highly or moderately hydrophobic molecular level chemicals such as endocrine disrupting chemicals (EDCs) (Kwon et al. 2006) even though fullerene has been shown to exhibit stronger hydrophobicity (as discussed in more detail below in this chapter). The values obtained in this research are consistent with research by Hou et al. (Hou et al. 2011) examined partitioning between an egg phosphatidylcholine lipid bilayer and water in which they reported log distribution

coefficients of 3.2 and 3.7 at pH 7.4 using Freundlich and Langmuir models, respectively, when fullerene concentration in water was 2 mg/L. Moreover, estimates of the bioconcentration factor (BCF) of fullerene by Jafvert and Kulkarni (Jafvert and Kulkarni 2008) (log BCF as 4.5, 5.4, and 5.7 for cod, earthworms, and salmon, respectively) and Tervonen et al. (Tervonen et al. 2010) (log BCF values of fullerene for *Daphnia magna* from 3.3 and 3.9) are in the range of the results of this study.

As shown in Table 3.1, regardless of lipid types, partition coefficients increase with increasing temperature. It has been reported that the polar head groups of phospholipid membranes lie in the bilayer plane at lower temperature (5 °C); however, those head groups increasingly submerge in the hydrocarbon tail with increasing temperature, causing enhanced lateral head group repulsion and increased distance between bilayers in water (Dill and Stigter 1988). Because fullerene dispersions in water have much larger particle diameters than molecular scale chemicals, they can more easily penetrate into lipid membranes when the distance between the lipid bilayers is held at higher temperature for longer periods to time. Therefore, the observed increase in the partitioning values with increasing temperatures may be attributed to thermal changes associated with the lipid membrane structure.

Table 3.1: Lipid-water partition coefficients of fullerene at five different temperatures using three unsaturated lipids (DMoPC, DOPC and DEruPC).

(Units : L/kg lipid)

Lipids	4 ˚C	11 ˚C	25˚C	30 ˚C	50 ˚C
DMoPC (C 14:1)	2.54 (±1.18)×10^3	5.87 (±3.08)×10^3	7.17 (±1.25)×10^3	1.51 (±0.13)×10^4	2.19 × 10^4
DOPC (C 18:1)	6.37×10^3	6.70 (±3.81)×10^3	1.27 (±0.34)×10^4	3.16 (±0.67)×10^4	5.05 × 10^4
DEruPC (C 22:1)	7.85 (±4.93)×10^3	1.03 (±0.70)×10^4	2.40 (±1.34)×10^4	6.51 (±1.55)×10^4	1.90 (±0.04)×10^5

Average (± standard deviation) of triplicate analyses. For duplicate analyses, average values are used without standard deviation.

Effects of acyl chain length of unsaturated lipid membranes. The main transition temperature of the unsaturated lipids DMoPC, DOPC, and DEruPC are less than -30, -22, and 11 °C, respectively. Thus, DMoPC and DOPC are present as liquid crystalline phase at all five temperatures, and only DEruPC has different physical states at the different temperatures studied: gel phase at 4 °C, ripple phase at 11 °C, and liquid crystalline phase above 25 °C. The K_{lipw} values of fullerene obtained in these experiments using three different unsaturated lipids were highest with DEruPC (C 22:1, 22:1) and lowest with DMoPC (C 14:1, 14:1) regardless of temperatures (Table 3.1). Based on this result, it can be concluded that partitioning values of fullerene are higher for unsaturated lipids composed of longer acyl chains. This result agrees with those in Yamamoto and Liljestrand (Yamamoto and Liljestrand 2004) that reported K_{lipw} values of 17 β-estradiol and p-nonylphenol in the order of DOPC (C18:1, 18:1) > POPC (C16:0, 18:1) above the transition temperature of each phospholipid. For saturated lipids which exist as a gel phase at room temperature, previous studies have reported that K_{lipw} values of hydrophobic organic pollutants are higher for shorter acyl chain (Antunes-Madeira and Madeira 1987, Yamamoto and Liljestrand 2004) because shorter acyl chain lengths yield

a more fluid conformation to the bilayer which leads to greater partitioning. However, for unsaturated lipids which exist as liquid crystalline phases at room temperature, lipid fluidity may not be affected significantly by acyl chain length. Instead, a stronger hydrophobic interaction between fullerene and lipids with a longer acyl chain may result in higher partitioning values. Since it is generally acknowledged that in natural environments biological membranes contain higher unsaturated lipid content on a relative basis, the result of this study suggests that strongly hydrophobic fullerene nanoparticles can partition and accumulate to a greater extent in membranes composed of longer unsaturated acyl chains found in aquatic organisms.

Differences in lipid-water partitioning mechanisms between hydrophobic chemicals and fullerene. For neutral organic chemicals such as endocrine disrupting chemicals (EDCs) and polycyclic aromatic hydrocarbons (PAHs), it is widely known that the relationship between octanol-water partition coefficients (K_{ow}) and lipid-water partition coefficients (K_{lipw}) generally follows a linear trend (Figure 3.4). This implies that more hydrophobic chemicals tend to have greater partitioning values between lipid and water. Although the log K_{ow} of fullerene, which is reported as 6.67 by Jafvert and Kulkarni (Jafvert and Kulkarni 2008), is higher than that of EDCs, K_{lipw} of fullerene is in the range of K_{lipw} values of EDCs. Moreover, although the log K_{ow} of fullerene is in the range of log K_{ow} values of strongly hydrophobic PAHs such as benzo[a]pyrene (6.35), dibenzo[a,c]anthracene (6.17), and benzo[ghi]perylene (6.90), K_{lipw} of fullerene is more than two orders of magnitude lower than the reported K_{lipw} of these three PAHs (Kwon et al. 2009). Due to similarities between the molecular features of PAHs and fullerene (such as fused pentagonal, hexagonal structures and an extended π electron system) properties of PAHs have been used to estimate fullerene properties such as solubility (Martin et al. 2007) and polarizability (Shanker and Applequist 1994). However, the results shown in

Figure 3.4 suggest that K_{lipw} values of hydrophobic chemicals cannot be used as a good predictor for the K_{lipw} values of fullerene. This may be explained by differences in the partitioning mechanisms between neutral organic chemicals and fullerene. First, in contrast to molecular fullerene (C_{60}), fullerene aggregates (nC_{60}) in water are negatively charged (Figure 3.1(b)), which can create electrostatic repulsion between fullerene aggregates and polar head groups of the lipid membranes, thereby increasing solubility in the polar aqueous phase. Second, the smaller K_{lipw} value of fullerene compared to the values for the PAHs may be attributed to the larger particle size and bulky structure of fullerene, which suggests that more thermodynamic energy is required for fullerene to partition into the lipid membranes due to the increased cavity space that must be created inside the organized lipid membranes. Further investigations (i.e. using lipids consisting of different polar head groups and evaluating the partitioning thermodynamics) were also conducted in Chapter 4 to confirm the lipid-water partitioning mechanisms associated with fullerene.

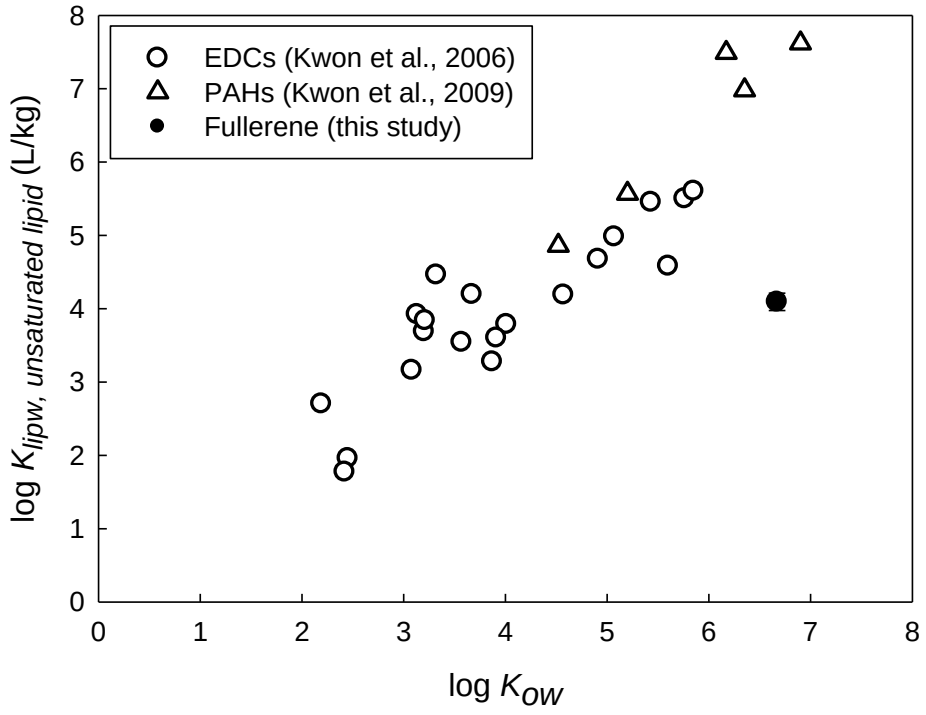

Figure 3.4: Relationship between reported octanol-water partition coefficient (K_{ow}) and unsaturated lipid-water partition coefficient (K_{lipw}) of 19 endocrine disrupting chemicals (EDCs), five polycyclic aromatic hydrocarbons (PAHs), and fullerene. Kwon et al., (2006) conducted experiments at 22 °C and used 1-palmitoyl-2-oleoyl-sn-glycero-3-phosphocholine (POPC, C 18:1, 16:0) as a representative unsaturated lipid, and K_{lipw} of fullerene in this figure was measured at 25 °C with DOPC (C 18:1, 18:1) unsaturated lipid.

3.4. CONCLUSIONS

An *in vitro* method for the quantitative measurement of lipid-water partitioning values of fullerene using SSLMs was developed and employed to study fullerene partitioning. The main focus of this study has been on the effects of lipid composition on partitioning coefficients. As noted above, the hydrophobic acyl chain length of lipid membranes significantly affected the partitioning of fullerene between the lipids and water. This result suggests that lipid components should be carefully chosen to assess bioaccumulation of fullerene into aquatic organisms. Moreover, partitioning increases with increasing temperature, regardless of lipid type, indicating that temperature is also of critical importance to assess toxicity and bioavailability of fullerene. The relationship between octanol-water partitioning (K_{ow}) and lipid-water partitioning (K_{lipw}) of hydrophobic organic chemicals and fullerene appears to be different, which implies that the partitioning mechanism of fullerene may also differ from that of other hydrophobic chemicals due to the unique properties of fullerene nanoparticles. These properties include the negative charge and large particle size of fullerene aggregates. The development of the *in vitro* method in this chapter makes it possible to determine the lipid-water partitioning thermodynamics of fullerene and to assess competitive lipid-fullerene interactions with organic matter constituents such as humic acid and protein.

3.5. REFERENCES

Antunes-Madeira, M.C. and Madeira, V.M. (1987) Partition of malathion in synthetic and native membranes. Biochim Biophys Acta 901(1), 61-66.

Baksh, M.M., Jaros, M. and Groves, J.T. (2004) Detection of molecular interactions at membrane surfaces through colloid phase transitions. Nature 427(6970), 139-141.

Bayerl, T.M. and Bloom, M. (1990) Physical properties of single phospholipid bilayers adsorbed to micro glass beads. A new vesicular model system studied by ^{2}H-nuclear magnetic resonance. Biophys J 58(2), 357-362.

Brant, J.A., Labille, J., Bottero, J.Y. and Wiesner, M.R. (2006) Characterizing the impact of preparation method on fullerene cluster structure and chemistry. Langmuir 22(8), 3878-3885.

Chen, Z., Westerhoff, P. and Herckes, P. (2008) Quantification of C_{60} fullerene concentrations in water. Environ Toxicol Chem 27(9), 1852-1859.

Dill, K.A. and Stigter, D. (1988) Lateral interactions among phosphatidylcholine and phosphatidylethanolamine head groups in phospholipid monolayers and bilayers. Biochemistry 27(9), 3446-3453.

Hou, W.C., Moghadam, B.Y., Westerhoff, P. and Posner, J.D. (2011) Distribution of fullerene nanomaterials between water and model biological membranes. Langmuir 27(19), 11899-11905.

Jafvert, C.T. and Kulkarni, P.P. (2008) Buckminsterfullerene's (C_{60}) octanol-water partition coefficient (Kow) and aqueous solubility. Environ Sci Technol 42(16), 5945-5950.

Kwon, J.H., Liljestrand, H.M. and Katz, L.E. (2006) Partitioning of moderately hydrophobic endocrine disruptors between water and synthetic membrane vesicles. Environ Toxicol Chem 25(8), 1984-1992.

Kwon, J.H., Liljestrand, H.M., Katz, L.E. and Yamamoto, H. (2007) Partitioning thermodynamics of selected endocrine disruptors between water and synthetic membrane vesicles: effects of membrane compositions. Environ Sci Technol 41(11), 4011-4018.

Kwon, J.H., Wuethrich, T., Mayer, P. and Escher, B.I. (2009) Development of a dynamic delivery method for in vitro bioassays. Chemosphere 76(1), 83-90.

Lovern, S.B. and Klaper, R. (2006) *Daphnia magna* mortality when exposed to titanium dioxide and fullerene (C_{60}) nanoparticles. Environ Toxicol Chem 25(4), 1132-1137.

Martin, D., Maran, U., Sild, S. and Karelson, M. (2007) QSPR modeling of solubility of polyaromatic hydrocarbons and fullerene in 1-octanol and n-heptane. J Phys Chem B 111(33), 9853-9857.

Oberdörster, E. (2004) Manufactured nanomaterials (fullerenes, C_{60}) induce oxidative stress in the brain of juvenile largemouth bass. Environ Health Perspect 112(10), 1058-1062.

Shanker, B. and Applequist, J. (1994) Polarizabilities of fullerenes C_{20} through C_{240} from atom monopole-dipole interaction theory. Journal of Physical Chemistry 98(26), 6486-6489.

Tervonen, K., Waissi, G., Petersen, E.J., Akkanen, J. and Kukkonen, J.V. (2010) Analysis of fullerene-C_{60} and kinetic measurements for its accumulation and depuration in Daphnia magna. Environ Toxicol Chem 29(5), 1072-1078.

Wang, I.C., Tai, L.A., Lee, D.D., Kanakamma, P.P., Shen, C.K., Luh, T.Y., Cheng, C.H. and Hwang, K.C. (1999) C_{60} and water-soluble fullerene derivatives as antioxidants against radical-initiated lipid peroxidation. J Med Chem 42(22), 4614-4620.

Wiesner, M.R., Hotze, E.M., Brant, J.A. and Espinasse, B. (2008) Nanomaterials as possible contaminants: the fullerene example. Water Sci Technol 57(3), 305-310.

Yamamoto, H. and Liljestrand, H.M. (2004) Partitioning of selected estrogenic compounds between synthetic membrane vesicles and water: effects of lipid components. Environ Sci Technol 38(4), 1139-1147.

Zhang, B., Cho, M., Hughes, J.B. and Kim, J.H. (2009) Translocation of C_{60} from aqueous stable colloidal aggregates into surfactant micelles. Environ Sci Technol 43(24), 9124-9129.

Chapter 4: Partitioning of fullerene nanoparticles between water and solid supported lipid membranes: Partitioning thermodynamics and effects of membrane composition on partitioning

ABSTRACT

The partition coefficient (K_{lipw}) of fullerene between water and solid supported lipid membranes (SSLMs) was examined using different lipid membrane compositions. K_{lipw} of fullerene was significantly higher with a cationic lipid membrane compared to that with a zwitterionic or anionic lipid membrane, potentially due to the strong interactions between negative fullerene dispersions and positive lipid head groups. The higher K_{lipw} for fullerene partitioning to ternary lipid mixture membranes was attributed to an increase in the interfacial surface area of the lipid membrane resulting from phase separation. These results imply that lipid composition can be a critical factor that affects bioconcentration of fullerene. Partitioning of fullerene into zwitterionic unsaturated lipid membranes was dominated by the entropy (ΔS) contribution and the process was endothermic ($\Delta H > 0$). This result contrasts the partitioning thermodynamics of highly and moderately hydrophobic chemicals indicating that the lipid-water partitioning mechanism of fullerene may be different from that of molecular level chemicals. Potential mechanisms for fullerene partitioning that may explain these differences include adsorption on the lipid membrane surfaces and partitioning into the center of lipid membranes (i.e. absorption).

Keywords

fullerene, lipid membranes, partitioning, thermodynamics

4.1. INTRODUCTION

The increased use of engineered nanomaterials (ENMs) has raised concerns associated with the unknown harmful effects of these materials on humans and the environment. Fullerene (C_{60}), one of the most prevalent carbon based nanomaterials, has been envisioned for numerous applications such as fuel cells (Wang et al. 2007), photovoltaic cells (McMahon et al. 2011), drug carriers (Hughes 2005), and face creams (Benn et al. 2011) due to its unique properties (e.g., electron-rich cage structure, antioxidant property, and high reactivity). Indeed, the global market for fullerene could approach $4.7 billion by 2016 (BCC research 2006). Due to the rapid increase in fullerene production, potential biological effects of this nanoparticle have been raised considerable concern.

To investigate possible harmful effects of nanoparticles on living organisms, bioaccumulation is of critical importance because it provides the link between chemical exposure in the environment and the uptake of nanoparticles through living organisms (Jonker and Van der Heijden 2007). A first step toward evaluating bioaccumulation is partitioning behavior into lipid membranes that act as biological barriers to target or reactive sites in cells. Bioaccumulation has been evaluated previously using lipid-water partitioning coefficients (K_{lipw}) of molecular level chemicals such as pharmaceuticals (Go and Ngiam 1997, Wenk et al. 1996), organic acids and bases (Escher et al. 2000), metal complexes (Kaiser and Escher 2006), and endocrine disrupting chemicals (EDCs) (Kwon et al. 2006, Yamamoto and Liljestrand 2004).

For the molecular organic chemicals, K_{lipw} have been measured using an equilibrium dialysis technique in which chemicals dissolved in water and liposome solutions are separated by a dialysis membrane, and chemicals can diffuse through the membrane but the liposome cannot. However, this technique cannot be applied to

measure K_{lipw} of nanoparticles because the diffusion of nanoparticles through a dialysis membrane may be limited by nanoparticle aggregation. Thus, it is essential to develop a new procedure to assess the lipid-water partitioning of nanoparticles.

Very recently, a few studies have examined K_{lipw} of nanoparticles. Hou *et al*. (Hou et al. 2011) performed a quantitative study measuring lipid-water association coefficients of fullerene using solid supported lipid membranes (SSLMs). They also applied SSLMs to investigate the equilibrium and kinetics of gold nanoparticle partitioning between water and lipid bilayers (Hou et al. 2012b). Applying SSLMs to investigate partitioning of nanoparticles between water and lipids is novel and relevant because SSLMs are stable (Bayerl and Bloom 1990) and preserve the fluidity of lipid membranes (Baksh et al. 2004). In addition, after interaction with nanoparticles, SSLMs can be separated from the nanoparticles easily via sedimentation in water. However, these previous studies (Hou et al. 2012b, Hou et al. 2011) used commercial SSLMs and focused on only one type of lipid, egg phospholipid, as a model membrane.

As nanoparticles are released to the environment, they will encounter a variety of organisms with different lipid membrane compositions. Even within a single organism, cell lipid composition can vary. For example, natural cell membranes consist of lipid membranes which have different head group charge (Ryhanen et al. 2006). Unlike molecular level chemicals, many nanoparticles in water have significant charge associated with their surfaces either because they accumulate solution species that impart charge or due to their inherent chemical structure. Thus, while it is critical to investigate the electrostatic interactions between nanoparticles and lipids with different head charges, to date, no studies have considered the effect of lipid head charge on lipid-nanoparticle interactions. In addition, cell membranes typically consist of three components: unsaturated lipids, saturated lipids, and cholesterol (Arnaud 2009). Ternary lipid

membranes composed of these three components exhibit a single liquid phase above the critical temperature (Tc). However, this single liquid phase undergoes phase separation below Tc, building raft domains which are enriched in saturated lipids (e.g., sphinogomyelin) and cholesterol (Arnaud 2009, Brown and London 2000, Garcia-Saez et al. 2007, Kuzmin et al. 2005, Stottrup et al. 2005, Veatch and Keller 2003). This lateral organization of ternary lipid mixture membranes creates a height mismatch between unsaturated lipids and saturated lipids/cholesterol (Figure 4.1.). For this reason the hydrophobic surface area of lipids might increase after phase separation, which can affect lipid water partitioning of nanoparticles. Even though recent studies (Kuzmin et al. 2005, Veatch and Keller 2003) have emphasized the importance of rafts in membrane biology, the phase separation of the lipid components has not been considered in previous studies designed to estimate K_{lipw} of various nanoparticles.

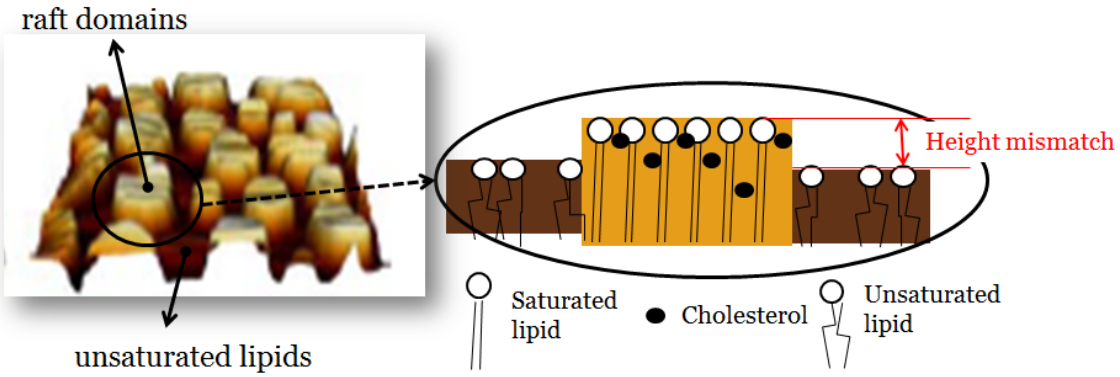

Figure 4.1: An AFM image of lipid membrane surface after phase separation in ternary lipid mixtures (DMoPC:SM:Cholesterol) provided by Garcia-Saez et al., (2007), and its schematic diagram.

Previously, we successfully synthesized solid supported lipid membranes (SSLMs) with three unsaturated lipids which have different acyl chain lengths in our lab and demonstrated the effects of acyl chain lengths on the K_{lipw} of fullerene (Ha et al. 2013). In

this study, SSLMs with lipid membranes containing different head charges, and ternary lipid membranes before and after phase separation were used to investigate the effects of lipid membrane composition. Partitioning thermodynamics (e.g., enthalpy change (ΔH) and entropy change (ΔS)) were evaluated to help identify plausible lipid-water partitioning mechanisms of fullerene.

4.2. MATERIALS AND METHODS

Chemicals. Carbon fullerene (C_{60}, 99.5+ %) was purchased from SES Research (Houston, TX). Three unsaturated phospholipids having zwitterion head groups were used in this study: (1,2-dimyristoleoyl-sn-glycero-3-phosphocholine (DMoPC, C 14:1, 14:1), 1,2-dioleoyl-sn-glycero-3-phosphocholine (DOPC, C 18:1, 18:1), and 1,2-dierucoyl-sn-glycero-3-phosphocholine (DEruPC, C 22:1, 22:1) . In addition, a lipid with a positively charged head group, 1,2-dioleoyl-3-trimethylammonium-propane (DOTAP) and a lipid with a negatively charge head group,1,2-dioleoyl-sn-glycero-3-phospho-(1'-rac-glycerol) (18:1 PG) were studied. Table 4.1 summarizes the main transition temperature, physical state at room temperature and charge of the lipid head groups for each of the lipids. Two sphinogomyelins (N-stearoyl-D-erythro-sphingosylphosphorylcholine (18:0 SM) and Brain SM (BSM)) and cholesterol (Aldrich Chemical Co, Milwaukee, WI) were used to make ternary lipid membranes. The lipids were obtained from Avanti Polar Lipids (Alabaster, AL). The composition of the ternary lipid mixtures included one of the three unsaturated zwitterion lipids listed in Table 4.1, either SM or BSM as representative saturated lipids, and cholesterol. Table 4.2 shows the estimated phase height differences between the unsaturated lipids and the saturated lipids/cholesterol components.

To make the solid supported lipid membranes, non-functionalized silica microspheres (mean diameter of 5.2 μm, 100 % solid content) were purchased from Bangs Laboratories, Inc. (Fishers, IN). To prepare TEM images of fullerene nanoparticles and fullerene associated with SSLMs, carbon film grids (400 mesh) were purchased from Electron Microscopy Science (Hatfield, PA).

Table 4.1: Summary of selected unsaturated phospholipid components

Phospholipids	Carbon chain: Double bonds	Main transition temperature (°C)	Physical state at room temperature	Charge of lipid head
DMoPC	(C14:1, 14:1)	<-30	Liquid crystalline	Zwitterion
DOPC	(C18:1, 18:1)	-22	Liquid crystalline	Zwitterion
DEruPC	(C22:1, 22:1)	11	Liquid crystalline	Zwitterion
DOTAP	(C18:1, 18:1)	~ -0	Liquid crystalline	Positive
18: 1 PG	(C18:1, 18:1)	-18	Liquid crystalline	Negative

Table 4.2: Summary of selected ternary lipid mixture membranes

Lipid composition of ternary mixture lipids (2:1:1, w/w)	Estimated critical temperature (°C)	Estimated phase height difference[a] (pm)	References
DMoPC/SM/Cholesterol	38 ± 1	1560 ± 130	(Garcia-Saez et al. 2007)
DOPC/SM/Cholesterol	46 ± 1	870 ± 100	(Garcia-Saez et al. 2007)
DEruPC/SM/Cholesterol	66 ± 3	170 ± 70	(Garcia-Saez et al. 2007)
DMoPC/BSM/Cholesterol	-	-	
DOPC/BSM/Cholesterol	28	-	(Veatch and Keller 2003)
DEruPC/BSM/Cholesterol	-	-	

[a]Height different is a length between raft domain and unsaturated lipid after phase separation in ternary lipid membranes

Aqueous fullerene suspensions. Fullerene suspensions in water were prepared by the modified SON/nC_{60} method described in Brant *et al* (Brant et al. 2006). After

dissolving 3 mg of fullerene in 5 mL of toluene, 20 mL of deionized water was added to the solution. Then, the toluene was removed by ultrasonication with air purging leaving a yellowish fullerene aqueous solution. This fullerene suspension was filtered through a 0.8 μm membrane filter (Millipore, Billerica, MA) to remove any large aggregates. The resultant fullerene suspension was characterized using Transmission Electron Microscopy (TEM, FEI Tecnai) and Dynamic Light Scattering (DLS, Malvern Zetasizer Nano ZS). The shape of the fullerene nanoparticles in the suspensions was spherical (Figure 4.2). The average diameter and zeta potential of the fullerene aggregates ranged from 120-130 nm, and -35 - -50 mV, respectively.

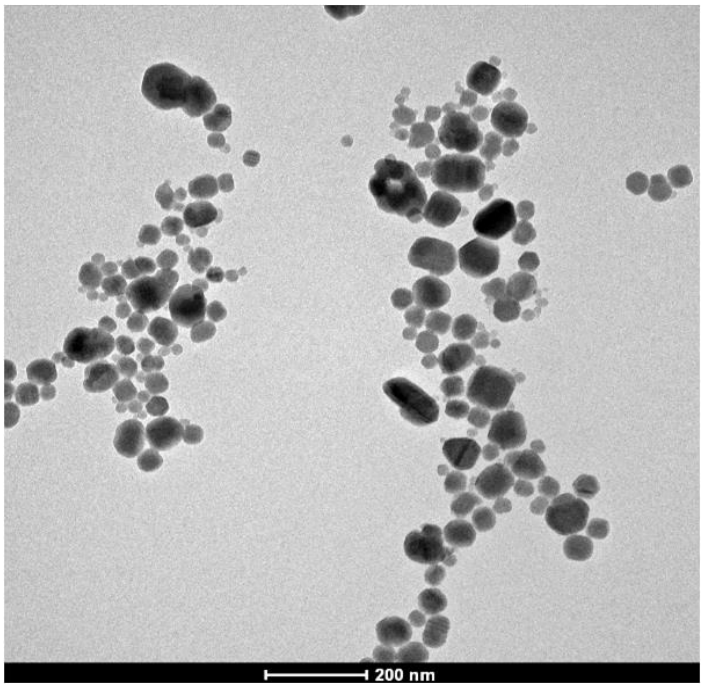

Figure 4.2: TEM image of fullerene aggregates (nC_{60})

Solid supported lipid membranes (SSLMs). The synthetic membrane vesicles for each lipid composition were prepared using the thin film hydration technique

followed by the rapid extrusion process. The detailed procedure is described elsewhere (Escher et al. 2000, Kwon et al. 2006). Solid supported lipid bilayers were made using modified methods described in Bayerl and Bloom. (Bayerl and Bloom 1990), and Baksh *et al.* (Baksh et al. 2004). Silica beads were washed with methanol followed by extensive rinsing with water and nitric acid. The lipid vesicle dispersions were poured onto the silica beads with 60 sec of rigorous vortex mixing followed by 2 hrs of gentle mixing on a shaker. Then, the silica beads and lipid dispersion mixtures were centrifuged and the supernatants were discarded to remove excess vesicles not adsorbed on the solid surface. The mass of the lipids adsorbed on the silica beads was determined by measuring the difference between initial lipid concentration and supernatant concentration. Lipid concentrations were measured using a total organic carbon (TOC) analyzer (Tekmar Dohrmann Apollo 9000, Cincinnati, OH).

For the solid supported ternary lipid mixture membrane vesicles, the weight ratio of unsaturated lipids: SM: cholesterol = 2:1:1 were used. Two replicate samples were prepared. One sample was stored at room temperature which is below the critical temperature (T_c). The other was initially stored at 70 ˚C (above T_c of all ternary lipid mixtures) overnight and transferred to room temperature to create a phase height difference between the unsaturated lipids and the saturated lipids/cholesterol.

The formation of a uniform coating of the micro silica beads with lipid membranes was confirmed by confocal fluorescence microscopy and reported previously (Ha et al. 2013).

Determination of lipid-water partition coefficient (K_{lipw}). The solid supported lipid bilayer and aqueous fullerene dispersions were placed into 1.8 mL amber vials with PTFE/silicon septa. The vials were incubated for 80 hrs using custom-made tumbling devices or shakers over a range of temperatures. For the ternary lipid mixtures and

DOTAP, PG lipids, vials were incubated at room temperatures with a tumbling device. After an 80 hr incubation period, each vial sat quiescently for 1 hr to allow the solid supported lipid membranes (SSLMs) to settle. The fullerene concentration in the supernatant (C_w) was measured using a Waters 2690 high-performance liquid chromatography system equipped with a Waters 996 photodiode array detector (Milford, MA, USA) after extraction with toluene and 0.1 M of $Mg(ClO_4)_2$. K_{lipw} values were calculated using equation (4-1)

$$K_{lipw}(L/kg-lipid) = \frac{C_{lip}}{C_w m} = \frac{C_0 - C_w}{C_w m} \qquad (4\text{-}1)$$

where C_{lip} is the fullerene concentration in the lipid side, which is equal to the difference between the initial or reference fullerene concentration (C_0) and the fullerene concentration in the supernatant (C_w). m is the concentration of lipid (kg-lipid/L).

Determination of thermodynamics of lipid-water partitioning. To assess lipid-water partitioning mechanisms of fullerene, partitioning thermodynamics were investigated. K_{lipw} values using three zwitterion unsaturated lipid membranes measured at five different temperatures (4, 11, 25, 30, and 50 ˚C). The enthalpy (ΔH) and entropy (ΔS) of lipid-water partitioning were determined using the van't Hoff equation:

$$\log K_{lipw} = -\frac{\Delta H}{2.303R}\frac{1}{T} + \frac{\Delta S}{2.303R} \qquad (4\text{-}2)$$

where R is the ideal gas constant (8.314 J/mol-K) and T is temperature (K).

4.3. RESULTS AND DISCUSSION

Apparent time to equilibrium. To determine the apparent time for partitioning between the two phases to reach equilibrium, the concentration of fullerene in an aqueous suspension in contact with a solid supported lipid membrane was monitored over time (Figure 4.3). Bare silica beads (control) and silica beads coated with zwitterion DOPC lipids were prepared and combined with fullerene suspensions. As shown in Figure 4.3, apparent equilibrium was attained within 72 hrs. After 90 hrs, the concentration of free fullerene in water decreased suddenly possibly due to changes in the properties of the solid supported lipid membranes such as lipid fouling after a long incubation time (not shown here). Therefore, we chose 80 hrs as the apparent equilibrium time for lipid-water partitioning of fullerene. In addition to the zwitterion lipids, we confirmed that fullerene interactions with cationic and anionic lipids reached equilibrium within 80 hrs as well. Fullerene rarely interacted with bare nonporous silica beads as shown in Figure 4.3 and verified by TEM (Figure 4.4).

For molecular organic chemicals, the lipid-water partitioning equilibrium time varies from a few hours to days. For example, it was reported that less hydrophobic and smaller chemicals such as phenol, aniline, and hydroxyquinoline ligands reached equilibrium in 12 hrs (Escher et al. 2000, Kaiser and Escher 2006). On the other hand, the equilibrium time for endocrine disruptors, which are bulky and hydrophobic, was not obtained until 14 days (Kwon et al. 2006, Kwon et al. 2007). For engineered nanomaterials, which have sizes from a few to a hundred nanometers, it can be expected that the lipid water partitioning equilibrium may require a relatively long time compared to that of molecular level chemicals. However, fullerene reached equilibrium in 72 hrs in this study. Also a few recent studies have reported that the interaction of lipid membranes with fullerene (Hou et al. 2011) and gold nanoparticles (Hou et al. 2012b)

reached equilibrium in 48 hrs and 24 hrs, respectively. This might be attributed to the different lipid-water partitioning mechanisms between molecular organic chemicals and nanomaterials. Details on the partitioning mechanisms of fullerene are discussed later in this chapter.

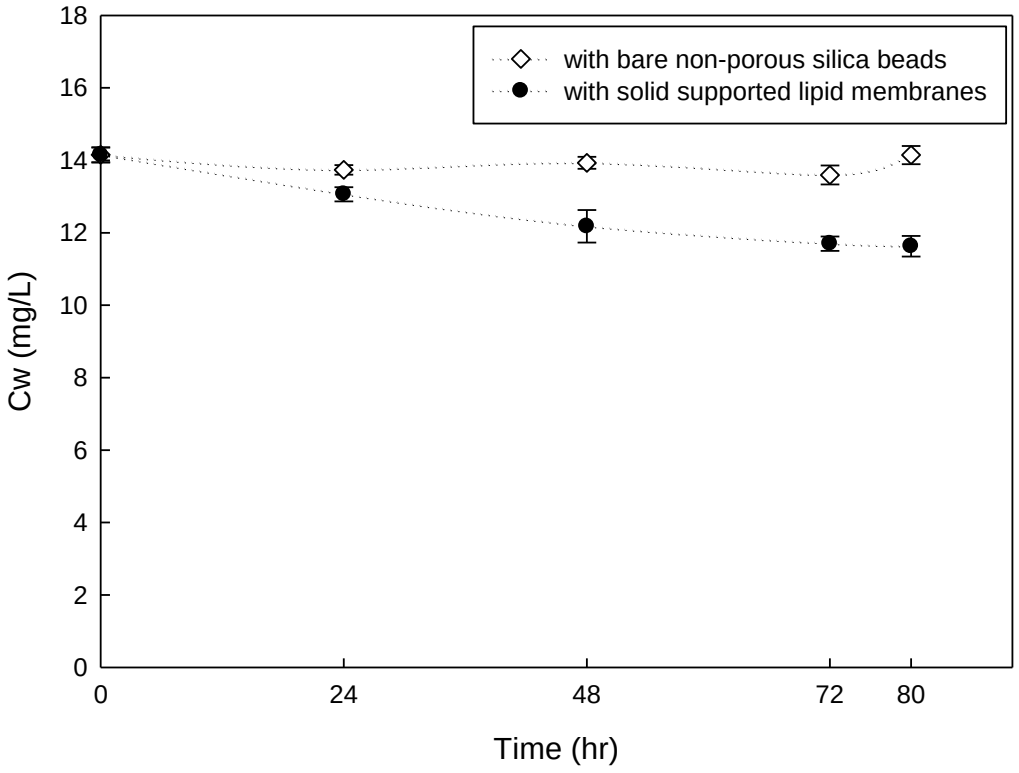

Figure 4.3: Interaction of fullerene suspensions with bare non porous silica beads (open diamond) and solid supported lipid membranes with DOPC (closed circle). C_w is free concentration of fullerene in water side after settling bare silica beads or solid supported lipid membranes (SSLMs). The error bars indicate standard deviations of triplicate analyses (not shown when the error bars are smaller than the symbol).

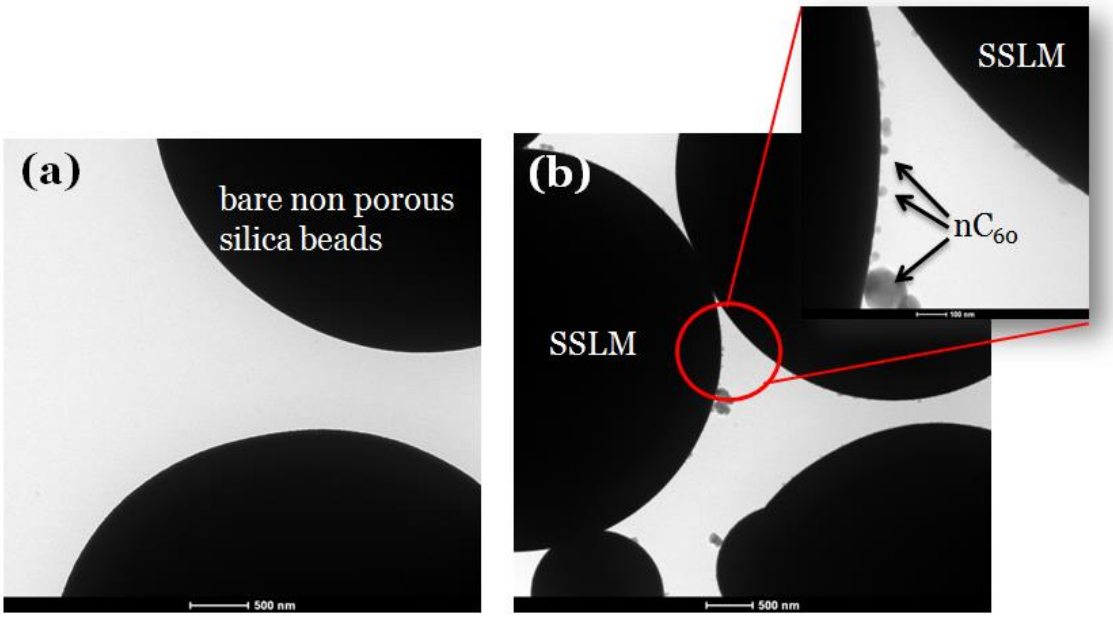

Figure 4.4: TEM images of (a) bare non porous silica beads (control) and (b) solid supported lipid membranes with DOPC lipids interaction with fullerene aggregates in water. Scale bar indicate 500 nm for Figure 4.4 (a) and (b), and 200 nm for the inset of Figure 4.3 (b).

Effects of head charges of lipid membranes. To investigate the effects of lipid membrane head charge on partitioning, solid supported lipid membranes (SSLMs) with DOTAP, DOPC, and PG which have positive, zwitterion and negative charged head groups, respectively, were prepared. These are all unsaturated lipids and have identical acyl chain lengths (C18:1) (Table 4.1). After 80 hrs of incubation of the fullerene with SSLMs containing a DOTAP lipid membrane, more than 95 % (96.03 ± 1.27) of the fullerene nanoparticles were removed. However, with SSLMs containing only DOPC or PG, only 9.24 % (±0.84), and 3.40 % (±0.49) of the fullerene was removed from solution. As shown in Figure 4.5(a), the log K_{lipw} values for fullerene between water and SSLMS

with DOTAP (5.82 ± 0.16) was significantly higher than that with DOPC (4.09 ± 0.12) and PG (3.25 ± 0.065). Also, we confirmed that many fullerene nanoparticles adsorbed onto the SSLMs coated with DOTAP, and the surfaces of some SSLMs were covered almost entirely by fullerene nanoparticles (Figure 4.5(b)). On the other hand, fullerene rarely adsorbed onto SSLMs with PG (Figure 4.5(c)).

Because fullerene particles in water are typically negatively charged (Brant et al. 2006, Labille et al. 2009) there can be a strong affinity between fullerene particles and positive lipid head groups. This implies that non-specific interactions between charged nanoparticles and oppositely charged lipid membranes are of critical importance for bio-nanoparticle interactions. Indeed, previous studies have demonstrated that positively charged nanoparticles are more likely to be adsorbed and internalized into cell membranes compared to neutral and negatively charged nanoparticles due to the strong interactions between positively charged nanoparticles and the negative surface charge of many lipid membranes (Cho et al. 2009a, Santhosh et al. 2014, Verma and Stellacci 2010). Even though the overall charge of most cell membranes is negative, some positively charged sites on cell surfaces have also been reported (Ghinea and Simionescu 1985). Thus, it is possible that fullerene dispersions in water can be strongly adsorbed onto positively charged surface sites and internalized into cells. This internalization is likely responsible for the harmful effects of fullerene towards living cells.

(a)

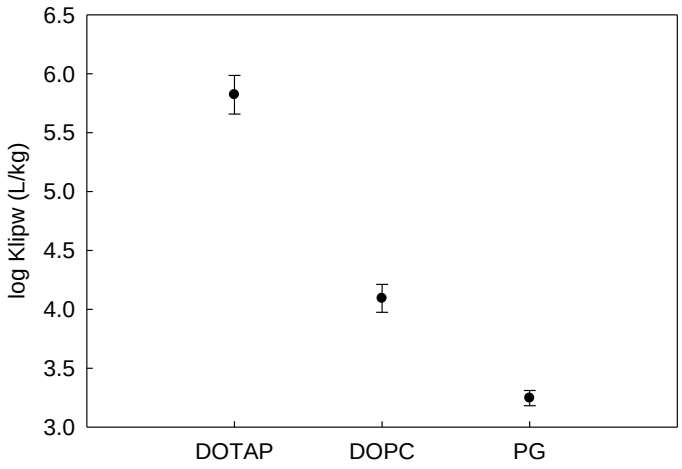

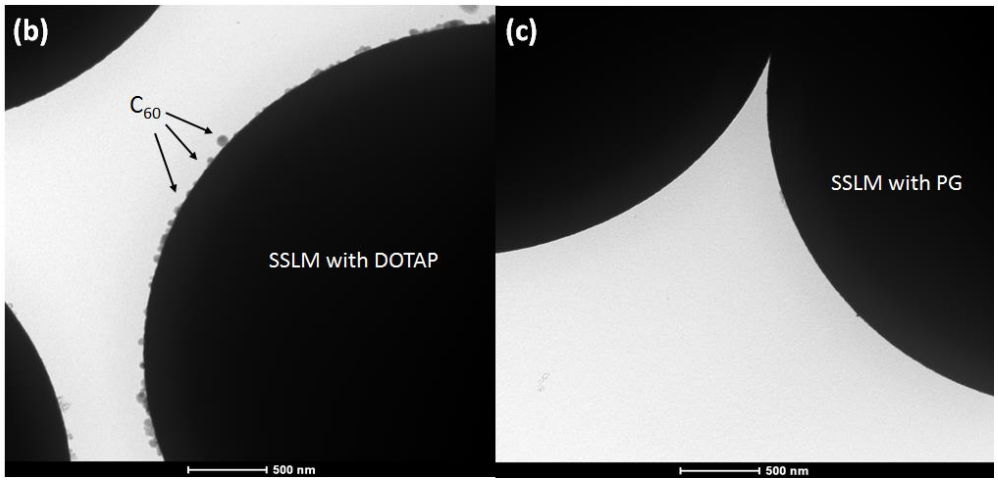

Figure 4.5: Effects of charge of lipid head groups on lipid-water partitioning of fullerene. (a) K_{lipw} of fullerene using three lipid membranes with different head charges. DOTAP, DOPC, and PG are 18:1 lipids which have positive, zwitterion, and negative head charges, respectively. The error bars denote standard deviations of triplicate analyses. (b) and (c) are TEM images of solid supported lipids with DOTAP and PG after interaction with fullerene. Scale bar indicates 500 nm.

Effects of surface structure of ternary lipid mixtures. Lipid rafts are liquid ordered phases which are enriched in sphingolipids and cholesterols, and the rafts coexist with unsaturated lipids which are considered liquid disordered phases (Garcia-Saez et al. 2007). The formation of lipid rafts can create a phase separation between rafts and unsaturated lipids which affects the surface structure of lipid membranes (Chiantia et al. 2006, Dietrich et al. 2001, Garcia-Saez et al. 2007). Figure 4.6 shows the effect of phase separation on partitioning values. For all ternary lipid membranes except DMoPC/SM/Cholesterol (whose estimated critical temperature of 66 ˚C is not high enough to achieve phase separation) and DEruPC/BSM/Cholesterol (K_{lipw} using DEruPC/BSM/Cholesterol before phase separation was not determined due to the negligible amount of fullerene that partitioned into the lipid membrane), the presence of cholesterol decreased K_{lipw} values, and K_{lipw} values increased after phase separation. One possible explanation for this effect is that the interfacial surface area covered by the lipid molecules decreases for the ternary mixtures. Indeed, previous research has shown that Cholesterol in a bilayer before phase separation decreases the surface area covered by lipid molecules (Hofsass et al. 2003). On the other hand, the height mismatch between saturated lipids/cholesterol and unsaturated lipids increases the interfacial surface area by creating raft domains after phase separation. Therefore, the decrease in surface area of lipid molecules due to cholesterol lowers K_{lipw} values whereas increasing lipid surface area due to phase separation increases K_{lipw} values. Thus, surface structure changes due to cholesterol content and phase separation in ternary lipid membranes are critical factors that impact fullerene partitioning.

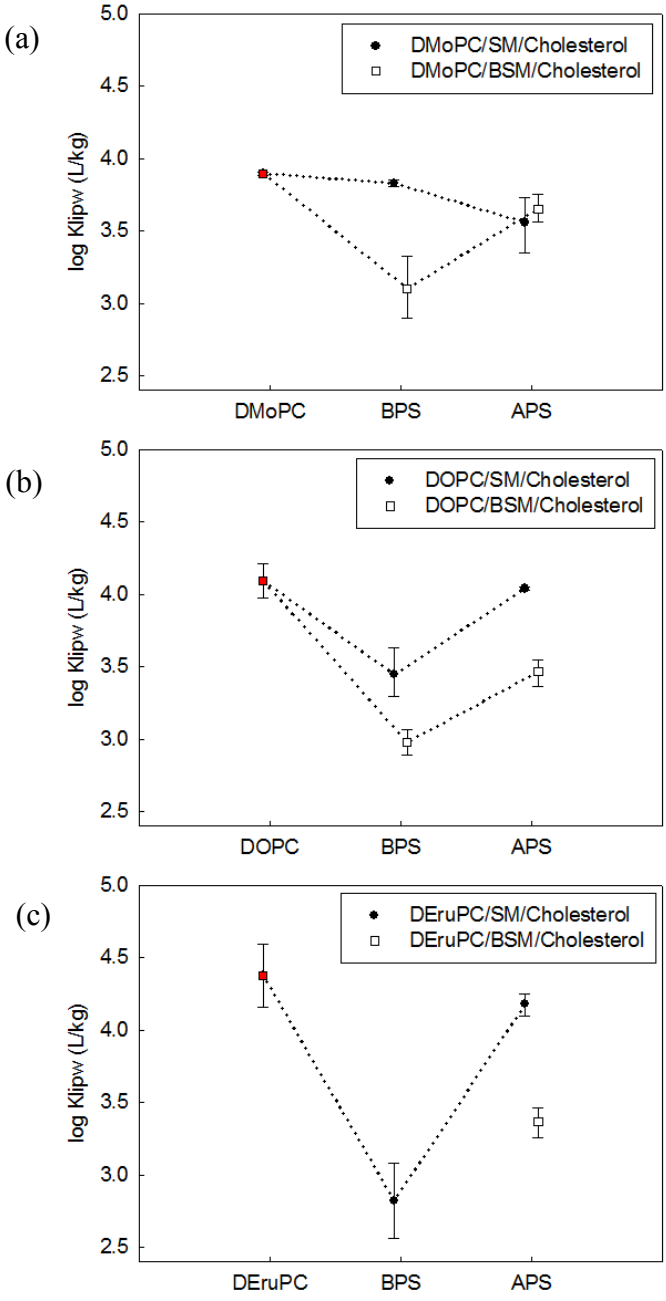

Figure 4.6: Effects of phase separation of ternary lipid mixtures on K_{lipw} values of fullerene. (a) DMoPC, (b) DOPC, and (c) DEruPC are the unsaturated lipids and SM and BSM are the saturated lipids. BPS and APS indicate before phase separation and after phase separation, respectively. The error bars indicate standard deviations of triplicate analyses.

Partitioning thermodynamics. The fullerene K_{lipw} values estimated with three unsaturated lipids (DMoPC (C14:1), DOPC (C18:1), DEruPC (C22:1)) (reported previously in Chapter 3) were used to determine enthalpy (ΔH) and entropy change (ΔS) via regression based on the van't Hoff equation (Figure 4.7, and Table 4.3). As can be seen in Table 4.3, the partitioning of fullerene into the unsaturated lipids was driven by entropy gains (ΔS > 0), and the process was endothermic (ΔH > 0).

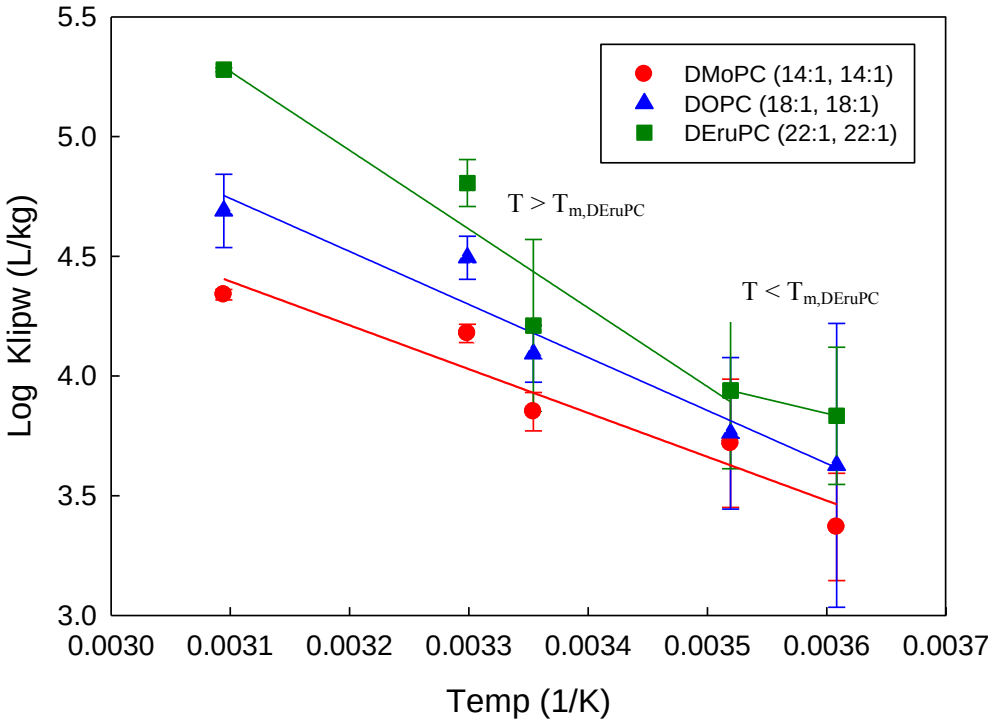

Figure 4.7: Determination of enthalpy (ΔH) and entropy (ΔS) values for lipid-water partitioning of fullerene using three unsaturated lipids (DMoPC, DOPC, and DEruPC). The error bars indicate standard deviations of triplicate analyses. For duplicate analyses, average values were used.

Table 4.3: Enthalpies (ΔH) and entropies (ΔS) for fullerene partitioning between water and selected zwitterion unsaturated lipids.

		Δ H (KJ/mol)	TΔ S* (KJ/mol)	r^2
$K_{lipw,DMoPC}$		35.07 (±6.14)**	57.51 (±5.67)	0.92
$K_{lipw,DOPC}$		42.40 (±6.26)	66.26 (±5.78)	0.94
$K_{lipw, DeruPC}$	$T < T_m$	22.67 (-)	46.28 (-)	-
	$T > T_m$	62.01 (±13.28)	87.53 (±12.04)	0.96

*. Entropy contribution (T ΔS) calculated at 25 ˚C

**. Values in parentheses are standard deviations of the regression

Partitioning thermodynamic values previously reported for molecular chemicals were significantly different from the results of this study. For endocrine disrupting chemicals and pharmaceuticals, partitioning has been driven by the enthalpy change of the liquid crystalline phase (Ávila and Martínez 2003, Go and Ngiam 1997, Kwon et al. 2007, Seelig and Ganz 1991, Wenk et al. 1996). As shown in Figure 4.8, the partitioning process of selected EDCs and pharmaceuticals into the unsaturated lipids was exothermic ($\Delta H < 0$), whereas in most cases partitioning into the saturated lipids was endothermic ($\Delta H > 0$). These differences between unsaturated and saturated lipids were attributed to the additional energy required for the chemicals to partition into the dense tail structures of saturated lipids. Both enthalpy and entropy contributions in fullerene partitioning into unsaturated lipids were higher than the reported values for the molecular chemicals– even when the values were similar to those for the saturated lipids (Figure 4.8). These results imply that the partitioning process of fullerene differs from that of molecular chemicals.

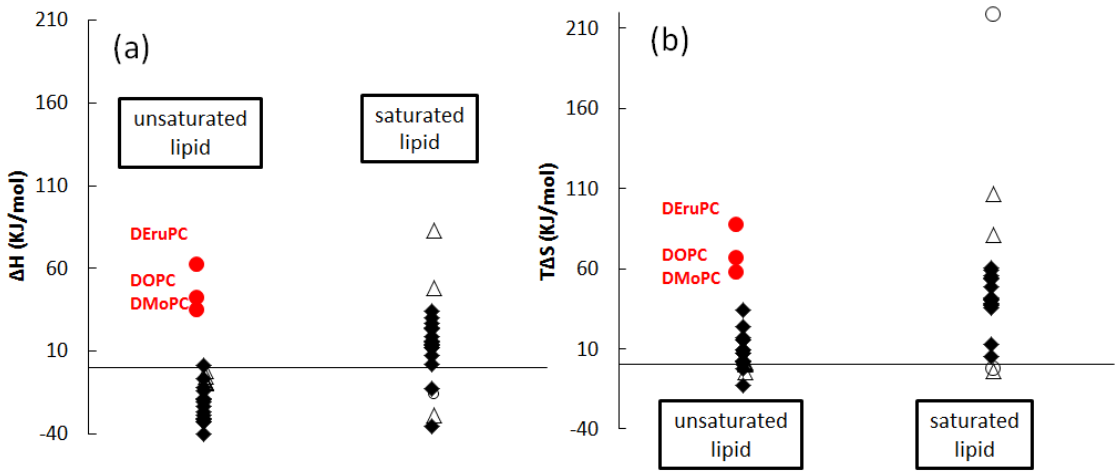

Figure 4.8: (a) Enthalpy (ΔH) and (b) entropy (ΔS) contributions of molecular level chemicals and fullerene. Closed diamond (♦), open triangle(△), open circle(○), red closed circle (●)are partitioning thermodynamics values of EDCs (Kwon et al. 2007), Pharmaceuticals (Go and Ngiam 1997, Seelig and Ganz 1991, Wenk et al. 1996), Benzocaine (Ávila and Martínez 2003), and fullerene (this study), respectively. Enthalpy contribution calculated at 25 ˚C

It is generally acknowledged that highly and moderately hydrophobic chemicals enter the hydrophobic tail region or center of the lipid bilayer. However, for nanoparticles, we hypothesize that the partitioning mechanism is a combination of adsorption and absorption: Large fullerene aggregates adsorb onto the head group of lipid membranes, and the fullerene aggregates partially disaggregate into small aggregates or molecular level fullerene which can then penetrate into lipid membranes (i.e., absorption) (Figure 4.9). TEM images of the interaction of solid supported lipid membranes (SSLMs) and fullerene suspensions (Figure 4.4) clearly show fullerene aggregates adsorbed onto the head groups of lipid membranes. In addition, previous molecular modeling studies (Bedrov et al. 2008, Qiao et al. 2007) simulated that pristine fullerene can easily diffuse into lipid bilayers and translocate the membrane within a few seconds. Wong-Ekkbut *et al.* (Wong-Ekkabut et al. 2008) reported that fullerene aggregates located close to the

lipid head group can form only small clusters and rapidly penetrate into the lipid bilayer. Also, Ikeda *et al.* (Ikeda et al. 2011) used differential scanning calorimetry (DSC) and ^{13}C NMR to confirm that the location of fullerene in the liposome is the hydrophobic core of the lipid membrane. These results suggest the absorption is a possible mechanism of fullerene partitioning into lipid membranes. Thus, the total Gibbs free energy change ($\Delta G_{partitioning}$) of lipid-water partitioning of fullerene can be determined from its components as shown below:

$$\Delta G_{partitioning} = \Delta G_{adsorption} + \Delta G_{adsorption} \qquad (4\text{-}3)$$

As illustrated in Figure 4.9, enthalpy and entropy changes depend on the operative partitioning processes. It is suggested that exothermic binding ($\Delta H < 0$) initially occurs between negatively charged fullerene suspensions and the N^+ terminus of lipid membranes. This binding is followed by an endothermic process ($\Delta H > 0$) which is induced by partial gelation of the lipid membrane (Wang et al. 2008). Wang *et al.* (Wang et al. 2008) suggested that the adsorption of negatively charged nanoparticles onto the lipid membrane resulted in a local gelation of the lipid membrane. This gelation can cause shrinkage of the lipid membrane surface because the surface area of the lipid membrane is dominated by the fluid phase rather than the gel phase. The shrinkage induced by adsorption is considered an endothermic process ($\Delta H > 0$). In addition, an adsorption mechanism can cause water molecules to be released from the lipid head groups. Consequently, adsorption can result in positive ΔS values (Li and Gu 2010).

When relatively large fullerene particles penetrate into lipid membranes (e.g., absorption process), the distance between highly organized lipid membranes increases. Generally, positive ΔH and positive ΔS values are attributed to the introduction of large molecules into the lipid membranes (Kwon et al. 2007). These changes in enthalpy and

entropy contributions would be greater for fullerene compared to molecular chemicals because of the larger size of fullerene nanoparticles.

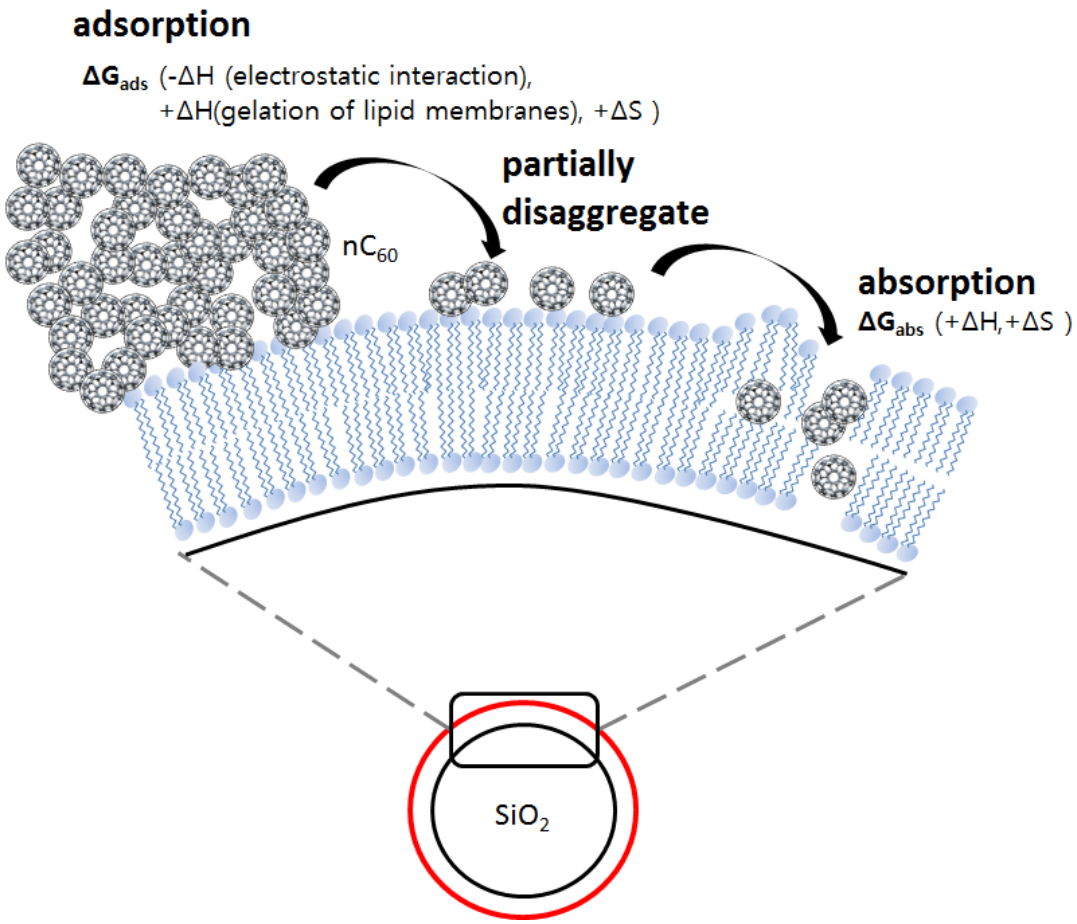

Figure 4.9: Schematic illustrating the possible partitioning mechanism of fullerene between solid supported lipid membranes (SSLMs) and water, and its thermodynamics.

Limitation of solid supported lipid membranes (SSLMs). To investigate the effect of various lipid components on the partitioning values, we tried to use saturated lipids which mostly exhibit a gel phase in the temperature range employed in this study. However, the partitioning values obtained using these saturated lipids were not reproducible, particularly in the gel phase. Previous studies (Feng et al. 2005, Tokumasu et al. 2003) have reported that for gel-phase saturated lipid membranes, SSLMs generate cracks on the surface. However, when the transition from gel to liquid crystalline phase was completed, the solid supports were covered with a thin lipid bilayer that formed a featureless and homogeneous surface. Thus, it is difficult to precisely measure K_{lipw} by applying solid supported lipid membranes using a gel phase consisting of saturated lipids which likely have defects on their surfaces. Figure 4.10 shows K_{lipw} values for fullerene using 1,2-distearoyl-sn-glycero-3-phosphocholine (DSPC, C 18:0, T_m = 55˚C) and DSPC/cholesterol mixtures at different temperatures below and above the transition temperature. DSPC exists a gel phase at 22, 30, 45, and 50 ˚C and liquid crystalline phase at 60 and 65 ˚C. On the other hand, the DSPC/cholesterol mixture is considered to be a liquid phase for all temperatures used in this study. As shown in Figure 4.10, the K_{lipw} value determined using a DSPC/cholesterol mixture increased gradually across the transition temperature. However, for DSPC only, the K_{lipw} value increased more dramatically above the transition temperature. It is possible that SSLMs have surface numerous defects below T_m, causing less fullerene attachment on the lipid membrane. However, above T_m, the SSLM surface is homogeneously covered by the lipid membrane leading to higher K_{lipw} values. Further investigations examining K_{lipw} values using gel-phase lipid membranes are warranted.

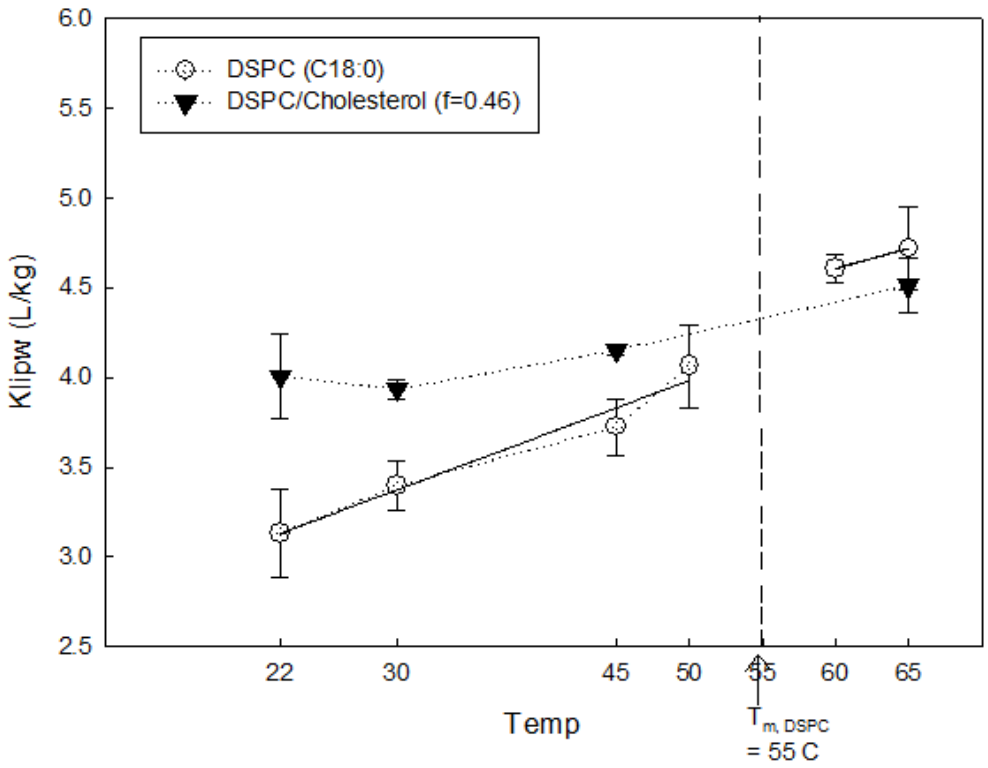

Figure 4.10: Lipid-water partition coefficients using one saturated lipids (DSPC), and DSPC/cholesterol mixture. The error bar indicates standard deviations of triplicate analyses. The transition temperature of DSPC is 55 ˚C, thus DSPC exists as gel phase at 22, 30, and 45 ˚C and liquid crystalline phase at 60 and 65 ˚C. Phase pf DSPC/cholesterol (f=0.46) is liquid ordered phase for all temperatures ranges in this figure. f denotes mole fraction of cholesterol.

4.4 ENVIRONMENTAL IMPLICATIONS

This study demonstrates that fullerene nanoparticles accumulate in unsaturated lipid membranes depending on the membrane composition (i.e. the lipid head charge and phase separation of ternary lipid membrane mixtures). Cells of living organisms mainly consist of unsaturated lipids, which have varying head charges, and raft domains have been observed in various cell membranes (Jacobson et al. 2007). Therefore, the lipid surrogates used in this study are appropriate for mimicing actual living cells. Results of this study suggest that fullerene nanoparticles in water have higher affinity for cationic lipid membranes and lipid membranes containing raft domains after phase separation. It is generally acknowledged that cationic lipid membranes play a critical role in gene delivery due to interactions between cationic head groups and anionic phosphate groups of the genes (Zhi et al. 2013). In addition, raft domain formations in ternary lipid membranes are responsible for many biological functions such as endocytosis, adhesion, signaling, and protein transport (Stottrup et al. 2005, Veatch and Keller 2003). Thus, findings from this study can be used for the further evaluation of fullerene uptake and toxicity in organisms subjected to fullerene exposure.

The partitioning process of fullerene was significantly different from that of molecular chemicals based on thermodynamic partitioning values determined in this study. It is proposed that the possible partitioning mechanisms are a combination of adsorption and absorption based on enthalpy and entropy contributions. This is the first study which presents partitioning thermodynamics via an *in vitro* method that includes both experimental and theoretical bases. The techniques used in this research with fullerene can also be used to understand the bioavailability of other engineered nanomaterials (e.g., nano-Ag, Carbon nanotubes, and TiO_2) with lipid membranes.

4.5. REFERENCES

Arnaud, C.H. (2009) Simulating Life's Envelopes. Chemical & Engineering News 87(6), 31-33.

Ávila, C.M. and Martínez, F. (2003) Thermodynamics of partitioning of benzocaine in some organic solvent/buffer and liposome systems. Chem Pharm Bull (Tokyo) 51(3), 237-240.

Baksh, M.M., Jaros, M. and Groves, J.T. (2004) Detection of molecular interactions at membrane surfaces through colloid phase transitions. Nature 427(6970), 139-141.

Bayerl, T.M. and Bloom, M. (1990) Physical properties of single phospholipid bilayers adsorbed to micro glass beads. A new vesicular model system studied by ^{2}H-nuclear magnetic resonance. Biophys J 58(2), 357-362.

BCC research (2006) Accssed on http://www.bccresearch.com/.

Bedrov, D., Smith, G.D., Davande, H. and Li, L. (2008) Passive transport of C_{60} fullerenes through a lipid membrane: a molecular dynamics simulation study. J Phys Chem B 112(7), 2078-2084.

Benn, T.M., Westerhoff, P. and Herckes, P. (2011) Detection of fullerenes (C_{60} and C_{70}) in commercial cosmetics. Environ Pollut 159(5), 1334-1342.

Brant, J.A., Labille, J., Bottero, J.Y. and Wiesner, M.R. (2006) Characterizing the impact of preparation method on fullerene cluster structure and chemistry. Langmuir 22(8), 3878-3885.

Brown, D.A. and London, E. (2000) Structure and function of sphingolipid- and cholesterol-rich membrane rafts. J Biol Chem 275(23), 17221-17224.

Chiantia, S., Ries, J., Kahya, N. and Schwille, P. (2006) Combined AFM and two-focus SFCS study of raft-exhibiting model membranes. Chemphyschem 7(11), 2409-2418.

Cho, E.C., Xie, J., Wurm, P.A. and Xia, Y. (2009) Understanding the role of surface charges in cellular adsorption versus internalization by selectively removing gold nanoparticles on the cell surface with a I_2/KI etchant. Nano Lett 9(3), 1080-1084.

Dietrich, C., Bagatolli, L.A., Volovyk, Z.N., Thompson, N.L., Levi, M., Jacobson, K. and Gratton, E. (2001) Lipid rafts reconstituted in model membranes. Biophys J 80(3), 1417-1428.

Escher, B.I., Schwarzenbach, R.P. and Westall, J.C. (2000) Evaluation of liposome-water partitioning of organic acids and bases. 1. Development of a sorption model. Environ Sci Technol 34(18), 3954-3961.

Feng, Z.V., Spurlin, T.A. and Gewirth, A.A. (2005) Direct visualization of asymmetric behavior in supported lipid bilayers at the gel-fluid phase transition. Biophys J 88(3), 2154-2164.

Garcia-Saez, A.J., Chiantia, S. and Schwille, P. (2007) Effect of line tension on the lateral organization of lipid membranes. J Biol Chem 282(46), 33537-33544.

Ghinea, N. and Simionescu, N. (1985) Anionized and cationized hemeundecapeptides as probes for cell surface charge and permeability studies: differentiated labeling of endothelial plasmalemmal vesicles. J Cell Biol 100(2), 606-612.

Go, M.L. and Ngiam, T.L. (1997) Thermodynamics of partitioning of the antimalarial drug mefloquine in phospholipid bilayers and bulk solvents. Chem Pharm Bull (Tokyo) 45(12), 2055-2060.

Ha, Y., Liljestrand, H.M. and Katz, L.E. (2013) Effects of lipid composition on partitioning of fullerene between water and lipid membranes. Water Sci Technol 68(2), 290-295.

Hofsass, C., Lindahl, E. and Edholm, O. (2003) Molecular dynamics simulations of phospholipid bilayers with cholesterol. Biophys J 84(4), 2192-2206.

Hou, W.C., Moghadam, B.Y., Corredor, C., Westerhoff, P. and Posner, J.D. (2012) Distribution of functionalized gold nanoparticles between water and lipid bilayers as model cell membranes. Environ Sci Technol 46(3), 1869-1876.

Hou, W.C., Moghadam, B.Y., Westerhoff, P. and Posner, J.D. (2011) Distribution of fullerene nanomaterials between water and model biological membranes. Langmuir 27(19), 11899-11905.

Hughes, G.A. (2005) Nanostructure-mediated drug delivery. Nanomedicine 1(1), 22-30.

Ikeda, A., Kiguchi, K., Shigematsu, T., Nobusawa, K., Kikuchi, J. and Akiyama, M. (2011) Location of [60]fullerene incorporation in lipid membranes. Chem Commun (Camb) 47(44), 12095-12097.

Jacobson, K., Mouritsen, O.G. and Anderson, R.G. (2007) Lipid rafts: at a crossroad between cell biology and physics. Nat Cell Biol 9(1), 7-14.

Jonker, M.T. and Van der Heijden, S.A. (2007) Bioconcentration factor hydrophobicity cutoff: an artificial phenomenon reconstructed. Environ Sci Technol 41(21), 7363-7369.

Kaiser, S.M. and Escher, B.I. (2006) The evaluation of liposome-water partitioning of 8-hydroxyquinolines and their copper complexes. Environ Sci Technol 40(6), 1784-1791.

Kuzmin, P.I., Akimov, S.A., Chizmadzhev, Y.A., Zimmerberg, J. and Cohen, F.S. (2005) Line tension and interaction energies of membrane rafts calculated from lipid splay and tilt. Biophys J 88(2), 1120-1133.

Kwon, J.H., Liljestrand, H.M. and Katz, L.E. (2006) Partitioning of moderately hydrophobic endocrine disruptors between water and synthetic membrane vesicles. Environ Toxicol Chem 25(8), 1984-1992.

Kwon, J.H., Liljestrand, H.M., Katz, L.E. and Yamamoto, H. (2007) Partitioning thermodynamics of selected endocrine disruptors between water and synthetic membrane vesicles: effects of membrane compositions. Environ Sci Technol 41(11), 4011-4018.

Li, Y. and Gu, N. (2010) Thermodynamics of charged nanoparticle adsorption on charge-neutral membranes: a simulation study. J Phys Chem B 114(8), 2749-2754.

McMahon, D.P., Cheung, D.L. and Troisi, A. (2011) Why holes and electrons separate so Well in polymer/fullerene photovoltaic cells. Journal of Physical Chemistry Letters 2(21), 2737-2741.

Qiao, R., Roberts, A.P., Mount, A.S., Klaine, S.J. and Ke, P.C. (2007) Translocation of C_{60} and its derivatives across a lipid bilayer. Nano Lett 7(3), 614-619.

Ryhanen, S.J., Saily, V.M. and Kinnunen, P.K. (2006) Cationic lipid membranes-specific interactions with counter-ions. J Phys Condens Matter 18(28), S1139-1150.

Santhosh, P.B., Velikonja, A., Perutkova, S., Gongadze, E., Kulkarni, M., Genova, J., Elersic, K., Iglic, A., Kralj-Iglic, V. and Ulrih, N.P. (2014) Influence of nanoparticle-membrane electrostatic interactions on membrane fluidity and bending elasticity. Chem Phys Lipids 178, 52-62.

Seelig, J. and Ganz, P. (1991) Nonclassical hydrophobic effect in membrane binding equilibria. Biochemistry 30(38), 9354-9359.

Stottrup, B.L., Stevens, D.S. and Keller, S.L. (2005) Miscibility of ternary mixtures of phospholipids and cholesterol in monolayers, and application to bilayer systems. Biophys J 88(1), 269-276.

Tokumasu, F., Jin, A.J., Feigenson, G.W. and Dvorak, J.A. (2003) Atomic force microscopy of nanometric liposome adsorption and nanoscopic membrane domain formation. Ultramicroscopy 97(1-4), 217-227.

Veatch, S.L. and Keller, S.L. (2003) Separation of liquid phases in giant vesicles of ternary mixtures of phospholipids and cholesterol. Biophys J 85(5), 3074-3083.

Verma, A. and Stellacci, F. (2010) Effect of surface properties on nanoparticle-cell interactions. Small 6(1), 12-21.

Wang, B., Zhang, L., Bae, S.C. and Granick, S. (2008) Nanoparticle-induced surface reconstruction of phospholipid membranes. Proc Natl Acad Sci U S A 105(47), 18171-18175.

Wang, H.B., DeSousa, R., Gasa, J., Tasaki, K., Stucky, G., Jousselme, B. and Wudl, F. (2007) Fabrication of new fullerene composite membranes and their application in

proton exchange membrane fuel cells. Journal of Membrane Science 289(1-2), 277-283.

Wenk, M.R., Fahr, A., Reszka, R. and Seelig, J. (1996) Paclitaxel partitioning into lipid bilayers. Journal of Pharmaceutical Sciences 85(2), 228-231.

Wong-Ekkabut, J., Baoukina, S., Triampo, W., Tang, I.M., Tieleman, D.P. and Monticelli, L. (2008) Computer simulation study of fullerene translocation through lipid membranes. Nat Nanotechnol 3(6), 363-368.

Yamamoto, H. and Liljestrand, H.M. (2004) Partitioning of selected estrogenic compounds between synthetic membrane vesicles and water: effects of lipid components. Environ Sci Technol 38(4), 1139-1147.

Zhi, D., Zhang, S., Cui, S., Zhao, Y., Wang, Y. and Zhao, D. (2013) The headgroup evolution of cationic lipids for gene delivery. Bioconjug Chem 24(4), 487-519.

Chapter 5: Cellular uptake of fullerene nanoparticles: Elucidating the mechanism of cellular uptake

ABSTRACT

The degree of interaction of engineered nanoparticles with biological cells plays a key role in determining their possible harmful effects towards humans and the environment. In this study, we successfully developed a quantitative method to investigate the cellular uptake mechanism of carbon fullerene nanoparticles using Caco-2 cell lines. Data from uptake studies demonstrated that the mass of fullerene taken up by cells at 37 °C was significantly higher than at 4 °C, which is an energy depleted condition. Cellular uptake of fullerene increased with increasing temperature which indicates that passive diffusion is one of transport mechanisms. In addition, cellular uptake efficiency was higher at lower fullerene concentrations and did not change significantly over a wide range of initial concentrations, indicating that fullerene uptake reached a plateau and the lipid membrane was likely saturated. The temperature dependence and membrane saturability suggest that the main transport mechanism of fullerene through cell membranes is a combination of passive diffusion and energy dependent endocytosis. Metabolic inhibitors decreased the amount of fullerene taken up by cells, which suggests active transport of fullerene across the lipid cell membrane. The results of this study support the hypothesis that fullerene transport occurs through microtubules and this microtubule transport can be affected by changes in fullerene characteristics over time. The implication of these results is that simple partitioning models may be inappropriate for describing fullerene uptake in cells. Instead, models associated with active transport can be used to estimate cellular uptake of fullerene as well as to control and reduce fullerene toxicity toward living organisms.

Keywords

fullerene, cellular uptake, endocytosis

5.1. INTRODUCTION

As production of engineered nanoparticles (ENPs) rapidly increases due to the expanding range of applications, concerns associated with unknown harmful effects of ENPs towards humans and the environment have grown. One of the promising applications of ENPs is in the biomedical field where applications include drug carriers (Singh and Lillard 2009), gene delivery (Panyam and Labhasetwar 2003), and biomolecular sensors (Saha et al. 2012). In these applications and others, ENPs frequently encounter cells in various organisms, including humans. It has been reported that, due to their small size, nanoparticles easily enter cells (Shang et al. 2014, Wang et al. 2009) where they responsible for possible toxic effects. Thus, investigating cellular uptake of ENPs is of critical importance in order to understand the biological fate of nanoparticles as well as their possible harmful effects.

Cell membranes, which serve as biological barriers to target sites within cells, control the extent of cellular uptake of ENPs. Recently, the mechanism of cellular uptake of ENPs has been reported to differ from that of molecular level chemicals. It is generally acknowledged that small hydrophobic molecules can transport through the cell membrane via passive diffusion driven by concentration gradients (Camenisch et al. 1998, Pade and Stavchansky 1997). However, recent studies have suggested that ENPs such as gold nanoparticles (Chithrani and Chan 2007), silica nanoparticles (Rancan et al. 2012), and carbon nanotubes (Jin et al. 2008) enter the cells through energy dependent active processes.

Carbon fullerene (C_{60}) has emerged at the forefront of ENP production and application, and a number of previous studies have reported that fullerene dispersions exhibit toxicity toward human cell lines (Sayes et al. 2005), bacteria (Cho et al. 2009b, Lyon et al. 2006), and aquatic organisms (Lovern and Klaper 2006). The mechanisms of fullerene toxicity toward living organisms is still under debate and little is known about cellular uptake of fullerene due to the difficulties associated with quantitative measurement of fullerene nanoparticles taken up by cells. Previous studies examining cellular uptake of fullerene have used visualization techniques (e.g., transmission electron microscopy) to locate fullerene or water soluble fullerene derivatives inside cells (Foley et al. 2002, Porter et al. 2007, Porter et al. 2006, Rouse et al. 2006). A few studies have used radioactively or fluorescently labeled fullerene nanoparticles to easily quantify the fullerene particles from bio-matrices (Cagle et al. 1999, Gulson and Wong 2006). However, these labeled nanoparticles may have different characteristics compared to the bare fullerene dispersions in water, which may affect cellular uptake and toxicity of fullerene nanoparticles (Pycke et al., 2011). To our knowledge, only one qualitative study has shown that fullerene derivatives can translocate into the cell via active transport (Li et al. 2008). However, Li et al. (Li et al.2008) used synthesized fullerene derivatives, specifically the malonic acid derivative of fullerene ($C_{60}(C(COOH)_2)_3$), which may have different biological impacts than bare fullerene dispersions in water (Li et al. 2008). Thus, it is imperative to develop a quantitative method to directly evaluate the cellular uptake mechanism of fullerene.

In this study, the Caco-2 cell line was selected to describe cellular uptake of fullerene. The Caco-2 cell line is derived from a human colorectal adenocarcinoma and exhibits morphological and functional similarities to the small intestinal epithelium (Pade and Stavchansky 1997). Caco-2 cell monolayers have been successfully used to

determine the membrane permeability of drugs and molecular chemicals. In addition, unlike other *in vitro* models such as the parallel artificial membrane permeation assay (PAMPA) which can account for only passive transport of chemicals, Caco-2 cells can exhibit active transport as well as passive diffusion. Indeed, many previous studies characterized transport mechanisms through Caco-2 cell lines based on general features of passive and carrier-mediated transport (Buesen et al. 2003, Hidalgo and Borchardt 1990, Sugano et al. 2010, Vasiluk et al. 2007). In addition, previous pharmaceutical studies suggested that the primary membrane transport mechanism of nanosize particles is energy dependent endocytosis using Caco-2 cells (Ma and Lim 2003, Mao et al. 2005, Win and Feng 2005). Therefore, the *in vitro* model using Caco-2 cells can be a relevant model for determining the mechanism of cellular uptake of fullerene.

Here, we developed a quantitative *in vitro* method for cellular uptake of fullerene by applying a modified liquid-extraction method used with bio-matrices (Petersen and Henry 2012, Pycke et al. 2011, Xia et al. 2006b). The goal of the research was to use this method to identify the primary cellular uptake mechanism of fullerene from general features associated with different transport mechanisms such as temperature and concentration dependence. In addition, the mechanism was evaluated by employing metabolic inhibitors that eliminate active transport mechanisms.

5.2. MATERIALS AND METHODS

Preparation of nanoparticles. Carbon fullerene (C_{60}, 99.5+ %) was obtained from SES Research (Houston, TX). Fullerene dispersions in water were prepared by the modified sonication method in Brant et al. (Brant et al. 2006), and described in detail elsewhere (Ha et al. 2013). In brief, solid fullerene was dissolved in toluene followed by

adding a large volume of deionized water. Then, the toluene was removed by 4-5 hrs of ultrasonication with air-purging leaving yellowish fullerene aggregations in water. There are two purposes of air-purging: First, all residual toluene can be removed by air-purging, and second, air-purging can prevent fullerene adsorption on the glass vial during the ultrasonication. The resultant fullerene suspension in water was filtered through a 0.8 μm membrane filter (Millipore, Billerica, MA) to remove any large aggregations. Fullerene suspensions were stored in dark at 4 °C and applied to the cellular uptake test within 2 days to prevent any changes in particle characteristics over time. For the experiment involving inhibitors, we stored the fullerene particles up to 14 days and applied employed them in the cellular uptake test weekly to investigate any possible changes of fullerene uptake mechanism over time. Particle size and zeta potential were characterized using Dynamic Light Scattering (Malvern Zetasizer Nano ZS).

Cell culture. The Caco-2 cell line was obtained from American Type Culture Collection (ATCC, VA, USA). The procedure for culturing Caco-2 cells was described elsewhere (Hidalgo and Borchardt 1990, Pade and Stavchansky 1997). In short, Caco-2 cells are maintained in flasks in Dulbecco's modified Eagle medium (D-MEN) containing 10 % fetal bovine serum (FBS), 2 % nonessential amino acids, and 1 % L-glutamine and penicillin in an atmosphere of 5 % CO_2. The cells were transferred to tissue culture flasks and cell monolayers were incubated with trypsin and EDTA solution. Cells underwent at least two passages before being seeded on cellular uptake plates.

Cellular uptake studies. For cellular uptake studies, Caco-2 cells were washed with phosphate buffer solution (PBS) three times to remove metal ions and then trypsinized with trypsin and an EDTA solution. The cells were transferred into 6 polycarbonate plates (Corning Inc., Corning, NY) at a seeding density of 10^5 cells/cm^2, incubated for two days in an atmosphere of 5 % CO_2 at 37 °C. To perform uptake tests

under a fetal bovine serum (FBS) free condition, the cell culture medium was changed to a medium without FBS on the second day of incubation. After two days of incubation, the cell culture medium was changed to one made by diluting a 2 mL fullerene suspension 10 fold with cell culture medium without FBS. The solution was incubated for up to 24 hrs. Each experiment was terminated by washing cells with PBS to remove excess particles which had not interacted with the cells. Then, the cells were detached from the plates with 400 μL trypsin-EDTA solution, transferred into vials, and lysed under 30 min of ultrasonication. Fullerene was extracted from lysed cells in trypsin to 1 mL toluene via liquid extraction using 400 μL 0.1 $Mg(ClO_4)_2$ and 2.5 mL glacier acetic acid (GAA). Fullerene concentrations in toluene were analyzed using a Waters 2690 high-performance liquid chromatography system equipped with a Waters 996 photodiode array detector (Milford, MA, USA).

For experiments at 4 °C, preincubation of cells and fullerene in cell culture medium was conducted at 4 °C for at least 30 min, followed by injection of nanoparticle dispersions. To specify the cellular uptake mechanism of fullerene, cells were preincubated with the metabolic inhibitors, sodium azide and 2,4-dinitrophenol, and a microtubule transport inhibitor, nocodazole, for 20 min prior to the the trypan blue exclusion method (Strober 2001) and more than 95 % of the total cells were still alive 24 hrs after addition of the inhibitors. The applied concentration of each inhibitor and cell viability after 24 hrs of inhibitor injections are summarized in Table 5.1. After 20 min pre incubation with 2 mL of cell culture medium containing each inhibitor, 200 μl of fullerene suspensions in water were injected.

Table 5.1: Applied concentrations of inhibitors and cell viability after 24 hrs of injecting each inhibitor.

inhibitors	Sodium azide	2,4 dinitrophenol	nocodazole
Conc.	1.2 mM	0.17 mM	6.35 μM
Cell viability after 24hrs (%)	95.5	98.4	96.0

Determination of recovery ratio of fullerene after liquid extraction. Due to the difficulties associated with quantitative measurements of fullerene nanoparticles within bio-matrices, previous studies have only evaluated the cellular uptake of fullerene using qualitative methods such as TEM and confocal microscopy. Here, we carefully performed liquid extraction of fullerene nanoparticles from different bio-matrices (e.g., cell culture medium and trypsinized cells after cell lysis), and calculated the recovery ratio for each solution. To determine the recovery ratio of fullerene after liquid-extraction, four different concentrations of fullerene suspensions were prepared with different dilution factors. Then, we injected each fullerene suspension into the cell culture medium without fetal bovine serum. Also, different concentrations of fullerene were injected into the trypsinized cells after cell lysis. Cell lysis was performed with 30 min of sonication. For liquid extraction of fullerene from bio-matrices, 0.1 M $Mg(ClO_4)_2$, Glacier Acetic Acid (GAA), and toluene were added, followed by intensive mixing. We stored each sample after liquid extraction at -20 °C overnight to reduce emulsion formation after liquid extraction. Then, fullerene solutions in toluene were carefully transferred and concentrations were measured by HPLC.

As shown in Figure 5.1, fullerene concentrations extracted from each bio-matrix increased linearly with increasing injected fullerene concentrations. The mean liquid

extraction recovery ratios from cell culture media that were exposed to Caco-2 cells and trypsinized Caco-2 cells were 61 % and 32 %, respectively. These recovery ratios were applied to all experimental results in this chapter.

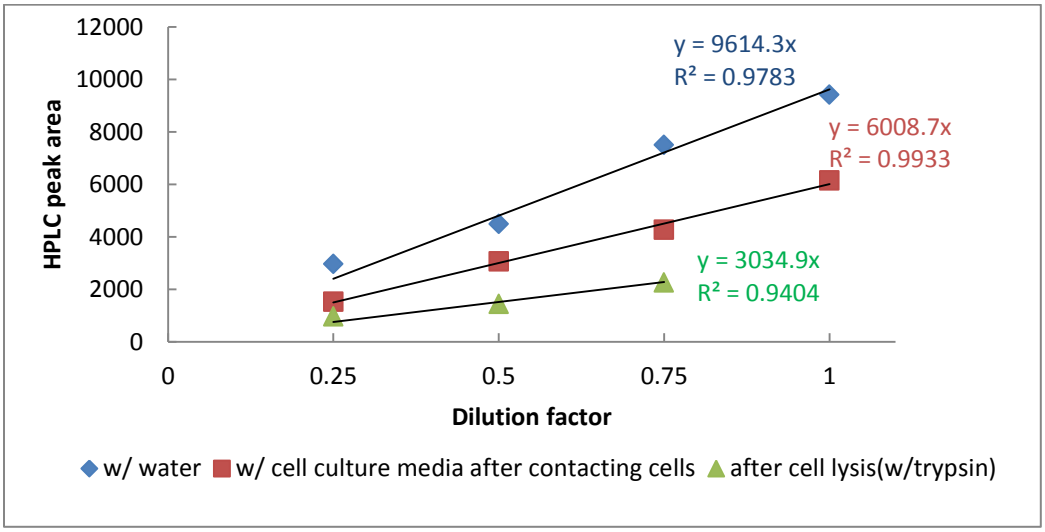

Figure 5.1: HPLC peak areas for fullerene concentration after liquid extraction from fullerene dispersion in water (blue diamond), with cell culture media after contacting cells (red square), and fullerene in trypsin after cell lysis (green triangle) with different dilution factors.

Transmission electron microscopy (TEM). To visualize fullerene nanoparticles internalized into the cells, transmission electron microscopy (TEM) was conducted on control Caco-2 cells and cells incubated with fullerene suspensions. Cells were trypsinized and transferred, and fixed with glutaraldehyde and paraformaldehyde. After one day, cells were washed with saline buffer and fixed with reduced osmium for 2-4 hrs in ice, dehydrated in an alcohol series, then embedded into epoxy resin, and sliced. Images of the cells were taken by FEI Tecnai TEM (Hillsboro, Oregon).

5.3. RESULTS AND DISCUSSION

Developing a quantitative method to assess fullerene cellular uptake. The rate of cellular uptake of fullerene was investigated to determine whether the extent of partitioning was a rate-limited process. We prepared two different cell culture media: one containing 10 % fetal bovine serum (FBS), and the other without FBS. Caco-2 cells were incubated with fullerene suspensions (C_0 = 0.8 mg/L) with and without FBS for up to 24 hrs at 37 °C. After incubation, fullerene particles in medium were carefully transferred and extracted for concentration measurement. As shown in Figure 5.2(a), fullerene concentrations in the medium containing FBS did not decrease until after 24 hrs. However, fullerene concentrations in FBS free medium decreased continuously and reached a steady state value within 12 hrs. Results presented in Figure 5.2(a) suggest that protein adsorption onto fullerene particles in the presence of FBS can reduce the efficiency of cellular uptake compared to bare fullerene suspensions in serum free conditions.

For all other experiments in this study, we studied uptake of fullerene suspensions in cell culture medium without FBS present. Figure 5.2(b) shows that the mass of fullerene taken up by the cells increased over time and reached equilibrium within 12 hrs A 24 hr equilibration period was selected as an appropriate fullerene incubation time with Caco-2 cells.

(a)

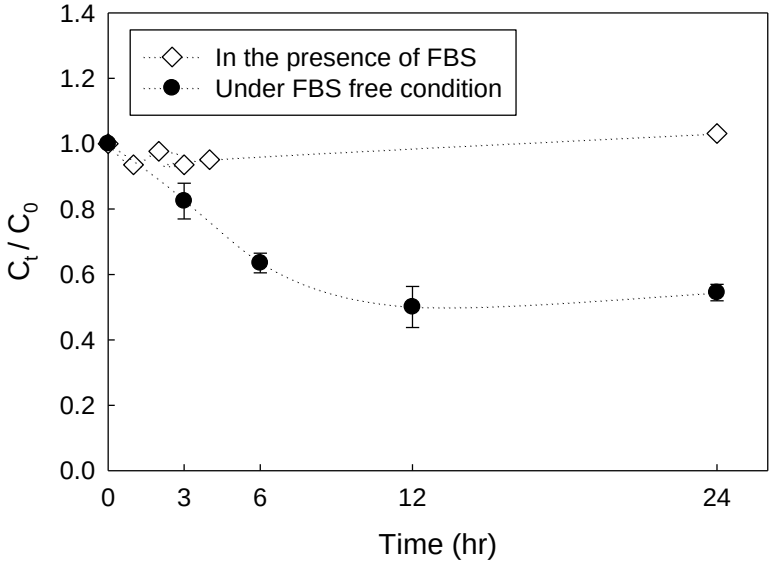

(b)

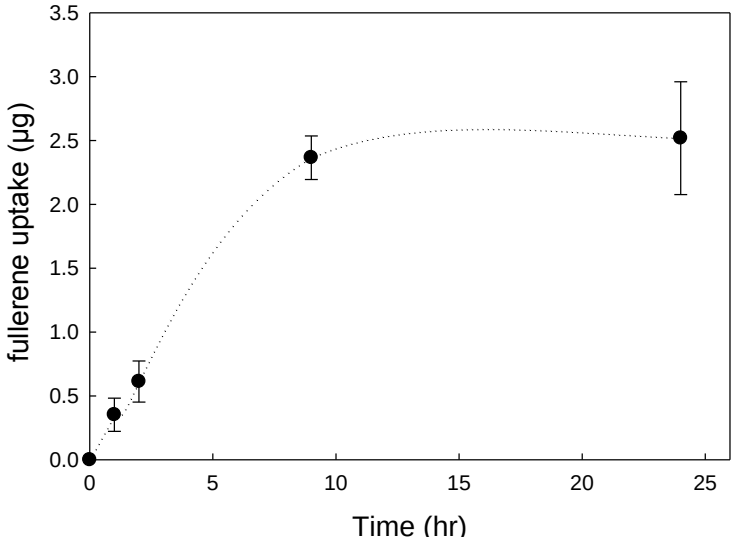

Figure 5.2: (a) Kinetics of fullerene nanoparticle (C_0 = 0.8 mg/L) removal in cell culture media in the presence of fetal bovine serum (FBS) and in FBS free media. (b) Kinetics of cellular uptake of fullerene nanoparticles (C_0 = 4.1 mg/L; Initial mass = 8.2 µg)

Triplicate experiments examining uptake in FBS free medium showed reasonably reproducible results (Figure 5.3) when the extraction efficiency of 61 percent was applied to the cell culture medium (after cell contact) and 32 percent from the cell lysis solution containing trypsin. While the majority of the fullerene was located within the cells, fullerene also remained in the cell culture medium and some fullerene was recovered from the PBS solution used to wash the cells. Total mass recovered from each reactor was calculated using equation (5-1).

$$total\,mass = \frac{mass\ from trypsinized\ cells}{0.32} + \frac{mass\ from cell\ culture medium}{0.61} + mass from PBS \quad (5\text{-}1)$$

As shown in Figure 5-3, the estimated total mass recovered from each reactor reached 74-98 %.

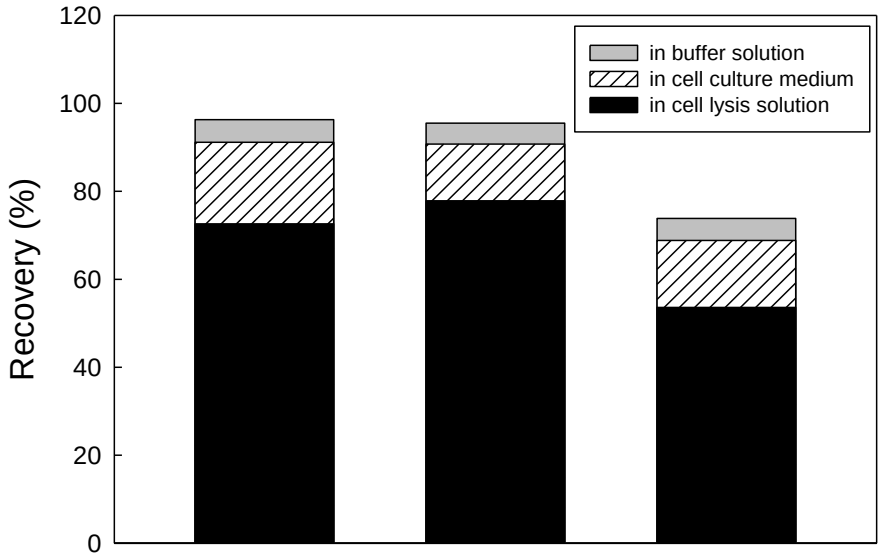

Figure 5.3: Mass of fullerene nanoparticles recovered from triplicate independent cellular uptake experiments. Gray bars show fullerene in saline phosphate buffer, white bars indicate fullerene remaining in the cell culture medium, and black bars represent fullerene taken up by Caco-2 cells. Initial fullerene concentration was 7.8 mg/L.

Temperature dependence on cellular uptake. Figure 5.4 shows the effect of temperature on fullerene uptake by Caco-2 cells. Cell viability was confirmed at 4 °C using the trypsin blue method, and more than 95 % of the cells were living after 4 hrs of incubation. As shown in Figure 5.4(a), cellular uptake at 37 °C is significantly higher than at 4 °C at each incubation time. Decreasing the temperature from 37 °C to 4 °C reduced cellular uptake of fullerene between 38-54 %. Temperature dependence on cellular uptake is consistent with studies conducted with other nanomaterials such as gold nanoparticles (Chithrani and Chan 2007), polymeric nanoparticles (Ma and Lim 2003), and chitosan-insulin nanocomplexes (Mao et al. 2005).

Figure 5.4(b) illustrates the possible cellular uptake mechanism of fullerene at two different temperatures. We postulate two steps associated with cellular uptake of fullerene: 1) physical adhesion on the cell surfaces, and 2) an internalization process such as passive diffusion into the cell membrane or energy dependent endocytosis. At 37 °C, fullerene first adheres on the cell surface due to electrostatic interactions. Because both the surface charge of the fullerene nanoparticles in water and the surface charge of the cells are negative, there is at best weak affinity between the particles and cell surface. However, a previous study (Cho et al. 2009a) suggested that SK-BR-3 Breast cancer cell surfaces have regions containing positively charged sites which allow negative particles to adhere to the cell surface. Once fullerene particles attach to the cell surfaces, they can translocate through lipid membranes by diffusion or internalization via endocytotic active transport. At 4 °C, the cells are expected to become energy-depleted; only adhesion and diffusion processes will be operative under these conditions. Therefore, the active transport mechanism of fullerene uptake may be partly responsible for the significant increase in uptake at higher temperature (diffusion processes are also faster at higher temperature). Also, our previous study (Ha et al. 2013) suggested that fullerene

association with lipid membranes increased with increasing temperatures possibly due to the thermal structural changes associated with lipid membranes. Thus, more fullerene adhesion on cell surfaces at 37 °C may be due to an increase in cellular uptake. In addition, molecular diffusion at 37 °C is higher than 4 °C, which may also contribute to differences in the rates of uptake at different temperatures.

Previous studies which considered cellular uptake of gold (Cho et al. 2009a) and iron nanoparticles (Wilhelm et al. 2002) have demonstrated that the adherence process is much slower than the internalization step, and the adsorption process is the rate-determining step that significantly affects the overall uptake rate as well as the number of nanoparticles associated with cells.

(a)

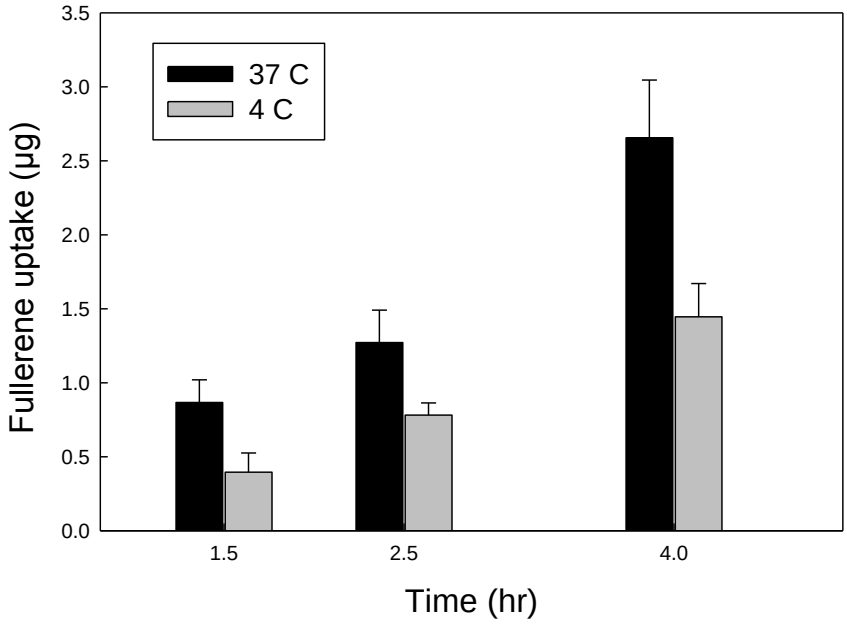

(b)

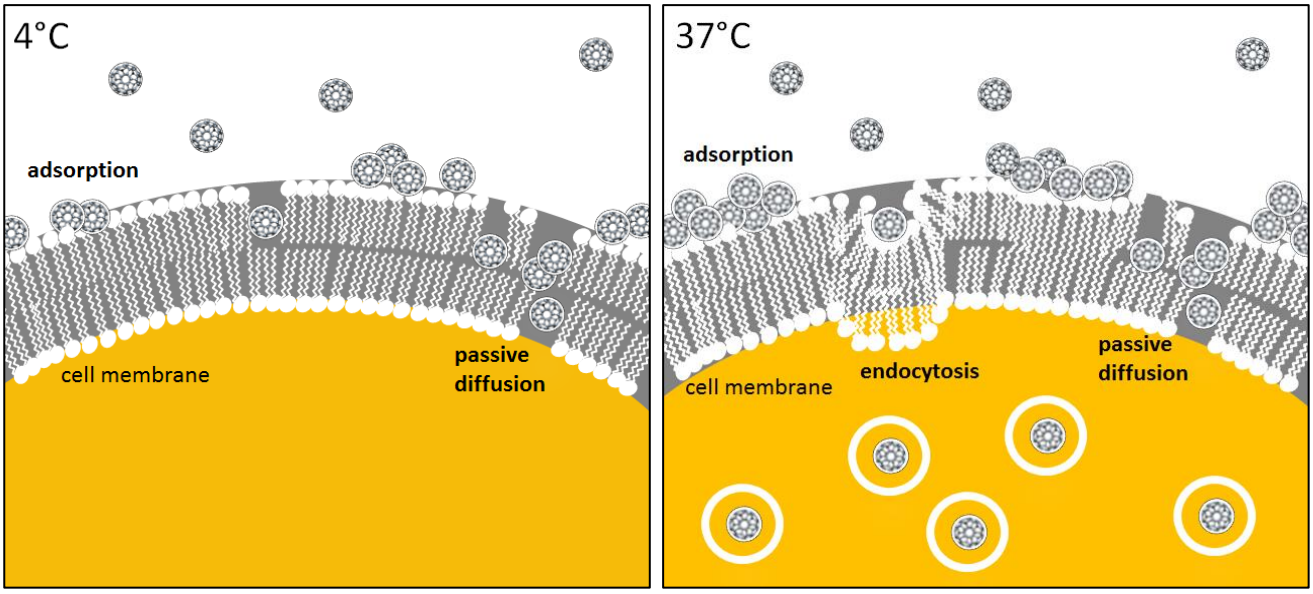

Figure 5.4: (a) Temperature dependence on the cellular uptake of fullerene nanoparticles (C_0 = 4.7 mg/L) (b) Schematic diagram of possible mechanisms of cellular uptake of fullerene at two different temperatures.

Concentration dependence on cellular uptake. To determine the effect of nanoparticle concentration on cellular uptake, two sets of fullerene suspensions were prepared at different fullerene concentrations. After preparing the fullerene suspensions using the sonication method, stock fullerene suspensions of 20 mg/L and 120 mg/L were prepared for set 1 and set 2, respectively, and different nanoparticle dilutions were prepared from each stock solutions. Each solution was then diluted 10 fold using cell culture medium, and the resultant concentration ranges were 1-2 mg/L and 3-12 mg/L for set 1 and set 2, respectively.

As shown in Figure 5.5(a), uptake increased with increasing concentration for both set 1 and set 2. This suggests that passive diffusion through the lipid membrane is at least partially responsible for the membrane transport of fullerene. However, cellular uptake efficiency was higher in the lower concentration range (set 1) compared with the higher concentration range (set 2) (Figure 5.5(b)). If the main cellular transport mechanism of fullerene is passive diffusion which depends on the concentration gradient, cellular uptake efficiency is expected to increase with increasing concentration. However, if the main mechanism is active transport, there will be a limited number of binding sites for internalization into the cells. Lower cellular uptake efficiency at higher concentration in Figure 5.5(b) indicates that cellular uptake of fullerene can be limited by the presence of saturable binding sites on the cell surfaces. The consistency of the percent uptake at high concentration is consistent with equilibrium partitioning to the surface. However, the plateau in cellular uptake at a relatively low concentration of 0.8 mg/L shown in Figure 5.5(b) suggests that there are a limited number of binding sites, and that the mechanism of uptake at low concentration results from a different uptake mechanism. Thus, this result suggests that a key transport mechanism of fullerene at low concentration is energy dependent endocytosis which has a limited number of binding

sites for active transport. At high concentration, cellular uptake efficiency did not change significantly, possibly indicating that more fullerene was adsorbed onto the lipid membrane surface with increasing concentration. Concentration dependence and saturability of cellular uptake in this study are consistent with other previous studies which concluded that uptake mechanisms of chitosan-insulin nanocomplexes (Ma and Lim 2003, Mao et al. 2005), polymer nanoparticles (Davda and Labhasetwar 2002), and oxide nanoparticles (Limbach et al. 2005) were dominated by endocytosis.

(a)

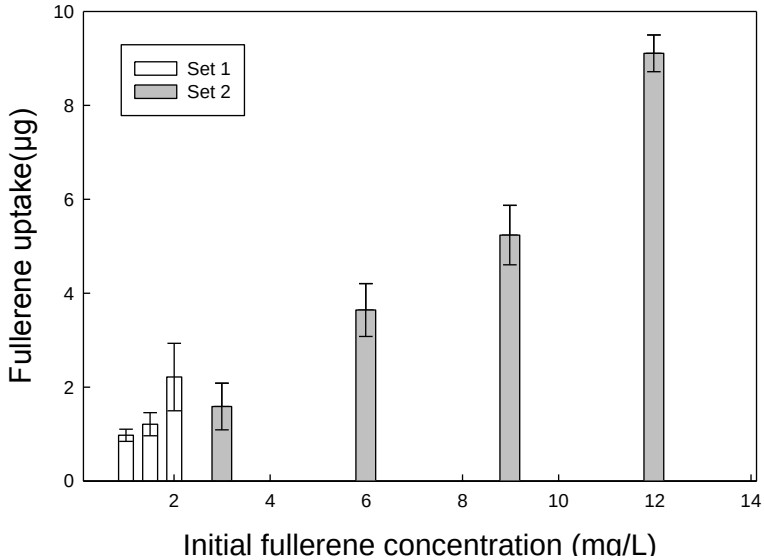

(b)

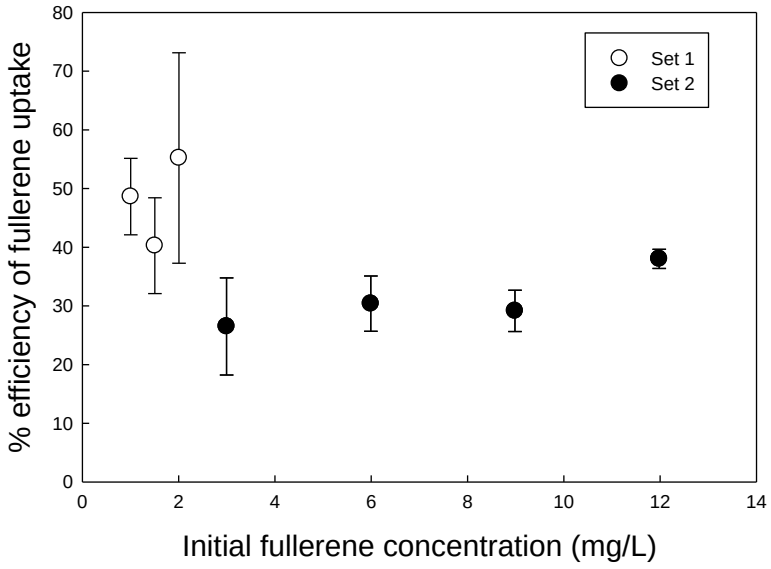

Figure 5.5: (a) The effect of concentration on the cellular uptake of fullerene nanoparticles. (b) The fullerene uptake efficiency related with initial fullerene concentration. For set 1 and set 2, 2 and 12 mg/L fullerene concentration were prepared, respectively and diluted for applying four different concentrations

Effect of inhibitors. To investigate the effect of inhibitors on cellular uptake of fullerene, three inhibitors — sodium azide, 2,4 dinitro-phenol, and nocodazole—were applied. In addition to specifying the uptake mechanism of fullerene aggregates over time with inhibitors, preliminary experiments were conducted to characterize changes in fullerene aggregations in the absence of inhibitors. Samples were examined weekly for up to 14 days and the size and zeta potential were measured to quantify potential changes in the fullerene dispersions in water over time. For every sampling event, fullerene aggregations were filtered using a 0.8 μm membrane filter to remove any large aggregates that would settle rapidly during the cellular uptake tests.

The size distribution of fullerene nanoparticles did not change significantly up to 14 days (Figure 5.6(a)), however, the zeta potential decreased continuously: Zeta potentials of initial fullerene, after 7 days, and after 14 days samples were -31.13 ± 0.58, -28.17 ± 0.58, and -19.37 ± 0.38, respectively (Figure 5.6(b)). These changes in the fullerene aggregates are consistent with previous results presented in Ma and Bouchard (Ma and Bouchard 2009) that reported variations in particle size and zeta potential of fullerene in de-ionized water over time. Fullerene aggregate surfaces are highly negatively charged. Thus, electrostatic repulsion can prevent further nanoparticle aggregation over time, which results in little change in the particle size distribution. The origin of the negative charge on the fullerene dispersions in water is still under debate. The main hypothesis for charge acquisition is adsorption of hydroxyl ions due to the donor-acceptor interaction of fullerene with water (Brant et al. 2006, Labille et al. 2009). During the 14 days of the experiment, the pH of the solution may decrease due to the dissolution of CO_2 from air. This decrease in pH leads to an increase in proton activity, which prevents the adsorption of OH- on the fullerene surface (Ma and Bouchard 2009).

This decrease in adsorption of OH- can be responsible for the zeta-potential reduction of fullerene over time.

To examine the impact of the sodium azide and 2,4 dinitro phenol inhibitors, the data from the experiments in which fullerene was incubated in distilled water and then cells and inhibitors were added either simultaneously at the start of incubation (Day 0) or after several days of fullerene/water incubation (Day 7 and Day 14) was pooled. The pooled data (see Appendix B) was analyzed to test the hypothesis that the mean value of uptake between controls (no inhibitors) and samples (with various inhibitors) were the same. The statistical analysis showed that the inhibitors significantly decreased the cellular uptake for a p value of 0.05. Thus, active transport is likely operative in these systems. However, it should be noted that the cellular uptake in these experiments (in which 2-3 mg/L of fullerene was added) was not completely reduced in these systems which is consistent with the observations in Figure 5.5 for higher concentrations. Thus, passive transport may also be operative or the inhibitors did not completely shut down active transport.

As shown Figure 5.6(c), with fullerene incubated for 7 days prior to addition of metabolic inhibitors and cells, sodium azide and 2,4 dinitro phenol, reduced fullerene uptake by the cells ($p < 0.05$), suggesting that energy dependent endocytosis is a key cellular transport mechanism of fullerene. However, when fullerene and cells and inhibitors were added simultaneously, the mean uptake was reduced in the presence of the inhibitors, but the differences were not statistically significant ($p < 0.05$). No statistically difference was observed for cellular uptake of fullerene by cells in control and fullerene samples that had been incubated for 14 days prior to cell and inhibitor additions either. While the lack of statistical significance of the impact of the inhibitors at 14 days may be due to the changes in the surface charge, no explanation other than the

relatively large standard deviation explains the lack of impact when the fullerene, cell suspension and inhibitors are added simultaneously (Day 0).

To further verify the endocytosis pathway, nocodazole, which inhibits microtubule transport, was applied. Microtubules are one of the cytoskeleton components and microtubule transport has been reported to be responsible for the cellular transport of polymer coated gold nanoparticles (Lin et al. 2012), polystyrene nanoparticles (Dausend et al. 2008, dos Santos et al. 2011) and quantum dots (Gao et al. 2008, Ruan et al. 2007, Sundara Rajan and Vu 2006). In addition, previous studies suggested that microtubule inhibition by nocodazole was affected by particle surface charge (Dausend et al. 2008, Lin et al. 2012) as well as particle size (dos Santos et al. 2011, Rejman et al. 2004). Once again, when all of the data is pooled (Day 0, Day 7 and Day 14), nocodazole, significantly decreases cellular uptake (See Appendix B). Interestingly, 7 days after the start of the incubation period as the zeta potential of the fullerene nanoparticles decreased, nocodazole inhibited fullerene transport to a greater extent compared to fullerene at the start of the incubation period. Incubation for 14 days led to significant reduction in both control and samples containing inhibitors which may be due to the reduced interaction between positively charged surface groups on the cells and the negatively charged fullerene (as described by Cho et al. (2009a) and in section 4.3 of this dissertation) rather than changes in hydrophobicity of the fullerene. Nevertheless, the nocozole had a significant impact on uptake of fullerene after 14 days of fullerene/water incubation compared to the 14 day control. Thus, it can be concluded that fullerene became more hydrophobic over time and this change may have lead to increased transport through cell membranes via the microtubule pathway which was inhibited by the nocozole. This result is consistent with results presented in Lin et al., (2012) (Lin et al. 2012) which indicated that more hydrophobic polymer coated gold nanoparticles have greater contributions

from microtubule transport to cellular uptake compared to that of hydrophilic nanoparticles.

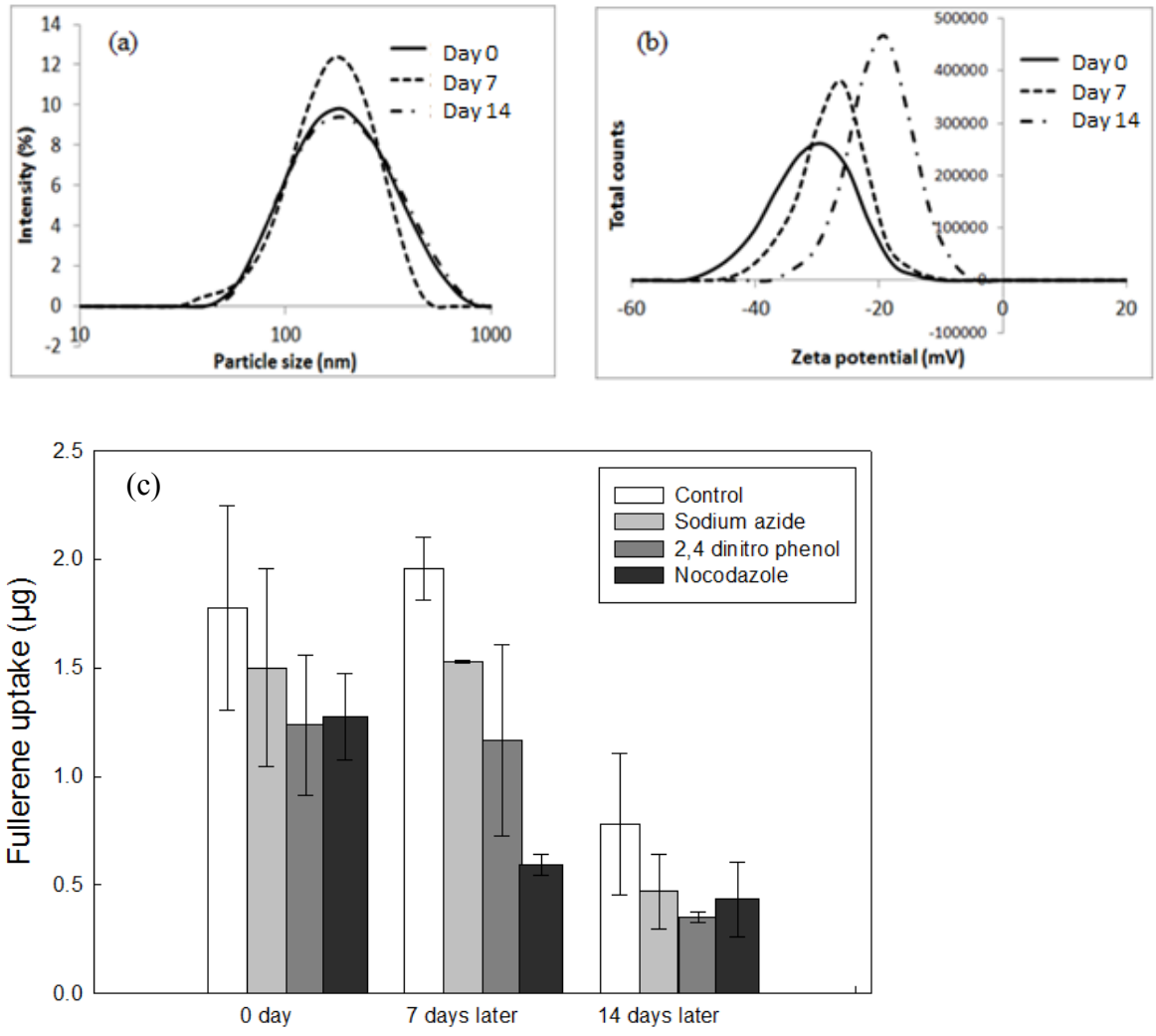

Figure 5.6: (a) Particle size and (b) zeta potential changes of fullerene nanoparticles in water as a function of incubation period. (c) Effect of inhibitors on fullerene uptake for varying fullerene incubation periods. Sodium azide and 2,4 dinitrophenol are metabolic inhibitors, and nocodazole is a microtubule inhibitor. All inhibitors and cells were added 24 hours prior to sampling on the day indicated.

TEM imaging. To locate the fullerene nanoparticles in the Caco-2 cells, TEM images were taken for control Caco-2 cells without fullerene (Figure 5.7(a)) and cells incubated for 24 hrs after fullerene injection (Figure 5.7(b)). Black dots in Caco-2 cells also found in TEM images provided by Sigma-aldrich (assess on http://www.sigmaaldrich.com/technical-documents/articles/biowire/cell-culture-collections.html). Unfortunately, because the control Caco-2 cells have small black particles along the plasma membranes as well as inside the cells (Figure 5.7(a)), it is difficult to distinguish the fullerene nanoparticles from particles that already existed inside the cells. For elemental analysis of the black spots on the control cells, we also performed TEM-EDS (insertion of Figure 5.7(a)). However, black particles in the control cells were predominantly carbon which is the main component of fullerene particles. Nonetheless, particles entrapped within vesicles (Figure 5.7(b)) were identified in Caco-2 cells incubated with fullerene. Previous studies also have shown that nanoparticles (Chithrani and Chan 2007, Wilhelm et al. 2002) can become entrapped within vesicles in the cells during the endocytosis process in which nanoparticles bind to the surface, the membrane wraps around the particles and the particles are internalized within the cells. Therefore, it appears that fullerene also can be deposited in small endocytic vesicles and fused into the cells.

(a)

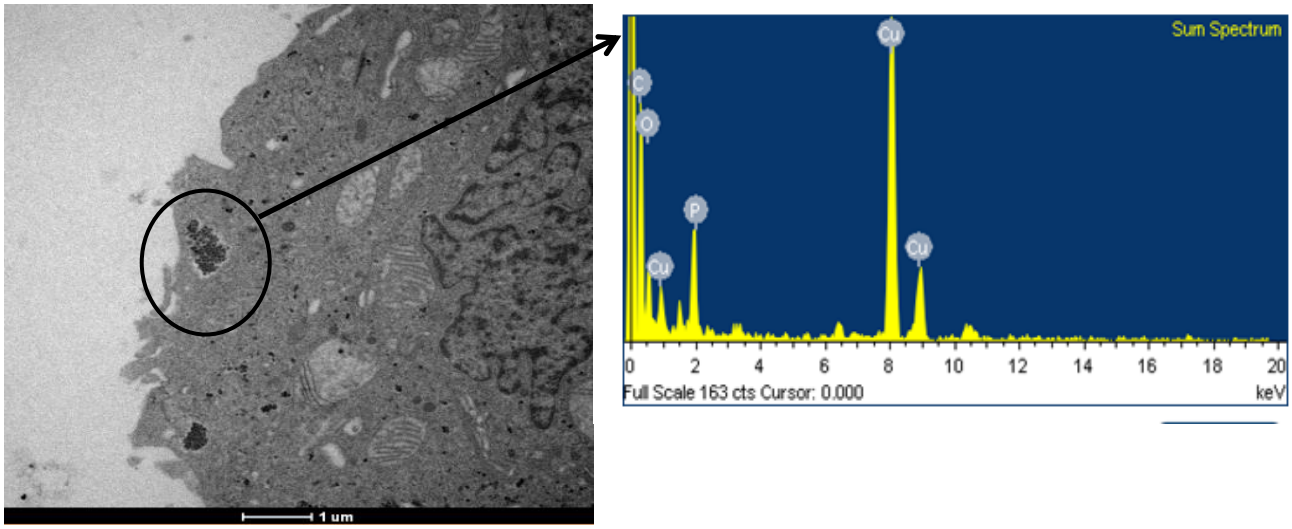

(b)

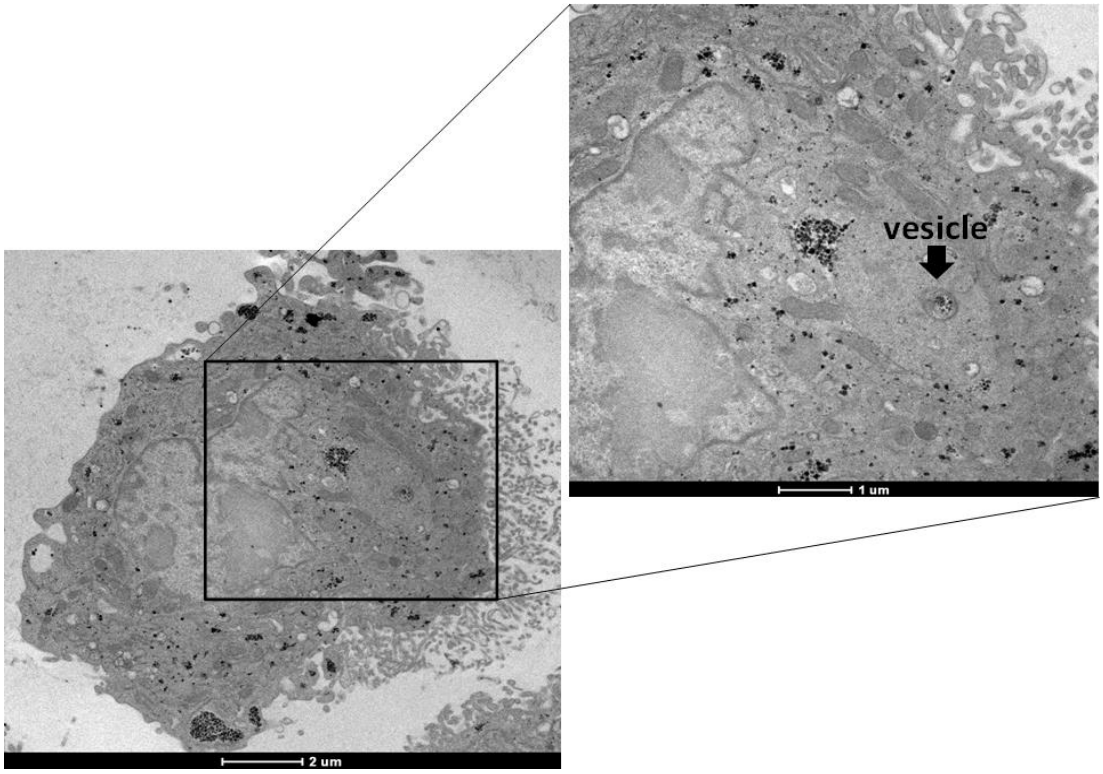

Figure 5.7: TEM images of (a) control Caco-2 cells (without fullerene injection) and (b) Caco-2 cells 24 hrs after fullerene nanoparticle injection. Insertion of Figure 5.7(a) is elemental analysis of black spots in control Caco-2 cells using TEM-EDS. Note: copper is present in the TEM grids.

5.4. ENVIRONMENTAL IMPLICATIONS

We compared the results of this study with reported values of bioconcentration of fullerene in aquatic organisms ($C_{biomass}$) (Chen et al. 2014, Oberdörster et al. 2006, Tao et al. 2009, Tervonen et al. 2010). To calculate $C_{biomass}$ of fullerene the mass of fullerene taken up by Caco-2 cells was divided by the dry Caco-2 cell biomass. With 10^5 cells/cm^2, the cell dry mass was 2.67 mg (± 0.06). The log($C_{biomass}$) of this study is 2-3.6 mg/kg which are in the ranges of the reported values of log($C_{biomass}$) with aquatic organisms (1.6-4.8 mg/kg for *Dalphnia* and 2.2-2.3 mg/kg for *Zebrafish*). However, with a similar concentration of fullerene in water, $C_{biomass}$ with real aquatic organisms is higher than $C_{biomass}$ values obtained from this study, possibly suggesting that accumulating fullerene into organs (e.g., gill, gut, and intestine) of real organisms which have different surface or volume ratio per mass can be higher than uptake into *in vitro* cell lines. Indeed, it was reported that nanoparticles such as titanium dioxide (TiO_2), silver nanoparticles, and cadmium accumulated considerably into fish gills and intestines (Farkas et al. 2011, Zhang et al. 2007). Thus, further work should be performed to estimate the bioaccumulations of fullerene in real organisms from quantitative *in vitro* studies.

In the present study, we provide information necessary to develop a quantitative model for predicting the cellular uptake of fullerene which is necessary for controlling and reducing toxicity and to improve the design of biomedical applications of this nanomaterial. In addition, this study is the first to identify the cellular transport mechanisms of fullerene based on a semi-quantitative approach. We suggest that not only passive diffusion but also energy dependent active transport contribute to the cellular transport of fullerene based on temperature dependence, concentration saturability, and uptake reduction with metabolic inhibitors. Thus, this research provides guidelines for developing experimental methods for cellular uptake of other nanoparticles

and provides the basis for future research that incorporates active transport processes into monitoring tools and environmental assessment protocols of fullerene nanoparticles. In addition, because active transport processes directly depend on cell type and function, the toxic effects of fullerene on different species and organs which have different cell membrane composition should be investigated in the future, and the results of this research provide the framework for such evaluation.

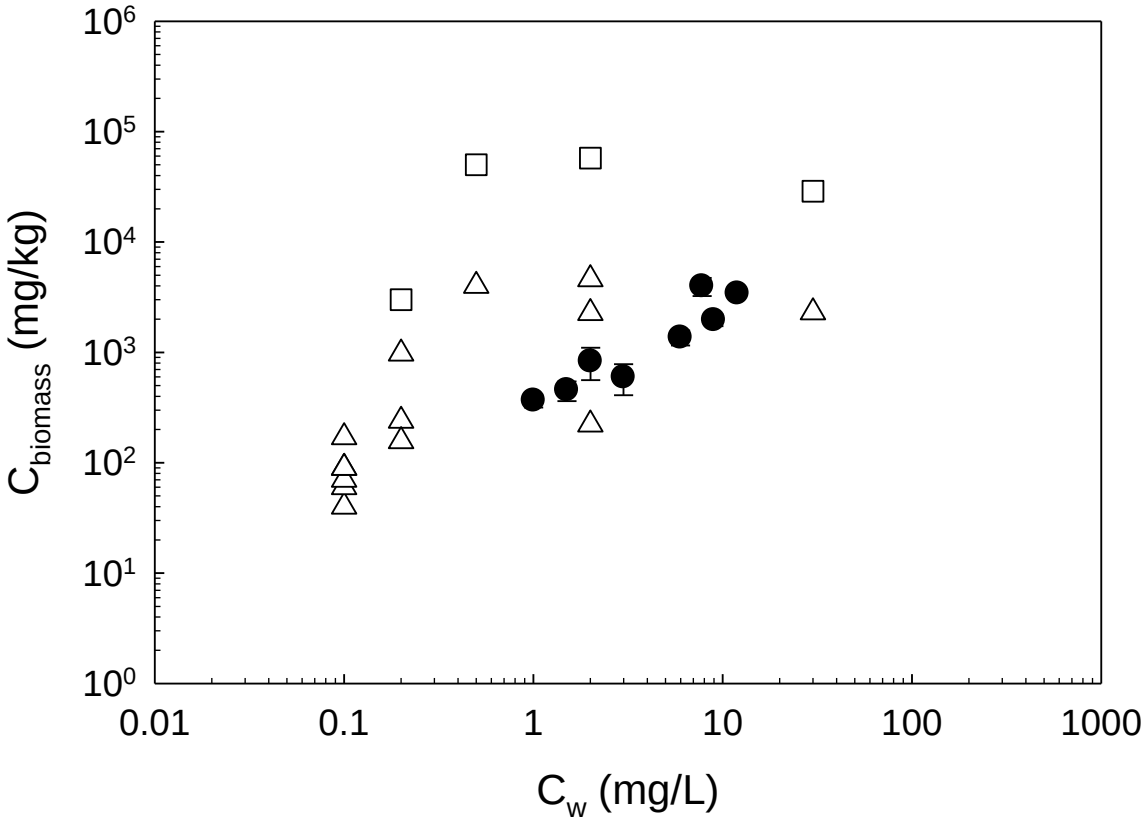

Figure 5.8: Comparisons of concentrations of fullerene taken up by Caco-2 cells compared to reported bioaccumulation values for *Dalphia* and *zebra fish*. Closed circles (●)fullerene uptake by cells (mass of fullerene per weight of dry cells) Open rectangles (□) and triangles (△) show the reported mass of fullerene that accumulates in the *Dalphia* normalized by dry and wet biomass weight, respectively. Open diamonds (◊) are determined from the bioconcentration factor of fullerene taken up by *Zebra fish*.

5.5. REFERENCES

Brant, J.A., Labille, J., Bottero, J.Y. and Wiesner, M.R. (2006) Characterizing the impact of preparation method on fullerene cluster structure and chemistry. Langmuir 22(8), 3878-3885.

Buesen, R., Mock, M., Nau, H., Seidel, A., Jacob, J. and Lampen, A. (2003) Human intestinal Caco-2 cells display active transport of benzo[a]pyrene metabolites. Chem Biol Interact 142(3), 201-221.

Cagle, D.W., Kennel, S.J., Mirzadeh, S., Alford, J.M. and Wilson, L.J. (1999) *In vivo* studies of fullerene-based materials using endohedral metallofullerene radiotracers. Proc Natl Acad Sci U S A 96(9), 5182-5187.

Camenisch, G., Alsenz, J., van de Waterbeemd, H. and Folkers, G. (1998) Estimation of permeability by passive diffusion through Caco-2 cell monolayers using the drugs' lipophilicity and molecular weight. Eur J Pharm Sci 6(4), 317-324.

Chen, Q., Yin, D., Li, J. and Hu, X. (2014) The effects of humic acid on the uptake and depuration of fullerene aqueous suspensions in two aquatic organisms. Environ Toxicol Chem 33(5), 1090-1097.

Chithrani, B.D. and Chan, W.C. (2007) Elucidating the mechanism of cellular uptake and removal of protein-coated gold nanoparticles of different sizes and shapes. Nano Lett 7(6), 1542-1550.

Cho, E.C., Xie, J., Wurm, P.A. and Xia, Y. (2009a) Understanding the role of surface charges in cellular adsorption versus internalization by selectively removing gold nanoparticles on the cell surface with a I_2/KI etchant. Nano Lett 9(3), 1080-1084.

Cho, M., Fortner, J.D., Hughes, J.B. and Kim, J.H. (2009b) Escherichia coli inactivation by water-soluble, ozonated C_{60} derivative: kinetics and mechanisms. Environ Sci Technol 43(19), 7410-7415.

Dausend, J., Musyanovych, A., Dass, M., Walther, P., Schrezenmeier, H., Landfester, K. and Mailander, V. (2008) Uptake mechanism of oppositely charged fluorescent nanoparticles in HeLa cells. Macromol Biosci 8(12), 1135-1143.

Davda, J. and Labhasetwar, V. (2002) Characterization of nanoparticle uptake by endothelial cells. Int J Pharm 233(1-2), 51-59.

dos Santos, T., Varela, J., Lynch, I., Salvati, A. and Dawson, K.A. (2011) Effects of transport inhibitors on the cellular uptake of carboxylated polystyrene nanoparticles in different cell lines. PLoS One 6(9), e24438.

Farkas, J., Christian, P., Gallego-Urrea, J.A., Roos, N., Hassellov, M., Tollefsen, K.E. and Thomas, K.V. (2011) Uptake and effects of manufactured silver nanoparticles

in rainbow trout (Oncorhynchus mykiss) gill cells. Aquat Toxicol 101(1), 117-125.

Foley, S., Crowley, C., Smaihi, M., Bonfils, C., Erlanger, B.F., Seta, P. and Larroque, C. (2002) Cellular localisation of a water-soluble fullerene derivative. Biochem Biophys Res Commun 294(1), 116-119.

Gao, X., Wang, T., Wu, B., Chen, J., Chen, J., Yue, Y., Dai, N., Chen, H. and Jiang, X. (2008) Quantum dots for tracking cellular transport of lectin-functionalized nanoparticles. Biochem Biophys Res Commun 377(1), 35-40.

Gulson, B. and Wong, H. (2006) Stable isotopic tracing-a way forward for nanotechnology. Environ Health Perspect 114(10), 1486-1488.

Ha, Y., Liljestrand, H.M. and Katz, L.E. (2013) Effects of lipid composition on partitioning of fullerene between water and lipid membranes. Water Sci Technol 68(2), 290-295.

Hidalgo, I.J. and Borchardt, R.T. (1990) Transport of a large neutral amino acid (phenylalanine) in a human intestinal epithelial cell line: Caco-2. Biochim Biophys Acta 1028(1), 25-30.

Jin, H., Heller, D.A. and Strano, M.S. (2008) Single-particle tracking of endocytosis and exocytosis of single-walled carbon nanotubes in NIH-3T3 cells. Nano Lett 8(6), 1577-1585.

Labille, J., Masion, A., Ziarelli, F., Rose, J., Brant, J., Villieras, F., Pelletier, M., Borschneck, D., Wiesner, M.R. and Bottero, J.Y. (2009) Hydration and dispersion of C_{60} in aqueous systems: the nature of water-fullerene interactions. Langmuir 25(19), 11232-11235.

Li, W., Chen, C., Ye, C., Wei, T., Zhao, Y., Lao, F., Chen, Z., Meng, H., Gao, Y., Yuan, H., Xing, G., Zhao, F., Chai, Z., Zhang, X., Yang, F., Han, D., Tang, X. and Zhang, Y. (2008) The translocation of fullerenic nanoparticles into lysosome via the pathway of clathrin-mediated endocytosis. Nanotechnology 19(14), 145102.

Limbach, L.K., Li, Y., Grass, R.N., Brunner, T.J., Hintermann, M.A., Muller, M., Gunther, D. and Stark, W.J. (2005) Oxide nanoparticle uptake in human lung fibroblasts: effects of particle size, agglomeration, and diffusion at low concentrations. Environ Sci Technol 39(23), 9370-9376.

Lin, I.C., Liang, M., Liu, T.Y., Monteiro, M.J. and Toth, I. (2012) Cellular transport pathways of polymer coated gold nanoparticles. Nanomedicine 8(1), 8-11.

Lovern, S.B. and Klaper, R. (2006) *Daphnia magna* mortality when exposed to titanium dioxide and fullerene (C_{60}) nanoparticles. Environ Toxicol Chem 25(4), 1132-1137.

Lyon, D.Y., Adams, L.K., Falkner, J.C. and Alvarezt, P.J. (2006) Antibacterial activity of fullerene water suspensions: effects of preparation method and particle size. Environ Sci Technol 40(14), 4360-4366.

Ma, X. and Bouchard, D. (2009) Formation of aqueous suspensions of fullerenes. Environ Sci Technol 43(2), 330-336.

Ma, Z. and Lim, L.Y. (2003) Uptake of chitosan and associated insulin in Caco-2 cell monolayers: a comparison between chitosan molecules and chitosan nanoparticles. Pharm Res 20(11), 1812-1819.

Mao, S., Germershaus, O., Fischer, D., Linn, T., Schnepf, R. and Kissel, T. (2005) Uptake and transport of PEG-graft-trimethyl-chitosan copolymer-insulin nanocomplexes by epithelial cells. Pharm Res 22(12), 2058-2068.

Oberdörster, E., Zhu, S.Q., Blickley, T.M., McClellan-Green, P. and Haasch, M.L. (2006) Ecotoxicology of carbon-based engineered nanoparticles: Effects of fullerene (C_{60}) on aquatic organisms. Carbon 44(6), 1112-1120.

Pade, V. and Stavchansky, S. (1997) Estimation of the relative contribution of the transcellular and paracellular pathway to the transport of passively absorbed drugs in the Caco-2 cell culture model. Pharm Res 14(9), 1210-1215.

Panyam, J. and Labhasetwar, V. (2003) Biodegradable nanoparticles for drug and gene delivery to cells and tissue. Adv Drug Deliv Rev 55(3), 329-347.

Petersen, E.J. and Henry, T.B. (2012) Methodological considerations for testing the ecotoxicity of carbon nanotubes and fullerenes: review. Environ Toxicol Chem 31(1), 60-72.

Porter, A.E., Gass, M., Muller, K., Skepper, J.N., Midgley, P. and Welland, M. (2007) Visualizing the uptake of C_{60} to the cytoplasm and nucleus of human monocyte-derived macrophage cells using energy-filtered transmission electron microscopy and electron tomography. Environ Sci Technol 41(8), 3012-3017.

Porter, A.E., Muller, K., Skepper, J., Midgley, P. and Welland, M. (2006) Uptake of C_{60} by human monocyte macrophages, its localization and implications for toxicity: studied by high resolution electron microscopy and electron tomography. Acta Biomater 2(4), 409-419.

Pycke, B.F., Benn, T.M., Herckes, P., Westerhoff, P. and Halden, R.U. (2011) Strategies for quantifying C_{60} fullerenes in environmental and biological samples and implications for studies in environmental health and ecotoxicology. Trends Analyt Chem 30(1), 44-57.

Rancan, F., Gao, Q., Graf, C., Troppens, S., Hadam, S., Hackbarth, S., Kembuan, C., Blume-Peytavi, U., Ruhl, E., Lademann, J. and Vogt, A. (2012) Skin penetration and cellular uptake of amorphous silica nanoparticles with variable size, surface functionalization, and colloidal stability. ACS Nano 6(8), 6829-6842.

Rejman, J., Oberle, V., Zuhorn, I.S. and Hoekstra, D. (2004) Size-dependent internalization of particles via the pathways of clathrin- and caveolae-mediated endocytosis. Biochem J 377(Pt 1), 159-169.

Rouse, J.G., Yang, J., Barron, A.R. and Monteiro-Riviere, N.A. (2006) Fullerene-based amino acid nanoparticle interactions with human epidermal keratinocytes. Toxicol In Vitro 20(8), 1313-1320.

Ruan, G., Agrawal, A., Marcus, A.I. and Nie, S. (2007) Imaging and tracking of tat peptide-conjugated quantum dots in living cells: new insights into nanoparticle uptake, intracellular transport, and vesicle shedding. J Am Chem Soc 129(47), 14759-14766.

Saha, K., Agasti, S.S., Kim, C., Li, X. and Rotello, V.M. (2012) Gold nanoparticles in chemical and biological sensing. Chem Rev 112(5), 2739-2779.

Sayes, C.M., Gobin, A.M., Ausman, K.D., Mendez, J., West, J.L. and Colvin, V.L. (2005) Nano-C_{60} cytotoxicity is due to lipid peroxidation. Biomaterials 26(36), 7587-7595.

Shang, L., Nienhaus, K. and Nienhaus, G.U. (2014) Engineered nanoparticles interacting with cells: size matters. J Nanobiotechnology 12, 5.

Singh, R. and Lillard, J.W., Jr. (2009) Nanoparticle-based targeted drug delivery. Exp Mol Pathol 86(3), 215-223.

Strober, W. (2001) Trypan blue exclusion test of cell viability. Curr Protoc Immunol Appendix 3, Appedix 3B.

Sugano, K., Kansy, M., Artursson, P., Avdeef, A., Bendels, S., Di, L., Ecker, G.F., Faller, B., Fischer, H., Gerebtzoff, G., Lennernaes, H. and Senner, F. (2010) Coexistence of passive and carrier-mediated processes in drug transport. Nat Rev Drug Discov 9(8), 597-614.

Sundara Rajan, S. and Vu, T.Q. (2006) Quantum dots monitor TrkA receptor dynamics in the interior of neural PC12 cells. Nano Lett 6(9), 2049-2059.

Tao, X., Fortner, J.D., Zhang, B., He, Y., Chen, Y. and Hughes, J.B. (2009) Effects of aqueous stable fullerene nanocrystals (nC60) on Daphnia magna: evaluation of sub-lethal reproductive responses and accumulation. Chemosphere 77(11), 1482-1487.

Tervonen, K., Waissi, G., Petersen, E.J., Akkanen, J. and Kukkonen, J.V. (2010) Analysis of fullerene-C_{60} and kinetic measurements for its accumulation and depuration in Daphnia magna. Environ Toxicol Chem 29(5), 1072-1078.

Vasiluk, L., Pinto, L.J., Walji, Z.A., Tsang, W.S., Gobas, F.A., Eickhoff, C. and Moore, M.M. (2007) Benzo[a]pyrene bioavailability from pristine soil and contaminated sediment assessed using two in vitro models. Environ Toxicol Chem 26(3), 387-393.

Wang, Z., Tiruppathi, C., Minshall, R.D. and Malik, A.B. (2009) Size and dynamics of caveolae studied using nanoparticles in living endothelial cells. ACS Nano 3(12), 4110-4116.

Wilhelm, C., Gazeau, F., Roger, J., Pons, J.N. and Bacri, J.C. (2002) Interaction of anionic superparamagnetic nanoparticles with cells: Kinetic analyses of membrane adsorption and subsequent internalization. Langmuir 18(21), 8148-8155.

Win, K.Y. and Feng, S.S. (2005) Effects of particle size and surface coating on cellular uptake of polymeric nanoparticles for oral delivery of anticancer drugs. Biomaterials 26(15), 2713-2722.

Xia, X.R., Monteiro-Riviere, N.A. and Riviere, J.E. (2006) Trace analysis of fullerenes in biological samples by simplified liquid-liquid extraction and high-performance liquid chromatography. J Chromatogr A 1129(2), 216-222.

Zhang, X., Sun, H., Zhang, Z., Niu, Q., Chen, Y. and Crittenden, J.C. (2007) Enhanced bioaccumulation of cadmium in carp in the presence of titanium dioxide nanoparticles. Chemosphere 67(1), 160-166.

Chapter 6: Bioavilability of fullerene under environmentally relevant conditions: Effects of humic acid and fetal bovine serum on the lipid accumulation and cellular uptake

ABSTRACT

Carbon fullerene (C_{60}) has emerged at the forefront of nanoscale research and application due to its unique properties. As the production of this nanoparticle rapidly increases, it can be released into natural aquatic environments and can accumulate in biological environments. This research examined the effects of humic acid and fetal bovine serum (FBS), which are ubiquitous in aquatic environments and blood plasma in living organisms, respectively, on bioavailability of fullerene. Bioavailability was investigated using *in vitro* methods for lipid membrane accumulation and cellular uptake studies. Humic acid and FBS significantly changed the characteristics of fullerene including its particle size and surface charge. The effects of humic acid on lipid accumulation of fullerene depended on the lipid head charge. For lipids with positively charged head groups, lipid accumulation of humic acid coated fullerene was similar to lipid accumulation of bare fullerene. However, with zwitterion and negatively charged lipids, humic acid coated fullerene exhibited reduced levels of accumulation compared to bare fullerene. FBS also significantly decreased the lipid accumulation values when positively charged and zwitterion head groups were present on the lipids, possibly due to the higher steric repulsion of the protein coated nanoparticles. In addition, both humic acid and protein effectively lowered the amounts of fullerene taken up by Caco-2 cells. Results of this study suggest that surface modification of fullerene by environmentally

relevant matrices can significantly affect the biological transport, as well as the possible toxicity of this nanoparticle.

Keywords

fullerene, lipid accumulation, cellular uptake, humic acid, fetal bovine serum

6.1. INTRODUCTION

Carbon fullerene (C_{60}) which was discovered by Kroto et al. (Kroto 1985) is at the center of nanotechnology due to its unique properties such as its electron rich cage structure, high reactivity, and ability to accept and release electrons. Recently, fullerene use has expanded to a broad range of commercial (Benn et al. 2011, McMahon et al. 2011, Wang 2007) (e.g., batteries, fuel cells, photovoltaics, and face cream) and biomedical applications (Chen et al. 2005, Fan et al. 2013, Friedman et al. 1993, Hughes 2005) (e.g., inhibitor of the HIV protease, drug carrier, and anti-cancer drug). As usage of this nanomaterial rapidly increases, the potential for release into aquatic environments also increases. Thus, concerns related to the possible harmful effects of fullerene nanoparticles within mammalian cells and aquatic organisms (Cho et al. 2009b, Lovern and Klaper 2006, Lyon et al. 2006, Sayes et al. 2005) must be addressed.

It is now well accepted that when nanoparticles are released into natural aquatic and biological environments, surface modification of nanoparticles occurs due to interactions with natural organic matter (NOM) present in aquatic environments (Baalousha 2009, Thio et al. 2011, Zhang et al. 2009b) and biological macromolecules

(Lynch and Dawson 2008) in living organisms. Many previous studies have reported that this surface modification of nanomaterials affects nanoparticle interactions with living systems as well as possible toxicity toward them (Ehrenberg et al. 2009, Fabrega et al. 2009, Giri et al. 2014, Guarnieri et al. 2011, Lesniak et al. 2012). Researchers have also suggested that NOM in natural waters as well as biological macromolecules (e.g., protein) affect the stability of carbon based nanomaterials such as fullerene and carbon nanotubes (Hyung and Kim 2009a, Li et al. 2009, Saleh et al. 2010, Xie et al. 2008, Zhu et al. 2009). In addition, it was suggested that protein coated nanoparticles can affect the immune system of living organisms (Dobrovolskaia and McNeil 2007). For example, when fullerene nanoparticles interact with protein, they can inhibit fibrillation of protein which can cause Alzheimer's disease (Podolski et al. 2007). Thus, it is imperative to investigate the influence of NOM and biomolecules in natural environments on bioavailability of nanomaterials.

The objective of this study is to explore the effect of environmentally and biologically relevant materials on the bioavailability of fullerene. To understand bioavailability, we used two *in vitro* methods developed previously (Chapters 3 - 5): (i) lipid accumulation by solid supported lipid membranes (SSLMs) with synthetic lipid bilayers of varying composition; and, (ii) cellular uptake experiments using Caco-2 cells consisting of monolayer membranes. Transport of fullerene nanoparticles from aquatic and biological environments to an organism occurs via lipid membranes which serve as cell barriers. Thus, bio-accumulation and bio-uptake of fullerene nanoparticles through

these lipid membranes is of critical importance to assess bioavailability of this nanoparticle. As a representative NOM and biomacromolecule, we chose a commercially available humic acid and fetal bovine serum (FBS), respectively. Humic acid is ubiquitous in aquatic environments, which consists of a hydrophobic backbone and various functional groups such as phenolic and carboxylic groups (Xie et al. 2008). Due to the hydrophilic functional groups of humic acid, nanoparticles which are coated with humic acid exhibit a different polarity compared to that of bare nanoparticles (Bian et al. 2011). FBS is a protein present in the blood plasma of living organisms, and it is usually used as protein supplement for cell cultures. As a rule of thumb, when nanoparticles contact protein, they are immediately covered by protein, forming a protective layer (Lynch and Dawson 2008, Zhu et al. 2009). This surface modification of nanoparticles by protein can influence the potential risk associated with these particles via occupational as well as environmental exposures. To date, only one study has suggested that humic acid reduced the uptake of fullerene through aquatic living organisms (Chen et al. 2014), and no study has reported the effects of humic acid and FBS on lipid accumulation and cellular uptake of fullerene. Thus, the focus of this research was to investigate changes in the particle characteristics of fullerene due to the presence of humic acid and FBS and evaluate the effect of these substances on fullerence cellular uptake.

6.2. MATERIALS AND METHODS

Materials. Carbon fullerene (100% solid, 99.5+ %) was obtained from SES Research (Houston, TX). Suwannee river humic acid standard II and FBS (FBS) were purchased from the International Humic Substances Society (IHSS, St.Paul, MN) and Life Technologies (Grand Island, NY), respectively. Non-functionalized silica microspheres (Bangs Laboratories, Inc., Fisher, IN) were used as the solid support for the solid supported lipid membranes (SSLMs). The mean diameter of the microspheres was 5.2 μm. Three lipids, 1,2-dioleoyl-3-trimethylammonium-propane (DOTAP), 1,2-dioleoyl-sn-glycero-3-phosphocholine (DOPC), and 1,2-dioleoyl-sn-glycero-3-phospho-(1'-rac-glycerol) (18:1 PG) were purchased from Avanti Polar Lipids (Alabaster, AL). To perform the cellular uptake tests, Caco-2 cells were purchased from American Type Culture Collection (ATCC, Manassas, VA). All solvents used in this study were of analytical grade.

Preparation of aqueous fullerene suspensions. Fullerene suspensions in water (nC_{60}) were prepared by a liquid exchange method by ultrasonication (SON/nC_{60}) and details are described elsewhere (Brant et al. 2006, Ha et al. 2013). After dissolving 3 mg of fullerene in 5 mL toluene, 30 mL of deionized water was added to the solution. Under ultrasonic treatment with air purging, the toluene layer was removed leaving yellowish fullerene aggregations in water. This fullerene suspension was filtered through a 0.8 μm membrane filter (Millipore, Billerica, MA) to remove particles that were not dispersed in water. The size and zeta potential of the resultant fullerene suspension were

measured using Dynamic Light Scattering (DLS, Malvern Zetasizer Nano ZS), and fullerene aggregates were used within 2 days to prevent any changes in particle characteristics. To investigate the effect of humic acid and FBS on bioavailability of fullerene, fullerene dispersions were incubated in the dark for 24 hours with humic acid (5-50 mg/L) or 10 % FBS for 24 hrs. Then, humic acid or FBS coated fullerene and was also characterized by DLS and used for lipid accumulation as well as cellular uptake experiments.

Determination of accumulation of fullerene in lipid membranes. SSLMs with three different lipid membranes (DOTAP, DOPC, and PG) were synthesized. The detailed procedure was reported in our previous study (Ha et al. 2013). In brief, the synthetic membrane vesicles for each lipid were mixed with silica microspheres and vigorously mixed (vortex mixing) prior to 2 hrs of gentle mixing on a shaker. Then, the mixtures were centrifuged and supernatants that contained excess lipids not adsorbed onto silica beads were transferred to other vials. The mass of lipids that adsorbed onto the SSLMs was determined by measuring differences between initial lipid concentration and supernatant concentration using a TOC analyzer (Tekmar Dohrmann Apollo 9000, Cincinnati, OH).

The synthesized solid supported lipid membranes and fullerene dispersions were placed into 40 mL vials with PTFE/silicon septa. The vials were incubated at room temperature using a custom-made tumbling device. After a certain incubation time, each vial sat for 1 hr to allow settling of the solid supported lipid membranes (SSLMs). Then,

0.5 mL of supernatant containing the fullerene particles that remained in solution were transferred to a new vial for liquid extraction of fullerene. For bare fullerene suspensions in water, liquid extraction was performed by adding 0.1 M $Mg(ClO_4)_2$ (0.4 mL) and toluene (0.5 mL) followed by vigorous mixing. After liquid extraction, the initial fullerene concentration (C_0) and supernatant concentration (C_w) were measured using a Waters 2690 high performance liquid chromatography system equipped with a Waters 996 photodiode array detector (Milford, MA). Fullerene accumulation in the lipids was calculated using equation (6-1)

$$Fullerene\ accumulated\ in\ lipid\ (mg/kg-lipid) = \frac{C_{lip}}{m} = \frac{C_0 - C_w}{m} \qquad (6\text{-}1)$$

where C_{lip} (mg/L) is the fullerene concentration in the lipid side, which can be determined from the difference between the initial fullerene concentration (C_0) and the fullerene concentration in the supernatant C (C_w). *m* is the concentration of lipid (kg-lipid/L) in the system.

For liquid extraction of fullerene dispersions incubated with humic acid and protein, we additionally added 2.5 mL of glacier acetic acid (GAA) to 0.1 M $Mg(ClO_4)_2$ and toluene to minimize emulsion creation. GAA was successfully used in previous studies for extracting fullerene suspensions from solutions containing environmentally relevant materials and biomolecules (Hyung and Kim 2009a, Pycke et al. 2011, Xia et al.

2006b). The fullerene recovery from the extracted solution was 110 (±0.29) % for 20 mg/L of humic acid and 96 (±23) % for 10 % FBS.

Cell culture. Caco-2 cells were maintained in flasks in Dulbecco's modified Eagle medium (D-MEN) containing 10 % FBS, 2 % nonessential amino acids, and 1 % L-glutamine and penicillin in an atmosphere of 5 % CO_2 at 37 °C. The cells were transferred to tissue culture flasks (75 cm^2) until they reached confluence. Then, cells were detached with trypsin and EDTA solution, and transferred to larger cell culture flasks (150 cm^2). Cell passages were performed every two to three days and we did at least two passages before being seeded on cellular uptake plates.

Cellular uptake studies. To investigate the effect of humic acid coating on cellular uptake of fullerenes, fullerene stock solutions incubated with different concentrations of humic acid (5, 10, and 20 mg/L) were prepared. Caco-2 cells placed in 150 cm^2 cell culture flasks were washed with phosphate buffer solution (PBS) three times to remove metal ions and detached with trypsin and an EDTA solution. Then, cells were seeded into 6 polycarbonate plates (Corning Inc., Corning, NY) at a density of 10^5 cells/cm^2 and incubated for two days in an atmosphere of 5 % CO_2 at 37 °C. Cellular uptake tests were performed under serum free conditions to prevent fullerene coating with protein. When the cells were initially seeded, a cell culture medium with 10 % FBS was used, and after one day of incubation, the cell culture medium was changed to a medium without FBS. After two days of incubation, the cell culture medium was changed to 2 mL of fresh medium with 200 μL of a fullerene stock solution incubated with one of

several concentrations of humic acid. After 24 hrs of incubation, cells were washed three times with PBS buffer and detached from the plates with 400 μL of a trypsin-EDTA solution. The cells were lysed with 30 min of ultrasonication. Then, fullerene was destabilized with 400 μL of 0.1 M $Mg(ClO_4)_2$ and 2.5 mL glacier acetic acid (GAA) and extracted with toluene. Fullerene concentrations were analyzed using a Waters 2690 high-performance liquid chromatography system equipped with a Waters 996 photodiode array detector (Milford, MA, USA).

To evaluate the effect of FBS on cellular uptake of fullerene, fullerene suspensions were incubated in cell culture medium with and without FBS for 12-24 hrs. Then, 2 mL of a fullerene suspension containing 10^5 cells/cm^2 were placed in 6 polycarbonate plates and incubated for two days. Other procedures (e.g., cell lysis, liquid extraction of fullerene, and fullerene concentration analysis) for performing the uptake experiments are as described above.

6.3. Results And Discussion

Impact of humic acid and FBS on the fullerene particle characteristics. To investigate the effects of humic acid and FBS on the fullerene particle characteristics, particle size and zeta potential were measured after 24 hrs of incubation of fullerene with humic acid and FBS. Figure 6.1 highlights the significant changes in particle size and zeta potential of fullerene due to the addition of 10 – 50 mg/L humic acid. As shown in Figure 6.1(a), the presence of humic acid significantly decreased the particle size,

indicating that humic acid can adsorb onto fullerene and prevent fullerene particle aggregation. This result is in agreement with Xie et al. (Xie et al. 2008) who concluded that the particle size distribution of fullerene shifted to smaller diameters when incubated with 20 mg/L humic acid. In addition, many previous studies (Bian et al. 2011, Ghosh et al. 2010, Zhang et al. 2009b) have reported that the presence of humic acid effectively prevents aggregation of other nanoparticles (e.g., ZnO, TiO_2, SiO_2, and Al_2O_3) over time, which implies increasing stability in natural aquatic environments. Also, the addition of humic acid decreased the surface charge of the fullerene nanoparticles (Figure 6.1(b)). This result is also consistent with other studies (Bian et al. 2011, Ghosh et al. 2010, Zhang et al. 2009b) that suggested that nanoparticles incubated with humic acid become more negatively charged due to the carboxylic acid functional groups on the humic acid which are typically deprotonated at circumneutral pH. It was suggested that the presence of multiple functional groups on the relatively large humic acid molecules can lead to steric hinderance effects which can increase the stability of nanoparticles that are coated with humic acid. As the humic acid concentration was increased in the experiments presented in Figure 6.1, differences in both size and zeta potential became negligible, indicating that 10 mg/L of humic acid was sufficient to saturate the fullerene surface (4.7 mg/L).

Figure 6.2 shows the effect of FBS on the particle size distributions. After 24 hrs of incubation with 10 % FBS, the size distribution becomes narrower, and there is a shift in the distribution to slightly higher mean particle size. This shift can be explained by non-specific adsorption of FBS on the fullerene surface. Deguchi et al., (2007) also

have reported that protein coated fullerene exhibits a slightly higher particle size compared to bare fullerene. When fullerene nanoparticles are exposed to protein containing solutions, the formation of a protein coating can prevent the formation of large particle aggregates, which increases the stability of the nanoparticles. Indeed, it has been reported that stability of fullerene increases due to protein adsorption (Deguchi et al. 2007). In addition, previous studies have indicated that the presence of protein makes carbon nanotubes (Casey et al. 2007, Zhu et al. 2009) and polystyrene particles (Ehrenberg et al. 2009) more stable in water. Studies (Ehrenberg et al. 2009, Guarnieri et al. 2011) have also demonstrated that the surface charge of negative polystyrene nanoparticles became less negative after adsorption of serum proteins. However, it was not possible to obtain zeta potential data for fullerene incubated with FBS (i.e., results did not meet quality criteria due to the increase number of sub-runs per measurement) possibly due to the fluid characteristics of the protein containing solution (e.g., color and viscosity).

(a)

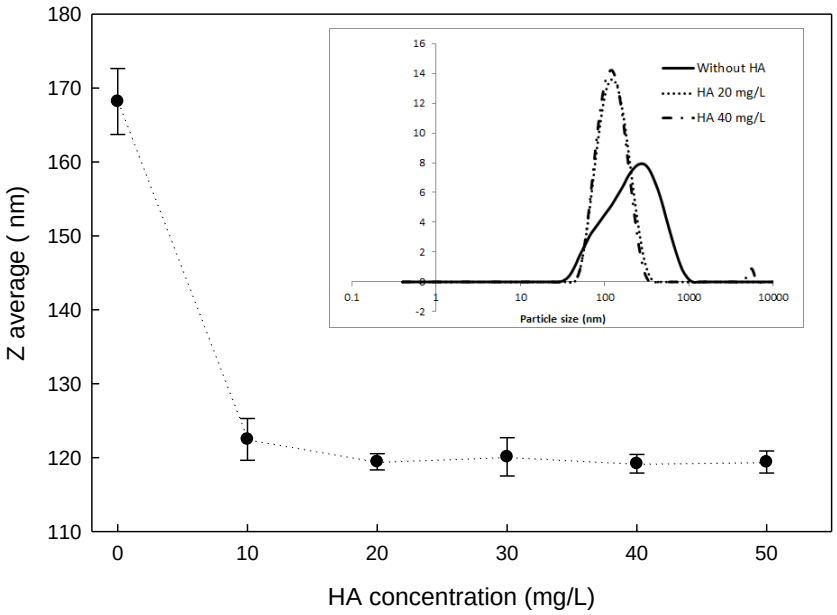

(b)

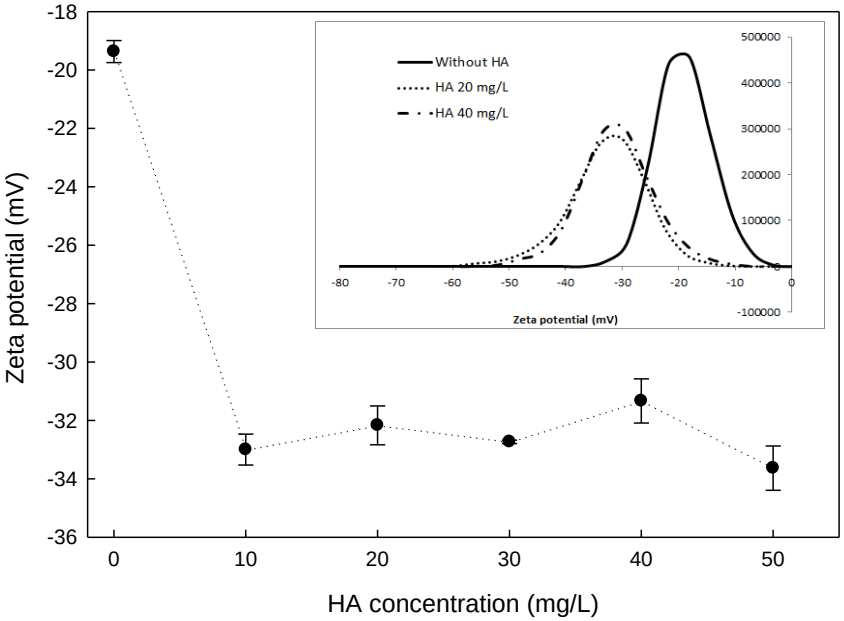

Figure 6.1: Effects of humic acid on (a) particle size and (b) zeta potential of fullerene nanoparticles (C_0 = 4.7 mg/L). Insertions in Figure 6.1(a) and Figure 6.1(b) are size distribution and zeta potential distribution of fullerene nanoparticle, respectively.

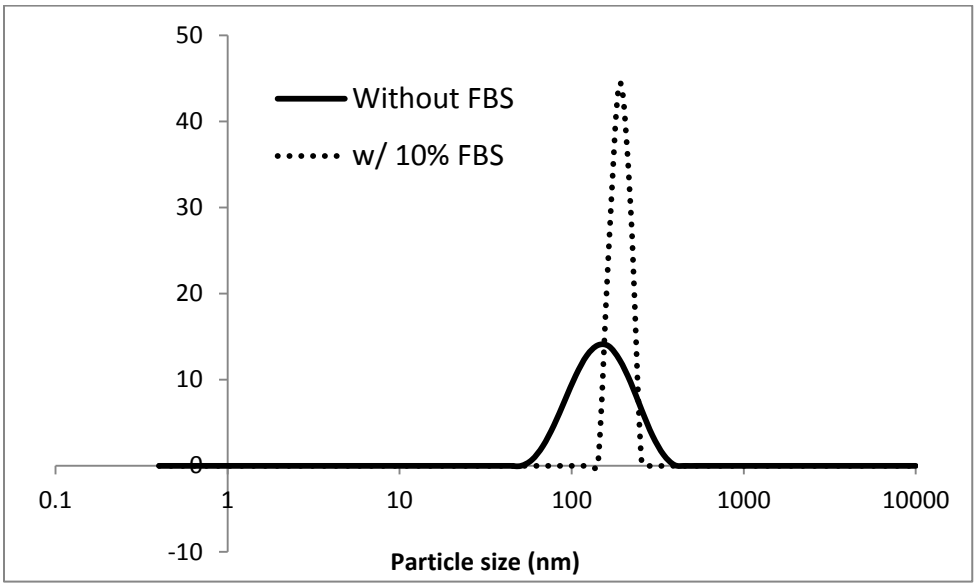

Figure 6.2**:** The effect of FBS on the fullerene particle distribution.

Kinetics of lipid accumulation of lipids. Time dependent lipid accumulation studies for bare fullerene nanoparticles were performed to investigate the effects of lipid surface charge on the rates of partitioning of fullerene between lipid and water. Results are shown in Figure 6.3. We chose three unsaturated lipids which have different head charges, but similar acyl chain length (C_{18}), and fluid phase at room temperature. Lipid accumulation of fullerene with DOTAP lipid reached steady state very quickly (within 30 min), and accumulation values with both DOPC and PG increased continuously reaching a plateau after approximately 24 hrs. At all times, fullerene accumulation values were highest for DOTAP, followed by DOPC, and then PG lipid. Due to the negative charge associated with the fullerene nanoparticle surface in water, a strong electrostatic

interaction between fullerene nanoparticles and DOTAP (positive) lipid would be expected compared to DOPC (zwitterion) and PG (negative) lipids. Thus, it can be concluded that adsorption of charged nanoparticles onto oppositely charged lipid membranes plays a critical role for bioaccumulation of nanoparticles..

To more fully understand the effects of lipid composition on the accumulation rates, we fit an empirical model to our experimental data and obtained rate parameters. This empirical model has been used in previous studies to describe cellular uptake kinetics of gold nanoparticles (Cho et al. 2009a) and oxide iron nanoparticles (Wilhelm et al. 2002). Also, this model was used by Hou et al. (Hou et al. 2012a) for describing the effect of gold nanoparticle size on lipid membrane accumulation. The model equation is :

$$C_{lip}\,(mg/kg-lipid) = \frac{k_a C C_{lip,0}}{k_a C + k_d}(1 - \exp(-(k_a C + k_d)t)) \qquad (6\text{-}2)$$

where C_{lip} (mg/kg-lipid) is the mass of fullerene that accumulated per unit mass of lipid as a function of time, t is time (hr), k_a (L/mg/h) is association rate constant, k_d (1/h) is a dissociation rate constant, C (mg/L) is the initial fullerene concentration, and $C_{lip,0}$ (mg/L) is the maximum concentration that can be adsorbed onto a unit mass of lipid membrane. It is difficult to calculate the exact $C_{lip,0}$ value because the size of the fullerene aggregates is not uniform. Here, we estimated $C_{lip,0}$ using an assumption that there is a single adsorbed layer of nanoparticle aggregates which have a uniform size of 150 nm on lipid membranes based on the calculations in Hou et al., (Hou et al. 2012a). Although $C_{lip,0}$ used in this study might not be accurate, that does not affect the lipid membrane composition dependence of the rate parameters summarized in Table 6.1. In Table 6.1, K

($=k_a/k_d$) the high affinity constant and high K value indicate a strong affinity between fullerene and the lipid membrane. Characteristic time (τ) is defined as $1/(k_aC+k_d)$ and a smaller τ value means faster rates. As shown in Table 6.1, the affinity constant is highest with DOTAP lipid and lowest with PG lipid. It is noteworthy that the affinity constant with the zwitterion lipid (DOPC) is slightly lower than with the positive lipid (DOTAP) but still much higher than with the negative lipid (PG), probably due to the electrostatic interaction between fullerene and positive portion of zwitterion lipid membrane (N^+ terminus).

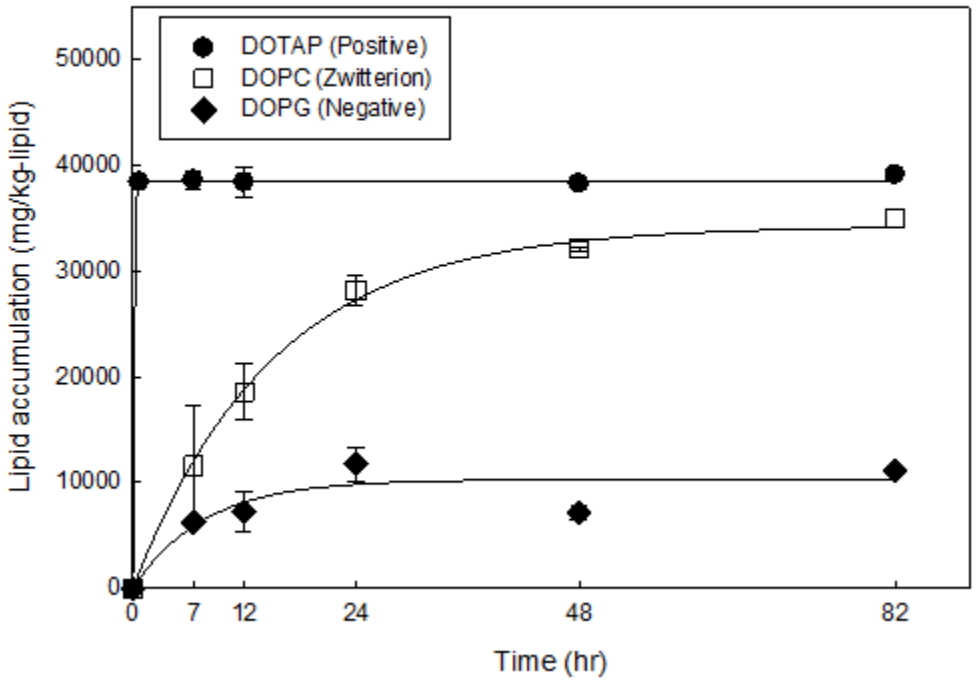

Figure 6.3: Rates of fullerene nanoparticle (C_0 = 4.7 mg/L) accumulation in three different lipid membranes which have different head charges. Solid lines are fitted according to equation 6-2.

Table 6.1: Rate parameters obtained by fitting the data using equation 6-2

Lipid membrane	Fullerene coating materials	$C_{lip,0}$ [a] (mg/kg-lipid)	k_a (L/mg/h)	k_d (1/h)	K [b] (L/mg)	τ [c] (h)	r^2
DOTAP	**Bare fullerene**	**3.93×10^8**	**1.80×10^{-4}**	**8.57**	**2.10×10^{-5}**	**0.12**	**99.8**
	Humic acid	3.14×10^8	1.49×10^{-6}	0.053	2.79×10^{-5}	18.73	99.9
	FBS	3.93×10^8	6.53×10^{-5}	3.72	1.75×10^{-5}	0.27	99.0
DOPC	**Bare fullerene**	**3.93×10^8**	**1.24×10^{-6}**	**0.066**	**1.86×10^{-5}**	**15.03**	**96.3**
	Humic acid	3.14×10^8	3.83×10^{-7}	0.022	1.72×10^{-5}	45.05	95.6
	FBS	3.93×10^8	4.04×10^{-7}	0.043	9.38×10^{-6}	23.20	89.2
PG	**Bare fullerene**	**3.93×10^8**	**7.33×10^{-7}**	**0.13**	**5.59×10^{-6}**	**7.63**	**82.6**
	Humic acid[d]	-	-	-	-	-	-
	FBS	3.93×10^8	5.16×10^{-7}	0.058	8.95×10^{-6}	17.33	61.8

[a] $C_{lip,0}$ for bare and FBS coated fullerene was estimated by assumption of single layer adsorption of 150 nm nanoparticles onto lipid membranes. Because humic acid decreased the mean size of fullerene nanoparticles, we used 120 nm instead of 150 nm for estimating $C_{lip,0}$ for humic acid coated fullerene.

[b] K ($=k_a/k_d$) is the affinity constant and high value of K indicates a strong affinity between fullerene and lipid membranes.

[c] Characteristic time (τ) is defined as $1/(k_aC+k_d)$ and smaller K indicates faster interaction.

[d] Rate parameters for interaction between PG lipid and humic acid coated fullerene are not available because regression did not converge.

Effects of humic acid and protein on lipid accumulation. Figure 6.4 shows the impact of humic acid on fullerene accumulation in three lipid membranes. With DOTAP lipid (Figure 6.4(a)), initial lipid accumulation values in the presence of 20 mg/L of humic acid were much lower than without humic acid, increased slowly, then finally reached a plateau at 80 hrs that was equivalent to the accumulation without humic acid. The possible reason for the slower adsorption process in the presence of humic acid may

be due to competitive adsorption of fullerene with humic acid in the background solution. Because humic acid is negatively charged, adsorption between the negatively charged humic acid and positively charged lipid membranes is favorable. Indeed, as shown in Figure 6.5, more than 20 % of the humic acid rapidly adsorbed onto the DOTAP lipids, however, humic acid did not adsorb onto DOPC or PG lipids. In Figure 6.4(a), lipid accumulation values with 20 mg/L humic acid decreased slightly after 6 hr of incubation. At early incubation times, adsorbed fullerene may have been desorbed due to the stronger interaction between humic acid and the lipid membrane.

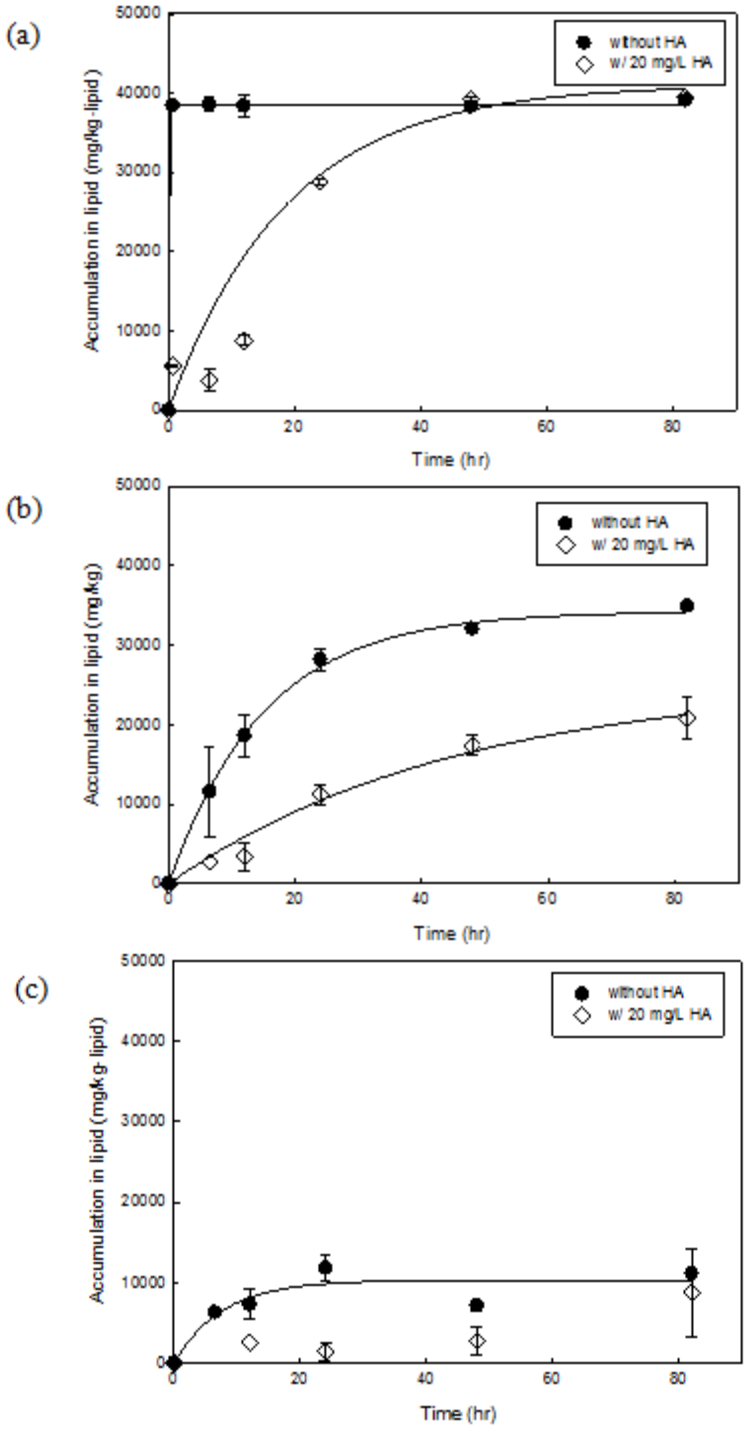

Figure 6.4: Rates of fullerene nanoparticle (C0 = 4.7 mg/L) accumulation in (a) DOTAP (positive head), (b) DOPC (zwitterion head), and (c) PG (negative head) with and without humic acid (20 mg/L). Solid lines are fits to equation 6-2.

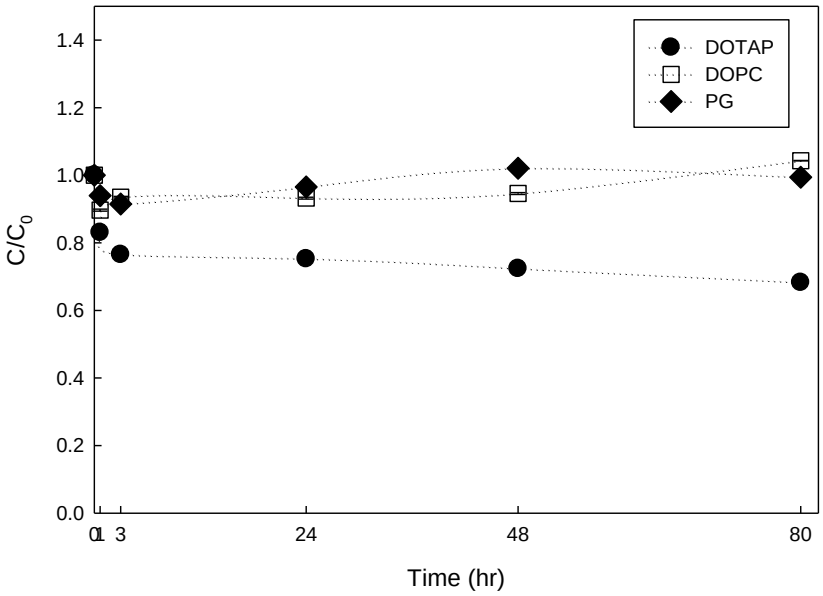

Figure 6.5: Adsorption of humic acid on three different lipid membranes with different head charges. Humic acid concentrations were measured by UV/vis spectrometer at 310 nm

To better understand the lipid accumulation of fullerene in the presence of humic acid, one additional test was performed. Two vials were prepared: a control vial containing only solid supported lipid membranes (SSLM) with DOTAP lipid in water, and another vial containing DOTAP lipid with 20 mg/L humic acid. After 80 hrs of incubation, fullerene dispersions were added in the presence of the same concentration of humic acid in both vials and incubated for an additional 80 hrs. As demonstrated in Figure 6.6, fullerene nanoparticles rapidly adsorbed onto the lipid membranes in the control vial. On the other hand, after 80 hrs of pre-incubation of the DOTAP lipid with humic acid, fullerene accumulation values were much lower than observed in the control vial. This result suggests that humic acid can strongly adsorb on the DOTAP lipid heads due to the electrostatic interaction, and prevent fullerene adsorption.

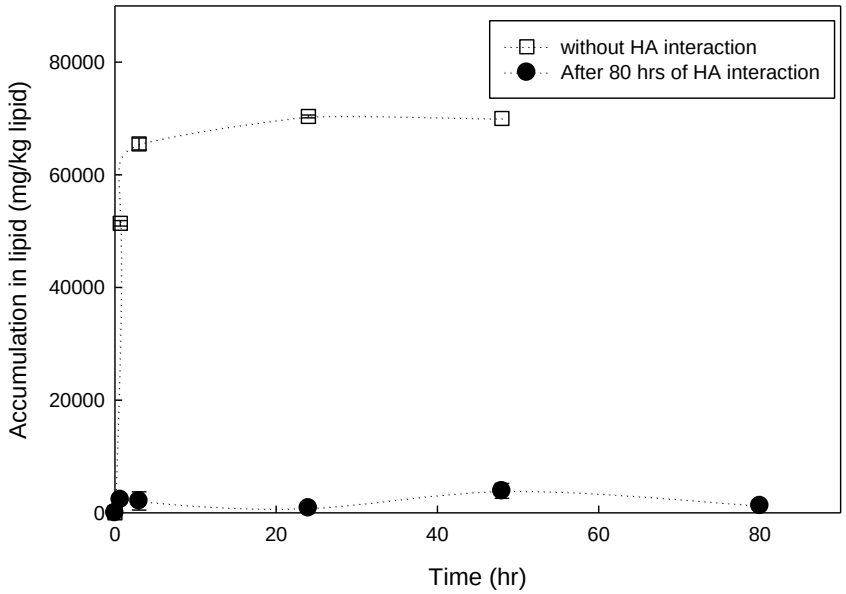

Figure 6.6: Rates of fullerene nanoparticles (C_0 = 8.3 mg/L) accumulated in DOTAP lipid membranes. Open rectangular represents fullerene accumulations in DOTAP lipid membrane and circle indicates accumulations of fullerene in lipid membranes which interacted with humic acid for 80 hrs.

With DOPC lipid (Figure 6.4(b)), humic acid effectively decreased lipid accumulation of fullerene at all incubation times. The main driving force of fullerene interaction with zwitterion lipid membranes can be electrostatic interaction between a positive portion of lipid membranes and fullerene, and steric effects associated with humic acid coated fullerene can prevent the approach of fullerene to the lipid membranes. Moreover, negatively charged deprotonated functional groups on the humic acid decrease the surface charge of the particles. With PG lipid (Figure 6.4(c)), in the presence of humic acid, fullerene accumulation within the lipid was lower than without humic acid

which can be explained by the stronger electrostatic repulsion between humic acid coated fullerene and a negatively charged lipid membrane (see Figure 6.1(b)).

Initial experiments confirmed that adsorption of FBS to any of the three lipid membranes is negligible (Figure 6.7). However, the presence of 10 % FBS significantly decreased the lipid accumulation of fullerene with both DOTAP (Figure 6.8(a)) and DOPC lipids (Figure 6.8(b)). When fullerene is exposed to the protein containing solution, fullerene was immediately coated with protein (Figure 6.2) which reduced its surface energy. This decrease in surface energy contributes to the decrease in accumulation of fullerene with FBS. With PG lipid (Figure 6.8(c)), there is not a significant difference between lipid accumulation with and without FBS. This is because both bare fullerene and FBS coated fullerene have strong electrostatic repulsion with negative lipid membranes.

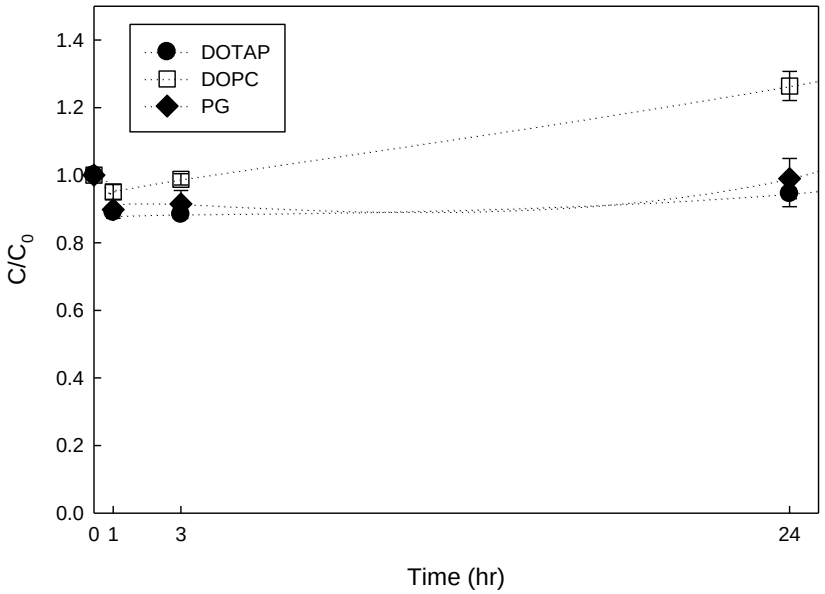

Figure 6.7: Adsorption of FBS on three different lipid membranes which have different head charges. FBS concentrations were measured by UV/vis spectrometer at 290 nm.

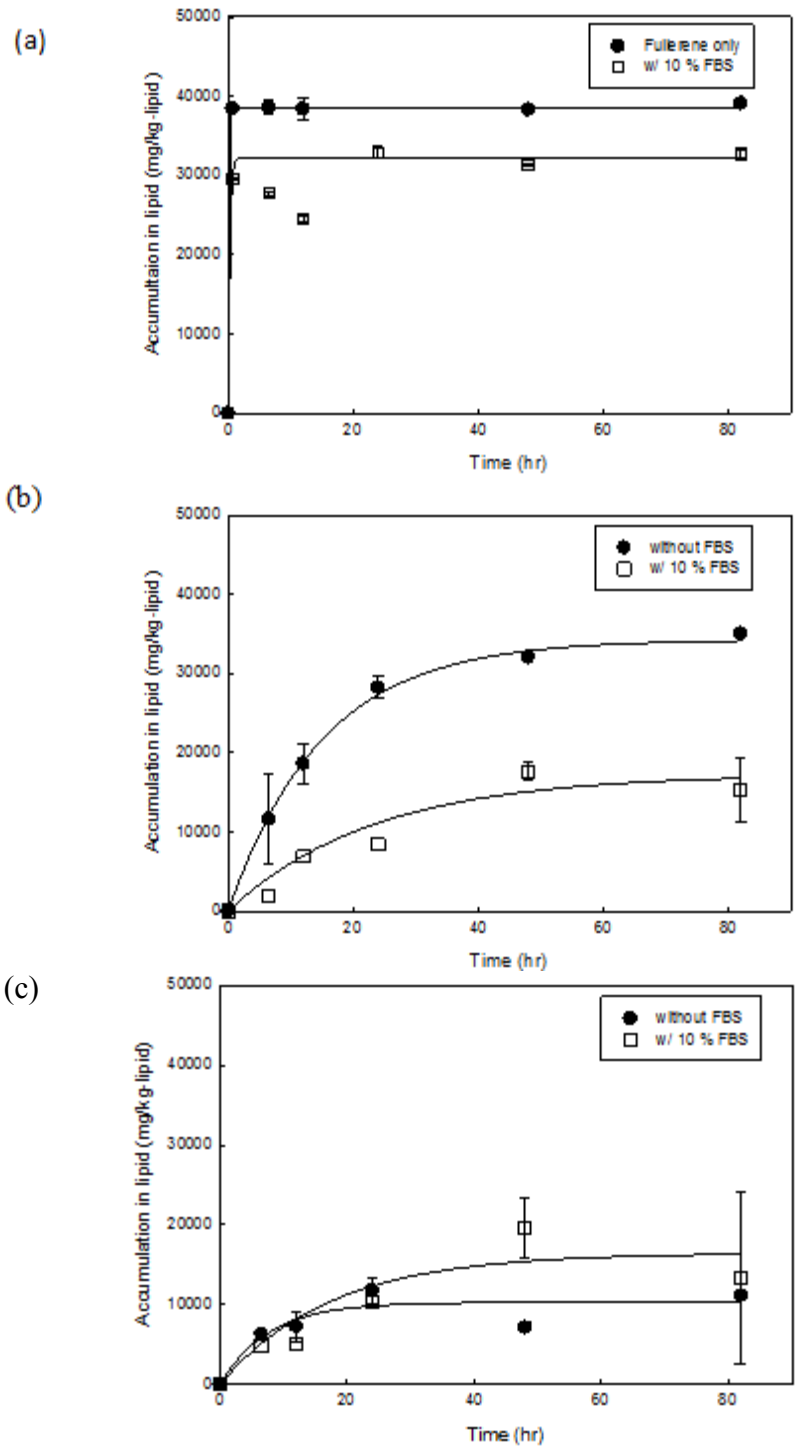

Figure 6.8: Rates of fullerene nanoparticles (C_0 = 4.7 mg/L) accumulated in (a) DOTAP (positive head), (b) DOPC (zwitterion head), and (c) PG (negative head) with and without 10 % FBS. Solid lines are fitted according to equation 6-2.

We also fit the model presented in equation (6-2) to the experimental data with humic acid and FBS and obtained rate parameters which are summarized in Table 6.1. To obtain a better fit, we ignored accumulation values at 6 hrs and 12 hrs in Figure 6.4(a) and Figure 6.8(a) (which decreased over time due to the significant release of attached fullerene nanoparticles at early incubation time). Rate parameters for the interaction between PG lipids and humic acid coated fullerene could not be obtained because the regression did not converge, exceed maximum number of iteration. For estimating $C_{lip,0}$ in equation (6-2) for fullerene coated with humic acid, we used a 120 nm particle size instead of 150 nm because humic acid significantly decreases particle size of fullerne (Figure 6.1(a)); the $C_{lip,0}$ value does not affect the dependence of humic acid and FBS on the rate parameters. With DOTAP lipids, humic coated fullerene and bare fullerene have similar affinity coefficients with the lipid due to the strong electrostatic interactions. With DOPC lipids, the presence of humic acid and FBS significantly decreases fullerene affinity with lipid membranes, and the affinity of FBS coated fullerene for lipid membranes is much lower than that of humic acid coated fullerene. This result suggests that FBS coating creates remarkably higher steric repulsion compared with the repulsion created by humic acid coating on nanoparticles. In addition, humic acid and FBS coated fullerene interacts with all three lipid membranes more slowly, and except for the PG lipid, adsorption rates are slower with humic acid than FBS. Because both fullerene dispersions and humic acid are hydrophobic and exhibit a similarly negative surface

charge, competitive adsorption of fullerene and humic acid can occur on the lipid, which results in slower lipid accumulation of fullerene in the presence of humic acid.

Effects of humic acid and protein on cellular uptake of fullerene. To investigate the effect of humic acid coating on the cellular uptake of fullerene, fullerene was incubated with humic acid (5, 10, 20 mg/L) for 12 hours prior to performing cellular uptake experiments. Results shown in Figure 6.9 demonstrate that humic acid coatings significantly decreased the overall mass of fullerene taken up by the cells for all humic acid concentrations. It is generally acknowledged that the net cell surface charge is negative and fullerene coated with humic acid has a lower surface charge compared to than bare fullerene and this was evident in Figure 6.1. Thus, electrostatic repulsion between humic acid coated fullerene and the cell surface can be higher than that of bare fullerene, resulting in less fullerene uptake by the cells in the presence of humic acid. This result is in agreement with a study of Chen et al. (Chen et al. 2014) that shows that humic acid addition decreased the uptake of fullerene by two aquatic organisms: *Daphnia magna* and *zebrafish* presumably due to more negatively charged surface of humic acid coated fullerene.

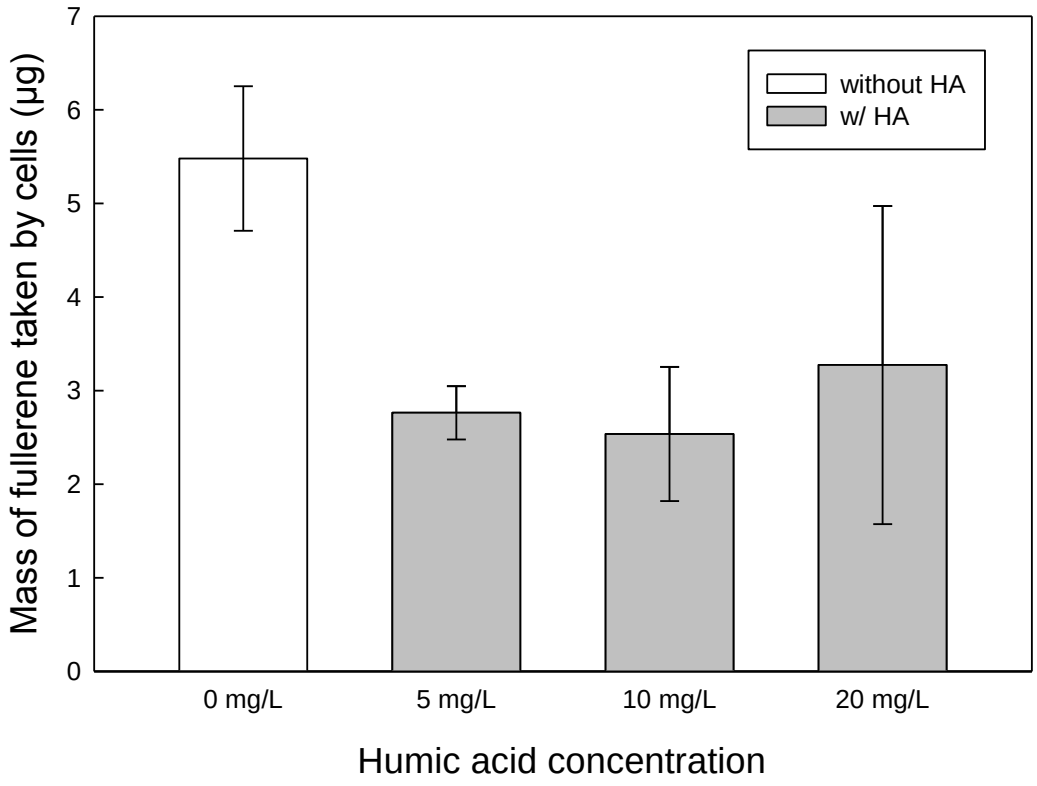

Figure 6.9: The effect of humic acid on cellular uptake of fullerene

The influence of FBS on cellular uptake of fullerene was also investigated (Figure 6.10). Interestingly, when higher concentrations of fullerene (> 7 mg/L) were injected into the cells under serum free conditions, fullerene particles associated with the cells were easily observed in the microscope images (Figure 6.10(b)). On the other hand, in the presence of FBS, fullerene was rarely observed on the cell surfaces (Figure 6.10(a)), indicating that serum protein affectively hindered the fullerene adsorption on the cells. Indeed, the mass of fullerene taken up by the cells when FBS was present is much lower than that under serum free conditions (Figure 6.10(c)). This result supports previous

results in this study which show that serum protein effectively decreased lipid accumulation of fullerene due to steric hinderance and a possible decrease in surface energy of FBS coated fullerene (Ehrenberg et al. 2009, Guarnieri et al. 2011). The proposed reduction in surface energy resulting from adsorption of protein onto the fullerene surface likely decreased the interaction between particles and cell membranes, which consequently contributed to reduced cellular uptake. Many previous studies also have reported that serum proteins drastically reduced cellular uptake of nanoparticles including polystyrene nanoparticle (Guarnieri et al. 2011), silica nanoparticles (Lesniak et al. 2012), and carbon nanotubes (Zhu et al. 2009). Thus, it can be concluded that humic acid and protein coated fullerene have different surface properties which lead to reductions in cellular uptake of fullerene.

In previous chapter, we proposed that the main cellular uptake mechanism of fullerene nanoparticle is energy dependent active transport (e.g., endocytosis). In the endocytosis process, nanoparticles first bind to the cell surface, followed by internalization inside the cells. Thus, adsorption of nanoparticles on the cell surface is a critical step for the cellular uptake. Humic acid coated fullerene has more polar surface area and FBS coated fullerene has less surface energy than bare fullerene, indicating that both humic acid and FBS can reduce the approach of fullerene to the cell surface. Thus, results of this study imply that humic acid and FBS can significantly affect the active transport of fullerene nanoparticles.

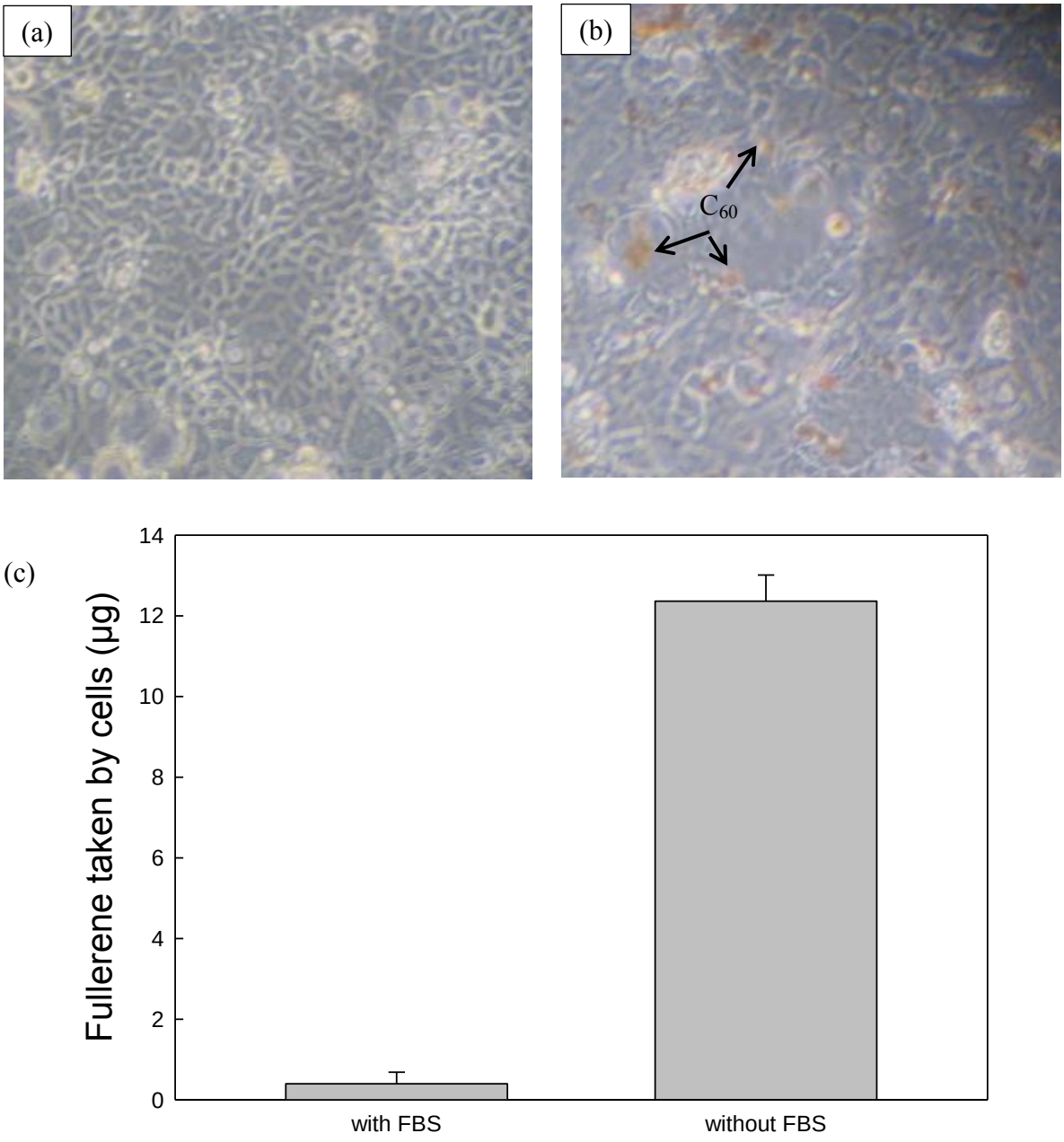

Figure 6.10: The effect of FBS on the cellular uptake of fullerene. Figure 6.10 (a) and (b) are Caco-2 cell microscope images taken after 24 hrs of fullerene injection with and without FBS in cell culture medium, respectively. Figure 6.10(c) shows the mass of fullerene taken by cells with and without FBS in cell culture medium. The injected fullerene concentration was 12 mg/L.

6.4. ENVIRONMENTAL IMPLICATIONS

Natural aquatic systems and biological systems are the most likely environments where the presence of fullerene nanoparticles will impart human and ecological effects. Humic acid and FBS, representative background organic species for each of these environments, were shown to alter the surface properties of fullerene nanoparticles and affect the interaction of this nanoparticle with living organisms. In this study, fullerene accumulation in lipids was significantly influenced by the presence of humic acid and FBS, but the impact of each depended on the composition of the lipid. With the positive lipid, DOTAP, fullerene coated with humic acid interacted more slowly with the lipid membrane but reached comparable accumulation levels relative to bare fullerene. For the zwitterion lipid (DOPC), both the rates and extent of partitioning was reduced in the presence of humic acid. In contrast, the presence of the negatively charged lipid, PG, did not have significant impacts on partitioning; however, the extent of partitioning into the lipid was minimal. In contrast to the humic acid coated fullerene, FBS coated fullerene did not yield the same extent of partitioning to the positive lipid, DOTAP, as bare fullerene, however, the accumulation level was higher than the accumulation of FBS coated fullerene and the other lipid membranes. Recent studies have shown that positive lipids can be used for gene therapy (Zhi et al. 2013). Thus, accumulation of fullerene in positive lipid membranes under environmentally and biologically relevant conditions has implications for biological applications of fullerene. With the zwitterion lipid (DOPC), both humic acid and FBS significantly reduced the amount of fullerene accumulated in

the lipid and both coatings affected the rates; however, the impact of FBS was greater. Considering the most prevalent lipid composition in living organism is zwitterion lipids, the results of this study can provide fundamental information to evaluate toxicity towards living organisms in real environments.

The effects of humic acid and FBS on cellular uptake of fullerene were also investigated. Results of this study have suggested that both humic acid and FBS decreased the quantitative mass of fullerene taken up by cells. The cellular uptake mechanism of nanoparticles into living cells is more complicated than the lipid accumulation mechanism: Using only lipid membrane components, we can envision passive adsorption and diffusion through lipid membranes, however, by evaluating cellular uptake using living cells, not only does passive diffusion impact rates of partitioning, but active transport (e.g., energy dependent endocytosis) is also likely. Thus, the results of this study indicate that humic acid and FBS affect fullerene transport through lipid membranes via active transport as well as passive diffusion.

To our knowledge, this is the first study to demonstrate how surface modification of fullerene in the presence of humic acid and FBS affects lipid accumulation as well as cellular uptake of this nanoparticle. In particular, the use of lipids of varying surface charge provides significant insight into the impact of natural organic matter (e.g., fulvic acid and polysaccharide) and biomacromolecules (e.g., lipids, other type of proteins) on bioavailability of fullerene nanoparticles.

6.5. REFERENCES

Baalousha, M. (2009) Aggregation and disaggregation of iron oxide nanoparticles: Influence of particle concentration, pH and natural organic matter. Sci Total Environ 407(6), 2093-2101.

Benn, T.M., Westerhoff, P. and Herckes, P. (2011) Detection of fullerenes (C_{60} and C_{70}) in commercial cosmetics. Environ Pollut 159(5), 1334-1342.

Bian, S.W., Mudunkotuwa, I.A., Rupasinghe, T. and Grassian, V.H. (2011) Aggregation and dissolution of 4 nm ZnO nanoparticles in aqueous environments: influence of pH, ionic strength, size, and adsorption of humic acid. Langmuir 27(10), 6059-6068.

Brant, J.A., Labille, J., Bottero, J.Y. and Wiesner, M.R. (2006) Characterizing the impact of preparation method on fullerene cluster structure and chemistry. Langmuir 22(8), 3878-3885.

Casey, A., Davoren, M., Herzog, E., Lyng, F.M., Byrne, H.J. and Chambers, G. (2007) Probing the interaction of single walled carbon nanotubes within cell culture medium as a precursor to toxicity testing. Carbon 45(1), 34-40.

Chen, C., Xing, G., Wang, J., Zhao, Y., Li, B., Tang, J., Jia, G., Wang, T., Sun, J., Xing, L., Yuan, H., Gao, Y., Meng, H., Chen, Z., Zhao, F., Chai, Z. and Fang, X. (2005) Multihydroxylated [Gd@$C_{82}(OH)_{22}$]n nanoparticles: antineoplastic activity of high efficiency and low toxicity. Nano Lett 5(10), 2050-2057.

Chen, Q., Yin, D., Li, J. and Hu, X. (2014) The effects of humic acid on the uptake and depuration of fullerene aqueous suspensions in two aquatic organisms. Environ Toxicol Chem 33(5), 1090-1097.

Cho, E.C., Xie, J., Wurm, P.A. and Xia, Y. (2009a) Understanding the role of surface charges in cellular adsorption versus internalization by selectively removing gold nanoparticles on the cell surface with a I_2/KI etchant. Nano Lett 9(3), 1080-1084.

Cho, M., Fortner, J.D., Hughes, J.B. and Kim, J.H. (2009b) Escherichia coli inactivation by water-soluble, ozonated C60 derivative: kinetics and mechanisms. Environ Sci Technol 43(19), 7410-7415.

Deguchi, S., Yamazaki, T., Mukai, S.A., Usami, R. and Horikoshi, K. (2007) Stabilization of C_{60} nanoparticles by protein adsorption and its implications for toxicity studies. Chem Res Toxicol 20(6), 854-858.

Dobrovolskaia, M.A. and McNeil, S.E. (2007) Immunological properties of engineered nanomaterials. Nat Nanotechnol 2(8), 469-478.

Ehrenberg, M.S., Friedman, A.E., Finkelstein, J.N., Oberdörster, G. and McGrath, J.L. (2009) The influence of protein adsorption on nanoparticle association with cultured endothelial cells. Biomaterials 30(4), 603-610.

Fabrega, J., Fawcett, S.R., Renshaw, J.C. and Lead, J.R. (2009) Silver nanoparticle impact on bacterial growth: effect of pH, concentration, and organic matter. Environ Sci Technol 43(19), 7285-7290.

Fan, J.Q., Fang, G., Zeng, F., Wang, X.D. and Wu, S.Z. (2013) Water-dispersible fullerene aggregates as a targeted anticancer prodrug with both chemo- and photodynamic therapeutic actions. Small 9(4), 613-621.

Friedman, S.H., Decamp, D.L., Sijbesma, R.P., Srdanov, G., Wudl, F. and Kenyon, G.L. (1993) Inhibition of the Hiv-1 Protease by Fullerene Derivatives - Model-Building Studies and Experimental-Verification. Journal of the American Chemical Society 115(15), 6506-6509.

Ghosh, S., Mashayekhi, H., Bhowmik, P. and Xing, B. (2010) Colloidal stability of Al_2O_3 nanoparticles as affected by coating of structurally different humic acids. Langmuir 26(2), 873-879.

Giri, K., Shameer, K., Zimmermann, M.T., Saha, S., Chakraborty, P.K., Sharma, A., Arvizo, R.R., Madden, B.J., McCormick, D.J., Kocher, J.P., Bhattacharya, R. and Mukherjee, P. (2014) Understanding protein-nanoparticle interaction: a new gateway to disease therapeutics. Bioconjug Chem 25(6), 1078-1090.

Guarnieri, D., Guaccio, A., Fusco, S. and Netti, P.A. (2011) Effect of serum proteins on polystyrene nanoparticle uptake and intracellular trafficking in endothelial cells. Journal of Nanoparticle Research 13(9), 4295-4309.

Ha, Y., Liljestrand, H.M. and Katz, L.E. (2013) Effects of lipid composition on partitioning of fullerene between water and lipid membranes. Water Sci Technol 68(2), 290-295.

Hou, W.C., Moghadam, B.Y., Corredor, C., Westerhoff, P. and Posner, J.D. (2012) Distribution of functionalized gold nanoparticles between water and lipid bilayers as model cell membranes. Environ Sci Technol 46(3), 1869-1876.

Hughes, G.A. (2005) Nanostructure-mediated drug delivery. Nanomedicine 1(1), 22-30.

Hyung, H. and Kim, J.H. (2009) Dispersion of C_{60} in natural water and removal by conventional drinking water treatment processes. Water Res 43(9), 2463-2470.

Kroto, H.W., Heath, J.R., O'Brein, S.C., Curl, R.F., Smalley, R.E. (1985) C_{60}: Buckminsterfullerene. Nature 318, 162-163.

Lesniak, A., Fenaroli, F., Monopoli, M.P., Aberg, C., Dawson, K.A. and Salvati, A. (2012) Effects of the presence or absence of a protein corona on silica nanoparticle uptake and impact on cells. ACS Nano 6(7), 5845-5857.

Li, Q., Xie, B., Hwang, Y.S. and Xu, Y. (2009) Kinetics of C_{60} fullerene dispersion in water enhanced by natural organic matter and sunlight. Environ Sci Technol 43(10), 3574-3579.

Lovern, S.B. and Klaper, R. (2006) Daphnia magna mortality when exposed to titanium dioxide and fullerene (C60) nanoparticles. Environ Toxicol Chem 25(4), 1132-1137.

Lynch, I. and Dawson, K.A. (2008) Protein-nanoparticle interactions. Nano Today 3(1-2), 40-47.

Lyon, D.Y., Adams, L.K., Falkner, J.C. and Alvarezt, P.J. (2006) Antibacterial activity of fullerene water suspensions: effects of preparation method and particle size. Environ Sci Technol 40(14), 4360-4366.

McMahon, D.P., Cheung, D.L. and Troisi, A. (2011) Why holes and electrons separate so Well in Polymer/Fullerene Photovoltaic Cells. Journal of Physical Chemistry Letters 2(21), 2737-2741.

Podolski, I.Y., Podlubnaya, Z.A., Kosenko, E.A., Mugantseva, E.A., Makarova, E.G., Marsagishvili, L.G., Shpagina, M.D., Kaminsky, Y.G., Andrievsky, G.V. and Klochkov, V.K. (2007) Effects of hydrated forms of C_{60} fullerene on amyloid 1-peptide fibrillization in vitro and performance of the cognitive task. J Nanosci Nanotechnol 7(4-5), 1479-1485.

Pycke, B.F., Benn, T.M., Herckes, P., Westerhoff, P. and Halden, R.U. (2011) Strategies for quantifying C_{60} fullerenes in environmental and biological samples and implications for studies in environmental health and ecotoxicology. Trends Analyt Chem 30(1), 44-57.

Saleh, N.B., Pfefferle, L.D. and Elimelech, M. (2010) Influence of biomacromolecules and humic acid on the aggregation kinetics of single-walled carbon nanotubes. Environ Sci Technol 44(7), 2412-2418.

Sayes, C.M., Gobin, A.M., Ausman, K.D., Mendez, J., West, J.L. and Colvin, V.L. (2005) Nano-C60 cytotoxicity is due to lipid peroxidation. Biomaterials 26(36), 7587-7595.

Thio, B.J., Zhou, D. and Keller, A.A. (2011) Influence of natural organic matter on the aggregation and deposition of titanium dioxide nanoparticles. J Hazard Mater 189(1-2), 556-563.

Wang, H.B., DeSousa, R., Gasa, J., Tasake, K., Stucky, G., Jousselme, B., Wudl, F. (2007) Fabrication of new fullerene composite membranes and their application in proton exchange membrane fuel cells. Jounal of membrane science 289(1-2), 277-283.

Wilhelm, C., Gazeau, F., Roger, J., Pons, J.N. and Bacri, J.C. (2002) Interaction of anionic superparamagnetic nanoparticles with cells: Kinetic analyses of

membrane adsorption and subsequent internalization. Langmuir 18(21), 8148-8155.

Xia, X.R., Monteiro-Riviere, N.A. and Riviere, J.E. (2006) Trace analysis of fullerenes in biological samples by simplified liquid-liquid extraction and high-performance liquid chromatography. J Chromatogr A 1129(2), 216-222.

Xie, B., Xu, Z., Guo, W. and Li, Q. (2008) Impact of natural organic matter on the physicochemical properties of aqueous C_{60} nanoparticles. Environ Sci Technol 42(8), 2853-2859.

Zhang, Y., Chen, Y., Westerhoff, P. and Crittenden, J. (2009) Impact of natural organic matter and divalent cations on the stability of aqueous nanoparticles. Water Res 43(17), 4249-4257.

Zhi, D., Zhang, S., Cui, S., Zhao, Y., Wang, Y. and Zhao, D. (2013) The headgroup evolution of cationic lipids for gene delivery. Bioconjug Chem 24(4), 487-519.

Zhu, Y., Li, W.X., Li, Q.N., Li, Y.G., Li, Y.F., Zhang, X.Y. and Huang, Q. (2009) Effects of serum proteins on intracellular uptake and cytotoxicity of carbon nanoparticles. Carbon 47(5), 1351-1358.

Chapter 7: Conclusions and recommendations

7.1. CONCLUSIONS

Engineered nanomaterials (ENMs) have appeared as emerging contaminants in the environment because production of ENMs has rapidly increased and the presence of these materials in the environment may have significant consequences with respect to human and ecological health. However, the potential harmful effects of ENMs to ecosystems and humans are still under debate due to the significantly different physical/chemical properties of nanoparticles compared to molecular level chemicals. Carbon fullerene was chosen as a representative ENM to address one of the major concerns with respect to ENMs, namely, bioavailability. The primary objectives of this research were to evaluate the bioavailability of aqueous fullerene dispersions by developing a more complete understanding of 1) partitioning of fullerene in lipid/water systems and, 2) the cellular uptake of fullerene.

To review, hypotheses tested in this dissertation were:

- Hypothesis I: The lipid water partitioning coefficients (K_{lipw}) of fullerene are affected by lipid composition.
- Hypothesis II: The lipid water partitioning mechanism of fullerene is different from that of molecular level chemicals and these differences can be explained by partitioning thermodynamics.
- Hypothesis III: Fullerene can be transported into the cell membrane via active transport.

- Hypothesis IV: Lipid accumulation and cellular uptake of fullerene are affected by the presence of natural organic matter and biological macromolecules under environmentally relevant conditions.

Partitioning between water and lipid membranes has been successfully used for evaluating bio-accumulation of molecular level chemicals. Lipid-water partitioning coefficients (K_{lipw}) of molecular level chemicals were measured by an equilibrium dialysis technique, however, this technique cannot be applied for measuring K_{lipw} of nanoparticles due to the aggregation of those materials. In Chapter 3, we developed a new technique to measure K_{lipw} of fullerene nanoparticles using solid supported lipid membranes (SSLMs) with different membrane composition. The major findings from Chapter 3 are listed below.

- Solid supported lipid membranes (SSLMs) were successfully synthesized in our lab. We confirmed that silica microspheres were uniformly coated with lipid bilayers using confocal microscopy of fluorescently labeled lipids.
- Log K_{lipw} (L/kg) values of fullerene with three different zwitterion unsaturated lipids ranged from 3.1 to 5.3, which are generally consistent with reported bioconcentration factors (BCF) of fullerene in previous studies.
- K_{lipw} values of fullerene increased with increasing temperature regardless of lipid membrane composition. Increasing temperature causes thermal changes to the lipid membrane, which may result in increasing partitioning values.
- K_{lipw} values of fullerene were higher with zwitterion unsaturated lipids composed of longer acyl chains. Stronger hydrophobic interactions between fullerene and lipids with longer acyl chains can contribute to higher partitioning values.

- The relationship between reported octanol-water partition coefficient (K_{ow}) and unsaturated lipid-water partitioning of hydrophobic molecular chemicals (K_{lipw}) was not applicable to fullerene. This result implies that the partitioning mechanism of fullerene is different from that of molecular level chemicals.

In Chapter 4, we used the *in vitro* method developed in Chapter 3 to investigate the effects of membrane composition on partitioning of fullerene as well as partitioning thermodynamics. In Chapter 4, three unsaturated lipids with different head charges were selected for investigating the effects of electrostatic forces between fullerene and lipids on the K_{lipw} values. In addition, ternary lipid mixtures were used to mimic actual cell membrane composition. The major conclusions from Chapter 4 are as follows:

- The K_{lipw} value of fullerene with a positively charged lipid membrane was significantly higher than that with either the zwitterion or negatively charged lipid membranes. Due to the negative surface charge of the fullerene dispersions in water, strong electrostatic interactions between fullerene dispersions and positive lipid head groups yielded a higher K_{lipw} value.
- With ternary lipid membranes consisting of a saturated lipid, an unsaturated lipid, and cholesterol, higher K_{lipw} values were obtained after phase separation. After phase separation, the surface area covered by the lipid molecules increased, which led to higher K_{lipw} values.
- Partitioning thermodynamics of fullerene between lipid and water were determined using the van't Hoff equation. The partitioning of fullerene with unsaturated lipids was driven by entropy ($\Delta S > 0$) and the process was endothermic ($\Delta H > 0$).

- Partitioning thermodynamics of fullerene were significantly different from reported thermodynamics of molecular level chemicals, indicating that the partitioning mechanism of fullerene differs from that of molecular chemicals. Here, we suggested that a combination of adsorption and absorption can be a plausible partitioning process of fullerene into lipid membranes.

In Chapters 3 and 4, we investigated fullerene interactions with synthetic lipid membranes, which can describe the passive adsorption and diffusion of fullerene into lipid membranes. However, active transport, which is an energy dependent process, can also be an important process for transport of nanoparticles through lipid membranes. In Chapter 5, we developed another *in vitro* method to perform experiments examining cellular uptake of fullerene nanoparticles. The main objective of Chapter 5 was to elucidate the main transport mechanism of fullerene through lipid membranes (passive *vs.* active transport) using Caco-2 cell lines. We reached the main conclusions listed below.

- The cellular uptake of fullerene was temperature dependent; more fullerene nanoparticles were taken up by cells at 37 °C compared to the mass of fullerene taken up by cells at 4 °C. Higher molecular diffusivity, more fullerene adsorption on the cell surface, and energy dependent active transport at 37 °C can be responsible for this temperature dependence.
- Lower cellular uptake was obtained at higher concentrations, and a plateau in cellular uptake was observed at relatively low concentrations. These results suggest that there are a limited number of binding sites on the cell surface, which suggests that a key mechanism of fullerene uptake at low concentration is active transport.

- Metabolic inhibitors (e.g., sodium azide and 2,4 dinitophenol) partly reduced the cellular uptake of fullerene. This result indicates that both passive diffusion and active transport contribute to fullerene nanoparticle transport through lipid membranes.
- A Microtubule inhibitor (e.g., nocodazole) also decreased the mass of fullerene taken up by cells. This result suggests that the microtubule transport, which is one of the active transport mechanisms, is also responsible for the cellular uptake of fullerene. We also demonstrated that the microtubule transport depends on surface characteristics of fullerene that may change over time possibly due to adsorption of OH^- on the fullerene surface.

When fullerene nanoparticles are released into natural aquatic and biological environments, surface modification of fullerene can occur due to coating of fullerene with environmentally relevant matrices such as natural organic matter and macro biomolecules. In Chapter 3, bioavailability of fullerene under environmentally relevant conditions was investigated. In particular, in the presence of humic acid or fetal bovine serum (FBS), we performed lipid accumulation and cellular uptake experiments, using the *in vitro* methods developed in Chapter 3 and Chapter 5, respectively. The conclusions from these experiments are as follows:

- Both humic acid and FBS significantly increased the stability of fullerene nanoparticles implying that fullerene nanoparticles can be coated with humic acid and FBS. Fullerene incubated with humic acid have more negatively charge than bare fullerene.
- The effect of humic acid on bioaccumulation of fullerene depends on the head charges of the lipid membrane. For positive lipids, bioaccumulation of

fullerene coated with humic acid is not significantly different from that of bare fullerene. However, when zwitterion and negative lipids are employed on SSLMs, the presence of humic acid effectively decreased the bioaccumulation values of fullerene.

- With zwitterion and negative lipid membranes, the presence of FBS also decreased fullerene affinity for the lipid membranes, and the affinity of FBS coated fullerene was much lower than that of humic acid coated fullerene due to the higher steric repulsion created by FBS coatings on fullerene.
- Both humic acid and FBS significantly lowered the amount of fullerene taken up by Caco-203 cells. Fullerene exhibits greater steric hindrance and less surface energy when coated with humic acid and FBS. Thus, fewer fullerene particles are adsorbed onto the cell surface in the presence of humic acid and FBS, which results in reduced cellular uptake.

7.2. RECOMMENDATIONS FOR FUTURE RESEARCH

This research has demonstrated that the lipid-water partitioning of fullerene is significantly different from that of traditional molecular level chemicals. In addition, we suggested that the main cellular uptake mechanism of fullerene is active transport, which is different from the main transport mechanism of molecular level chemicals (e.g., passive transport). We successfully developed *in vitro* methods to investigate lipid-water partitioning and the cellular uptake mechanism of fullerene. While partitioning thermodynamics indirectly inferred that the lipid water partitioning mechanism of fullerene is a combination of adsorption and absorption, we did not directly observe the absorption of fullerene into lipid bilayers. In addition, while cellular uptake tests provided the insights for the cellular uptake mechanism of fullerene, the *in vitro* method used in

this study cannot distinguish adsorbed fullerene onto the cell surface and fullerene internalized into the cell. Thus, the following recommendations for future research are related to the direct observation and refined experimental methods to elucidate the lipid membranes partitioning and transport mechanism of fullerene.

1) *Direct observation of fullerene located in the acyl chains of lipid membranes*: In Chapter 4, we hypothesized that fullerene nanoparticles first adhere on the lipid head groups (i.e., adsorption), and then, they can be located into the lipid membranes (i.e. absorption). TEM images (Figure 4.3, Figure 4.4) clearly show that fullerene adsorbs on the lipid surface. However, it is impossible to take TEM images of fullerene located inside the lipid bilayer because the thickness of the lipid bilayer is very small (4~5 nm) compared to the size of silica microspheres (diameter: 5 μm) which are used as solid for solid supported lipid membranes (SSLMs). Therefore, it will be important to develop a method for direct visualization of fullerene that is located inside the lipid bilayer to confirm the absorption mechanism of fullerene through the lipid membranes. We can suggest two possible methods for that: 1) take images by cryo-TEM, and 2) take fluorescent images of fluorescently labeled fullerene derivatives. Cryo-TEM can be used to confirm the molecular level lipid bilayers. Indeed, lipid bilayer in SSLMs successfully confirmed by cryo-TEM in previous studies (Gopalakrishnan et al. 2009, Mornet et al. 2005). Once cryo-TEM can focus on the lipid bilayer of SSLMs, fullerene which is located inside the lipid membranes can be easily seen. The other method is to obtain fluorescent images. In Chapter 3, we confirmed that in SSLMs, silica microspheres are uniformly coated with lipid bilayers with a help of fluorescently labeled lipid probe which color is red. If we can synthesize a fluorescently labeled fullerene derivative which has a different color, then fullerene imbedded inside the lipid membranes will be easily

seen using confocal microscopy. In this case, the physicochemical properties of fluorescently labeled fullerene derivatives should be similar to those of bare fullerene.

2) *Investigation of Caco-2 cell membrane permeation of fullerene*: In Chapter 6, the cellular uptake mechanism of fullerene was proposed: First fullerene adsorbed on the cell surface followed by internalization into the cells by energy dependent endocytosis. However, we cannot differentiate the fullerene that adhered on the cell surface from that internalized into cells. Here, we suggest the method for estimating membrane permeation of fullerene through Caco-2 cell monolayer. For the permeation study, Caco-2 cells will be seeded into Transwell™ microporous cell culture inserts and cultured for at least 21 days at 37 °C in a 5 % CO_2 to reach cell confluency. The integrity of the cell monolayer should be monitored by Trans Epithelial Electrical resistance (TEER). Figure 7.1 shows a diagram of Caco-2 monolayer on the Transwell™ filters, which can be used for the transport study.

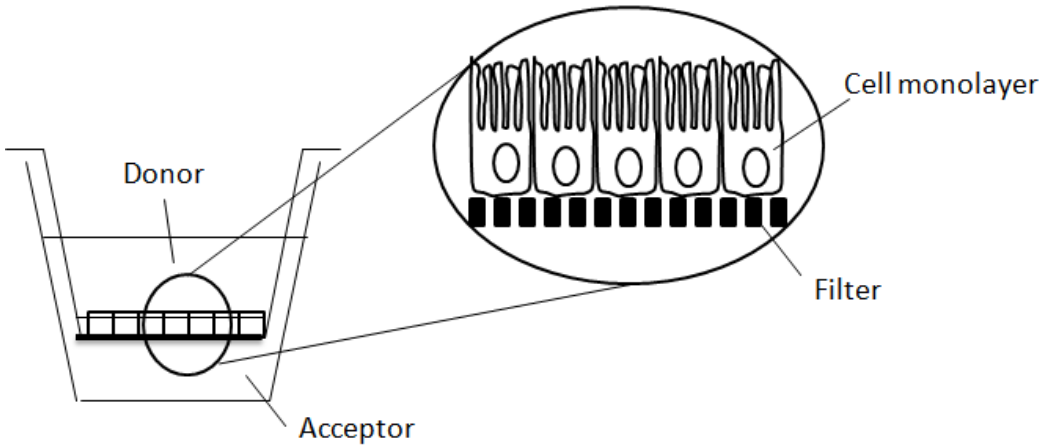

Figure 7.1: Diagram of Caco-2 monolayer on the Transwell™ filters

Fullerene aggregations in the cell culture medium are added to the donor chamber and cell culture medium without fullerenes is added to the acceptor chamber in Figure 7.1.

If fullerene can be detected in acceptor chambers, this can provide significant evidence that fullerene can transport through cell monolayer, not just adhere on the cell surface. In addition, this permeation study using Caco-2 cells has been widely used to investigate the cellular transport mechanism of various chemicals from molecular level chemicals (Hidalgo and Borchardt 1990, Pade and Stavchansky 1997) to nanoparticles (Lin et al. 2012). Thus, by using membrane permeation study, we can also confirm that the main cellular transport mechanism of fullerene is active transport.

7.3. REFERENCES

Gopalakrishnan, G., Rouiller, I., Colman, D.R. and Lennox, R.B. (2009) Supported bilayers formed from different phospholipids on spherical silica substrates. Langmuir 25(10), 5455-5458.

Hidalgo, I.J. and Borchardt, R.T. (1990) Transport of a large neutral amino acid (phenylalanine) in a human intestinal epithelial cell line: Caco-2. Biochim Biophys Acta 1028(1), 25-30.

Lin, I.C., Liang, M., Liu, T.Y., Monteiro, M.J. and Toth, I. (2012) Cellular transport pathways of polymer coated gold nanoparticles. Nanomedicine 8(1), 8-11.

Mornet, S., Lambert, O., Duguet, E. and Brisson, A. (2005) The formation of supported lipid bilayers on silica nanoparticles revealed by cryoelectron microscopy. Nano Lett 5(2), 281-285.

Pade, V. and Stavchansky, S. (1997) Estimation of the relative contribution of the transcellular and paracellular pathway to the transport of passively absorbed drugs in the Caco-2 cell culture model. Pharm Res 14(9), 1210-1215.

Appendix A. Analytical method for fullerene

HPLC PROTOCOL FOR MEASURING FULLERENE CONCENTRATION

Fullerene concentrations in toluene were measured by a Waters 2690 high performance liquid chromatography (HPLC) equipped with a Waters 996 photodiode array detector (Milford, MA). Mixture of hexane (70 %) and isopropyl alcohol (30 %) was used as an eluent. YMC-ODS-A column (5 µm, 6.0 × 150 mm, 120 Å, Allentown, PA) was used. With 382.6 nm UV wavelength, retention time for the fullerene detection is 6.5~7 min. The concentrations are proportional to the area of the peaks. With fullerene concentration ranged from 0.1 µM (0.084 mg/L) to 23 µM (16.8 mg/L), the R^2 of calibration curve was 0.9998 (Figure A-1).

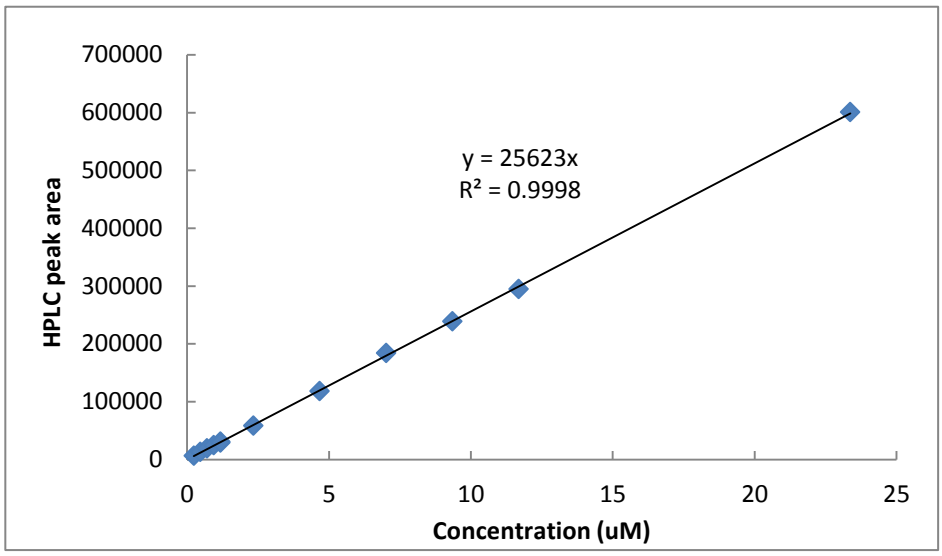

Figure A-1: Calibration curve for HPLCdetection of fullerene concentration (0.1 µM – 23 µM)

To determine the method detection limit (MDL), 7 samples at the low concentrations ranged from 0.1 µM (0.072 mg/L) to 2.3 µM (1.66 mg/L) were used

(Figure A-2). The standard deviation for these samples was 581.81 and slope for the calibration curve was 25302. The MDL for this method was calculated as 0.076 μM (0.054 mg/L) using equation (A-1).

$$MDL = (\text{standard deviation (STEYX)/slope}) \times 3.3 \qquad \text{(A-1)}$$

The reported fullerene concentration in water environments are ranged from 0.002 – 0.12 ng/L (Boxall et al. 2008, Gottschalk et al. 2009) , which are lower than MDL of this study. Thus, fullerene concentrations used in this study were higher than fullerene concentrations in the natural water environments.

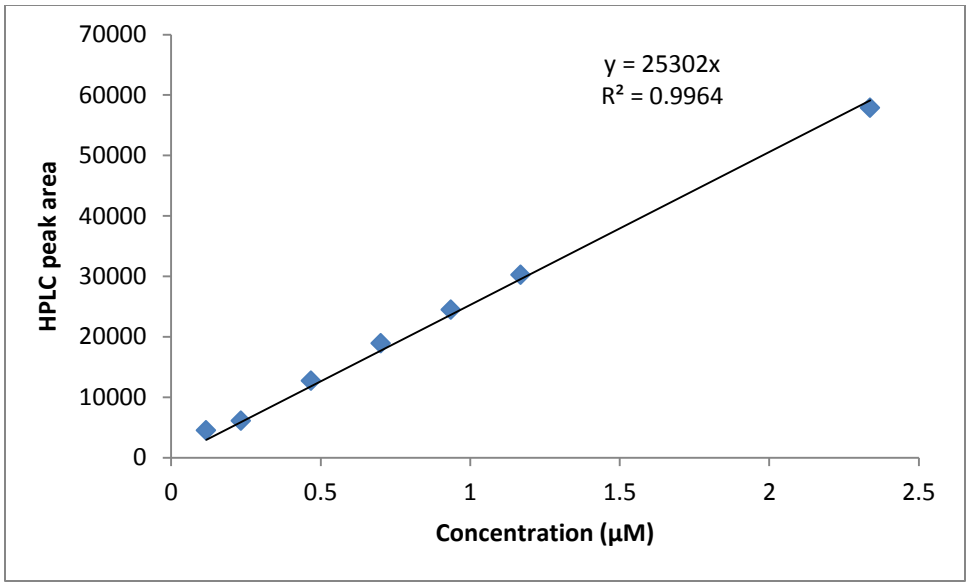

Figure A-2: Calibration curve for calculating method detection limit (MDL)

METHOD FOR LIQUID EXTRACTION OF FULLERENE

Fullerene concentrations in the water phase were extracted to a toluene phase using a liquid extraction method. 1 mL of fullerene suspensions in the water phase were first destabilized with 0.4 mL of 0.1 M $Mg(ClO_4)_2$, then 1 mL of toluene was added followed by vigorous mixing. $Mg(ClO_4)_2$ has been prevalently used for the liquid

extraction of fullerene, and it was reported that extraction recovery reached 100 % by using this destabilized material (Hyung and Kim 2009b) . We confirmed that HPLC peaks of fullerene concentrations in toluene phase increased with increasing fullerene concentrations in water phase (Figure A-3), and R^2 of this linear regression was 0.9965. For the liquid extraction of fullerene in solutions containing biomolecules and humic acid, 2.5 mL of glacier acetic acid (GAA) was additionally used to prevent emulsions.

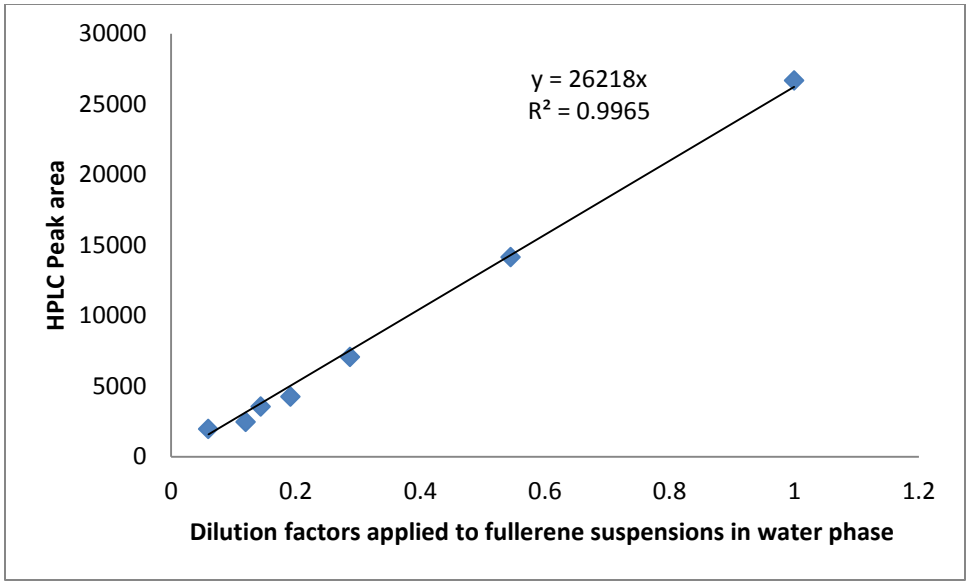

Figure A-3: Calibration curve for HPLC detection of fullerene in toluene phase after liquid extraction of fullerene in water phase.

We confirmed that after liquid extraction, fullerene in the toluene phase exists as molecular fullerene, not fullerene aggregates by taking TEM images. As shown in Figure A-4(a), fullerene aggregates in the water phase were easily observed in TEM images. However, in the toluene phase, we could not find any fullerene aggregates (Figure A-4(b)). This suggests that liquid extraction lead fullerene aggregates to break down and produce molecular fullerene in the toluene phase.

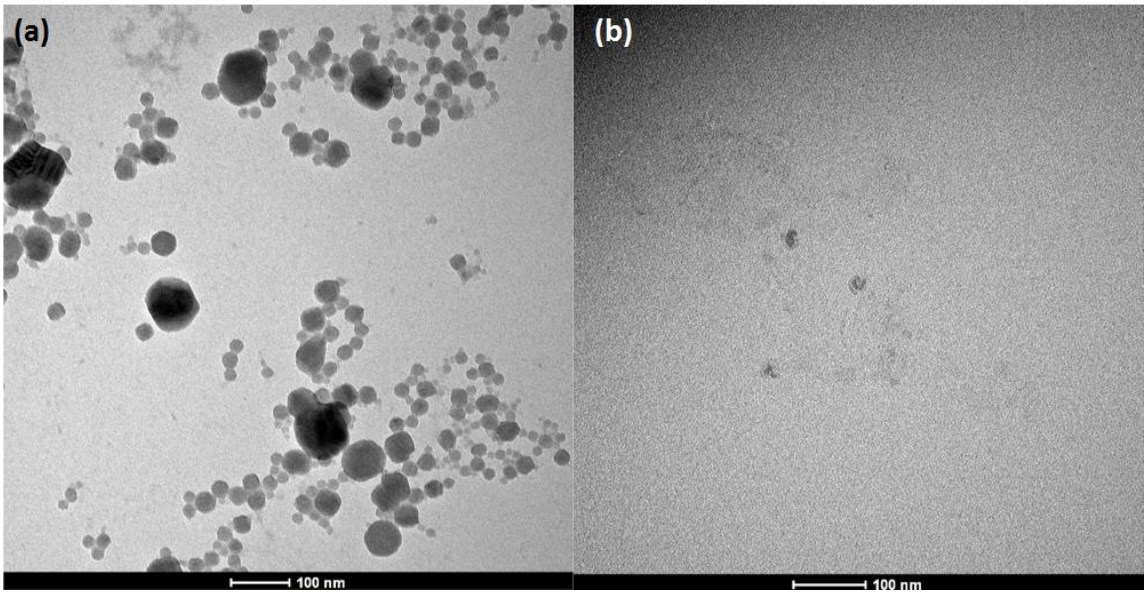

Figure A-4: TEM images of fullerene in (a) water phase before liquid extraction and (b) toluene phase after liquid extraction. Scales bar indicates 100 nm.

Appendix B. Pooled t test for investigating effects of inhibitors on cellular uptake of fullerene

To investigate the effects of inhibitors on cellular uptake of fullerene, we utilized a hypothesis testing using pooled data from five separate experiments (two for simultaneous addition of the fullerene, cells and inhibitors; one for addition of the cells and inhibitors 7 days after the fullerene was added to distilled water; and two for 14 day fullerene/water incubation prior to addition of the cells and the inhibitors). For each test, we prepared triplicate samples. Thus, total number of samples is 15. The mass of fullerene taken by cells for each test with or without inhibitors are shown in Table A-1. The t-statistic was used to evaluate the hypothesis of equal means between control samples without inhibitors and samples with inhibitors.

Table A-1: Mass of cellular uptake of fullerene in the presence of three different inhibitors for fullerene injections of 6 μg and 4 μg for test 1-3 and test 4-5, respectively. Results for tests1-3 are presented in Figure 5.6.

mass (μg)	Control	sodium azide	2,4 dinitrophenol	nocodazole
test1	1.947	1.068	0.989	1.107
	1.243	1.971	1.112	1.220
	2.135	1.463	1.604	1.494
test 2	1.998	1.520	0.819	0.583
	2.075	1.535	1.660	0.644
	1.797	1.528	1.012	0.548
test 3	1.144	0.425	0.321	0.339
	0.512	0.661	0.358	0.332
	0.681	0.322	0.372	0.630
test 4	2.512	1.104	2.201	1.749
	1.305	1.343	2.108	1.900
	2.891	1.735	1.556	1.095
test 5	1.348	1.229	1.101	0.583
	1.966	1.540	1.474	1.531
	1.660	1.467	1.995	0.517
average	1.681	1.261	1.246	0.951

For applying the t-test, two assumptions were applied: (1) all distributions are normal, and (2) the population variances $\sigma_{control}$ and $\sigma_{inhibitors}$ are equal. First we calculated a pooled estimator of the common variance s^2_{pooled} using equation (A-3).

$$S^2_{pooled} = \frac{\sum_{i=1}^{n_1}(x_i - \bar{x})^2 + \sum_{i=1}^{n_2}(y_i - \bar{y})^2}{n_1 + n_2 - 4} \qquad \text{(A-3)}$$

Where x_i values are the individual data for control cells, y_i values are the individual data for cells incubated with each inhibitor, $\bar{x}$ is the average of data for control cells, $\bar{y}$ is the average of data for samples with added inhibitor, and n_1 and n_2 are the number of control cells and samples with inhibitor, respectively (n_1=n_2=15). We used a value of 26 for the degrees of freedom (=15+15-4).

The test statistic, *t,* was calculated using equation (A-4) for all three inhibitors.

$$t = \frac{\bar{x} - \bar{y}}{s_{pooled}\sqrt{\frac{1}{n_1} + \frac{1}{n_2}}} \qquad \text{(A-4)}$$

t values for three inhibitors, sodium azide, 2,4 dinitro phenol, and nocodazole were 1.96, 1.81, and 3.26, respectively. The value of $t_{0.05}$ for 26 degree of freedom is 1.706. Thus, $t > t_{0.05}$, indicates that the mean value of the data for the control samples is significantly different from that with an inhibitor. Therefore, this result suggests that inhibitors used in this study significantly lowered the fullerene uptake by cells, indicating that active transport contributes to cellular transport of fullerene.

REFERENCES

Andrievsky, G.V., Kosevich, M.V., Vovk, O.M., Shelkovsky, V.S. and Vashchenko, L.A. (1995) On the production of an aqueous colloidal solution of fullerenes. J Chem Soc Chem Commun (12), 1281-1282.

Antunes-Madeira, M.C. and Madeira, V.M. (1987) Partition of malathion in synthetic and native membranes. Biochim Biophys Acta 901(1), 61-66.

Arnaud, C.H. (2009) Simulating Life's Envelopes. Chemical & Engineering News 87(6), 31-33.

Arts, M.T., Brett, M.T. and Kainz, M.J. (2009) Lipids in aquatic ecosystems, Springer, Dordrecht ; New York.

Ávila, C.M. and Martínez, F. (2003) Thermodynamics of partitioning of benzocaine in some organic solvent/buffer and liposome systems. Chem Pharm Bull (Tokyo) 51(3), 237-240.

Baalousha, M. (2009) Aggregation and disaggregation of iron oxide nanoparticles: Influence of particle concentration, pH and natural organic matter. Sci Total Environ 407(6), 2093-2101.

Baksh, M.M., Jaros, M. and Groves, J.T. (2004) Detection of molecular interactions at membrane surfaces through colloid phase transitions. Nature 427(6970), 139-141.

Bayerl, T.M. and Bloom, M. (1990) Physical properties of single phospholipid bilayers adsorbed to micro glass beads. A new vesicular model system studied by 2H-nuclear magnetic resonance. Biophys J 58(2), 357-362.

BCC Research (2006) Accessed on http://www.bccresearch.com/

Becker, L., Bada, J.L., Winans, R.E. and Bunch, T.E. (1994) Fullerenes in Allende meteorite. Nature 372(6506), 507.

Bedrov, D., Smith, G.D., Davande, H. and Li, L. (2008) Passive transport of C_{60} fullerenes through a lipid membrane: a molecular dynamics simulation study. J Phys Chem B 112(7), 2078-2084.

Benn, T.M., Westerhoff, P. and Herckes, P. (2011) Detection of fullerenes (C_{60} and C_{70}) in commercial cosmetics. Environ Pollut 159(5), 1334-1342.

Bian, S.W., Mudunkotuwa, I.A., Rupasinghe, T. and Grassian, V.H. (2011) Aggregation and dissolution of 4 nm ZnO nanoparticles in aqueous environments: influence of pH, ionic strength, size, and adsorption of humic acid. Langmuir 27(10), 6059-6068.

Boxall, A.B.A., Chaudhry, Q., Jones, A., Jefferson, B. and Watts, C.D. (2008) Current and future predicted environmental exposure to engineered nanoparticles, Central Science Laboratory, Sand Hutton, UK.

Brant, J., Lecoanet, H. and Wiesner, M.R. (2005) Aggretagion and deposition characteristics of fullerene nanoparticles in aqueous systems. Journal of Nanoparticle Research 7, 545-553.

Brant, J.A., Labille, J., Bottero, J.Y. and Wiesner, M.R. (2006) Characterizing the impact of preparation method on fullerene cluster structure and chemistry. Langmuir 22(8), 3878-3885.

Brown, D.A. and London, E. (2000) Structure and function of sphingolipid- and cholesterol-rich membrane rafts. J Biol Chem 275(23), 17221-17224.

Buesen, R., Mock, M., Nau, H., Seidel, A., Jacob, J. and Lampen, A. (2003) Human intestinal Caco-2 cells display active transport of benzo[a]pyrene metabolites. Chem Biol Interact 142(3), 201-221.

Buffle, J. and Leppard, G.G. (1995) Characterization of aquatic colloids and macromolecules. 1. Structure and behavior of colloidal material. Environ Sci Technol 29(9), 2169-2175.

Cagle, D.W., Kennel, S.J., Mirzadeh, S., Alford, J.M. and Wilson, L.J. (1999) *In vivo* studies of fullerene-based materials using endohedral metallofullerene radiotracers. Proc Natl Acad Sci USA 96(9), 5182-5187.

Camenisch, G., Alsenz, J., van de Waterbeemd, H. and Folkers, G. (1998) Estimation of permeability by passive diffusion through Caco-2 cell monolayers using the drugs' lipophilicity and molecular weight. Eur J Pharm Sci 6(4), 317-324.

Casey, A., Davoren, M., Herzog, E., Lyng, F.M., Byrne, H.J. and Chambers, G. (2007) Probing the interaction of single walled carbon nanotubes within cell culture medium as a precursor to toxicity testing. Carbon 45(1), 34-40.

Chae, S.R., Badireddy, A.R., Farner Budarz, J., Lin, S., Xiao, Y., Therezien, M. and Wiesner, M.R. (2010) Heterogeneities in fullerene nanoparticle aggregates affecting reactivity, bioactivity, and transport. ACS Nano 4(9), 5011-5018.

Chen, C., Xing, G., Wang, J., Zhao, Y., Li, B., Tang, J., Jia, G., Wang, T., Sun, J., Xing, L., Yuan, H., Gao, Y., Meng, H., Chen, Z., Zhao, F., Chai, Z. and Fang, X. (2005) Multihydroxylated [Gd@$C_{82}(OH)_{22}$]n nanoparticles: antineoplastic activity of high efficiency and low toxicity. Nano Lett 5(10), 2050-2057.

Chen, K.L. and Elimelech, M. (2007) Influence of humic acid on the aggregation kinetics of fullerene (C_{60}) nanoparticles in monovalent and divalent electrolyte solutions. J Colloid Interface Sci 309(1), 126-134.

Chen, K.L. and Elimelech, M. (2008) Interaction of fullerene (C_{60}) nanoparticles with humic acid and alginate coated silica surfaces: measurements, mechanisms, and environmental implications. Environ Sci Technol 42(20), 7607-7614.

Chen, Q., Yin, D., Li, J. and Hu, X. (2014) The effects of humic acid on the uptake and depuration of fullerene aqueous suspensions in two aquatic organisms. Environ Toxicol Chem 33(5), 1090-1097.

Chen, Z., Westerhoff, P. and Herckes, P. (2008) Quantification of C_{60} fullerene concentrations in water. Environ Toxicol Chem 27(9), 1852-1859.

Chiantia, S., Ries, J., Kahya, N. and Schwille, P. (2006) Combined AFM and two-focus SFCS study of raft-exhibiting model membranes. Chemphyschem 7(11), 2409-2418.

Chithrani, B.D. and Chan, W.C. (2007) Elucidating the mechanism of cellular uptake and removal of protein-coated gold nanoparticles of different sizes and shapes. Nano Lett 7(6), 1542-1550.

Chithrani, B.D., Ghazani, A.A. and Chan, W.C. (2006) Determining the size and shape dependence of gold nanoparticle uptake into mammalian cells. Nano Lett 6(4), 662-668.

Cho, E.C., Xie, J., Wurm, P.A. and Xia, Y. (2009a) Understanding the role of surface charges in cellular adsorption versus internalization by selectively removing gold nanoparticles on the cell surface with a I_2/KI etchant. Nano Lett 9(3), 1080-1084.

Cho, M., Fortner, J.D., Hughes, J.B. and Kim, J.H. (2009b) *Escherichia coli* inactivation by water-soluble, ozonated C_{60} derivative: kinetics and mechanisms. Environ Sci Technol 43(19), 7410-7415.

Cho, M., Snow, S.D., Hughes, J.B. and Kim, J.H. (2011) *Escherichia coli* Inactivation by UVC-Irradiated C_{60}: kinetics and mechanisms. Environ Sci Technol 45(22), 9627-9633.

Dausend, J., Musyanovych, A., Dass, M., Walther, P., Schrezenmeier, H., Landfester, K. and Mailander, V. (2008) Uptake mechanism of oppositely charged fluorescent nanoparticles in HeLa cells. Macromol Biosci 8(12), 1135-1143.

Davda, J. and Labhasetwar, V. (2002) Characterization of nanoparticle uptake by endothelial cells. Int J Pharm 233(1-2), 51-59.

Deguchi, S., Alargova, R.G. and GTsujii, K. (2001) Stable dispersions of fullerenes, C_{60} and C_{70} in water. Preparation and characterization. Langmuir 17, 6013-6017.

Deguchi, S., Yamazaki, T., Mukai, S.A., Usami, R. and Horikoshi, K. (2007) Stabilization of C_{60} nanoparticles by protein adsorption and its implications for toxicity studies. Chem Res Toxicol 20(6), 854-858.

Dietrich, C., Bagatolli, L.A., Volovyk, Z.N., Thompson, N.L., Levi, M., Jacobson, K. and Gratton, E. (2001) Lipid rafts reconstituted in model membranes. Biophys J 80(3), 1417-1428.

Dill, K.A. and Stigter, D. (1988) Lateral interactions among phosphatidylcholine and phosphatidylethanolamine head groups in phospholipid monolayers and bilayers. Biochemistry 27(9), 3446-3453.

Dobrovolskaia, M.A. and McNeil, S.E. (2007) Immunological properties of engineered nanomaterials. Nat Nanotechnol 2(8), 469-478.

dos Santos, T., Varela, J., Lynch, I., Salvati, A. and Dawson, K.A. (2011) Effects of transport inhibitors on the cellular uptake of carboxylated polystyrene nanoparticles in different cell lines. PLoS One 6(9), e24438.

Dresselhaus, M.S., Dresselhaus, G. and Eklund, P.C. (1996) Science of fullerenes and carbon nanotubes, Academic Press, San Diego.

Ehrenberg, M.S., Friedman, A.E., Finkelstein, J.N., Oberdörster, G. and McGrath, J.L. (2009) The influence of protein adsorption on nanoparticle association with cultured endothelial cells. Biomaterials 30(4), 603-610.

Eletskii, A.V. and Smirnov, B.M. (1995) Fullerenes and carbon structures. Physics-Uspekhi 38(9), 935-964.

Escher, B.I., Schwarzenbach, R.P. and Westall, J.C. (2000) Evaluation of liposome-water partitioning of organic acids and bases. 1. Development of a sorption model. Environ Sci Technol 34(18), 3954-3961.

Fabrega, J., Fawcett, S.R., Renshaw, J.C. and Lead, J.R. (2009) Silver nanoparticle impact on bacterial growth: effect of pH, concentration, and organic matter. Environ Sci Technol 43(19), 7285-7290.

Fan, J.Q., Fang, G., Zeng, F., Wang, X.D. and Wu, S.Z. (2013) Water-dispersible fullerene aggregates as a targeted anticancer prodrug with both chemo- and photodynamic therapeutic actions. Small 9(4), 613-621.

Farkas, J., Christian, P., Gallego-Urrea, J.A., Roos, N., Hassellov, M., Tollefsen, K.E. and Thomas, K.V. (2011) Uptake and effects of manufactured silver nanoparticles in rainbow trout (Oncorhynchus mykiss) gill cells. Aquat Toxicol 101(1), 117-125.

Farré, M., Pérez, S., Gajda-Schrantz, K., Osorio, V., Kantiani, L., Ginerbreda, A. and Barceló, D. (2010) First determination of C_{60} an C_{70} fullerenes and N-methylfulleropyrrolidine C60 on the suspended materaisl of wastwater effluents by liquid chromatography hybrid quadrupole linear ion trap tandem mass spectrometry. Journal of Hydrology 383, 44-51.

Feng, Z.V., Spurlin, T.A. and Gewirth, A.A. (2005) Direct visualization of asymmetric behavior in supported lipid bilayers at the gel-fluid phase transition. Biophys J 88(3), 2154-2164.

Foley, S., Crowley, C., Smaihi, M., Bonfils, C., Erlanger, B.F., Seta, P. and Larroque, C. (2002) Cellular localisation of a water-soluble fullerene derivative. Biochem Biophys Res Commun 294(1), 116-119.

Fortner, J.D., Lyon, D.Y., Sayes, C.M., Boyd, A.M., Falkner, J.C., Hotze, E.M., Alemany, L.B., Tao, Y.J., Guo, W., Ausman, K.D., Colvin, V.L. and Hughes, J.B. (2005) C_{60} in water: nanocrystal formation and microbial response. Environ Sci Technol 39(11), 4307-4316.

Friedman, S.H., Decamp, D.L., Sijbesma, R.P., Srdanov, G., Wudl, F. and Kenyon, G.L. (1993) Inhibition of the Hiv-1 Protease by Fullerene Derivatives - Model-Building Studies and Experimental-Verification. Journal of the American Chemical Society 115(15), 6506-6509.

Frontier Carbon Corporation (2012) Accessed on http://www.f-carbon.com/eng/.

Gao, X., Wang, T., Wu, B., Chen, J., Chen, J., Yue, Y., Dai, N., Chen, H. and Jiang, X. (2008) Quantum dots for tracking cellular transport of lectin-functionalized nanoparticles. Biochem Biophys Res Commun 377(1), 35-40.

Garcia-Saez, A.J., Chiantia, S. and Schwille, P. (2007) Effect of line tension on the lateral organization of lipid membranes. J Biol Chem 282(46), 33537-33544.

Gharbi, N., Pressac, M., Hadchouel, M., Szwarc, H., Wilson, S.R. and Moussa, F. (2005) [60]fullerene is a powerful antioxidant in vivo with no acute or subacute toxicity. Nano Lett 5(12), 2578-2585.

Ghinea, N. and Simionescu, N. (1985) Anionized and cationized hemeundecapeptides as probes for cell surface charge and permeability studies: differentiated labeling of endothelial plasmalemmal vesicles. J Cell Biol 100(2), 606-612.

Ghosh, S., Mashayekhi, H., Bhowmik, P. and Xing, B. (2010) Colloidal stability of Al_2O_3 nanoparticles as affected by coating of structurally different humic acids. Langmuir 26(2), 873-879.

Giri, K., Shameer, K., Zimmermann, M.T., Saha, S., Chakraborty, P.K., Sharma, A., Arvizo, R.R., Madden, B.J., McCormick, D.J., Kocher, J.P., Bhattacharya, R. and Mukherjee, P. (2014) Understanding protein-nanoparticle interaction: a new gateway to disease therapeutics. Bioconjug Chem 25(6), 1078-1090.

Go, M.L. and Ngiam, T.L. (1997) Thermodynamics of partitioning of the antimalarial drug mefloquine in phospholipid bilayers and bulk solvents. Chem Pharm Bull (Tokyo) 45(12), 2055-2060.

Gopalakrishnan, G., Rouiller, I., Colman, D.R. and Lennox, R.B. (2009) Supported bilayers formed from different phospholipids on spherical silica substrates. Langmuir 25(10), 5455-5458.

Gottschalk, F., Sonderer, T., Scholz, R.W. and Nowack, B. (2009) Modeled environmental concentrations of engineered nanomaterials (TiO_2, ZnO, Ag, CNT, Fullerenes) for different regions. Environ Sci Technol 43(24), 9216-9222.

Guarnieri, D., Guaccio, A., Fusco, S. and Netti, P.A. (2011) Effect of serum proteins on polystyrene nanoparticle uptake and intracellular trafficking in endothelial cells. Journal of Nanoparticle Research 13(9), 4295-4309.

Gulson, B. and Wong, H. (2006) Stable isotopic tracing-a way forward for nanotechnology. Environ Health Perspect 114(10), 1486-1488.

Ha, Y., Liljestrand, H.M. and Katz, L.E. (2013) Effects of lipid composition on partitioning of fullerene between water and lipid membranes. Water Sci Technol 68(2), 290-295.

Hendren, C.O., Mesnard, X., Droge, J. and Wiesner, M.R. (2011) Estimating production data for five engineered nanomaterials as a basis for exposure assessment. Environ Sci Technol 45(7), 2562-2569.

Hidalgo, I.J. and Borchardt, R.T. (1990) Transport of a large neutral amino acid (phenylalanine) in a human intestinal epithelial cell line: Caco-2. Biochim Biophys Acta 1028(1), 25-30.

Hofsass, C., Lindahl, E. and Edholm, O. (2003) Molecular dynamics simulations of phospholipid bilayers with cholesterol. Biophys J 84(4), 2192-2206.

Hou, W.C. and Jafvert, C.T. (2009a) Photochemical transformation of aqueous C_{60} clusters in sunlight. Environ Sci Technol 43(2), 362-367.

Hou, W.C. and Jafvert, C.T. (2009b) Photochemistry of aqueous C_{60} clusters: evidence of $^1O_2$ formation and its role in mediating C_{60} phototransformation. Environ Sci Technol 43(14), 5257-5262.

Hou, W.C., Kong, L., Wepasnick, K.A., Zepp, R.G., Fairbrother, D.H. and Jafvert, C.T. (2010) Photochemistry of aqueous C_{60} clusters: wavelength dependency and product characterization. Environ Sci Technol 44(21), 8121-8127.

Hou, W.C., Moghadam, B.Y., Corredor, C., Westerhoff, P. and Posner, J.D. (2012a) Distribution of functionalized gold nanoparticles between water and lipid bilayers as model cell membranes. Environ Sci Technol 46(3), 1869-1876.

Hou, W.C., Moghadam, B.Y., Corredor, C., Westerhoff, P. and Posner, J.D. (2012b) Distribution of functionalized gold nanoparticles between water and lipid bilayers as model cell membranes. Environ Sci Technol 46(3), 1869-1876.

Hou, W.C., Moghadam, B.Y., Westerhoff, P. and Posner, J.D. (2011) Distribution of fullerene nanomaterials between water and model biological membranes. Langmuir 27(19), 11899-11905.

Hughes, G.A. (2005) Nanostructure-mediated drug delivery. Nanomedicine 1(1), 22-30.

Hyung, H. and Kim, J.H. (2009a) Dispersion of C_{60} in natural water and removal by conventional drinking water treatment processes. Water Res 43(9), 2463-2470.

Ikeda, A., Kiguchi, K., Shigematsu, T., Nobusawa, K., Kikuchi, J. and Akiyama, M. (2011) Location of [60]fullerene incorporation in lipid membranes. Chem Commun (Camb) 47(44), 12095-12097.

Isaacson, C.W., Kleber, M. and Field, J.A. (2009) Quantitative analysis of fullerene nanomaterials in environmental systems: a critical review. Environ Sci Technol 43(17), 6463-6474.

Jacobson, K., Mouritsen, O.G. and Anderson, R.G. (2007) Lipid rafts: at a crossroad between cell biology and physics. Nat Cell Biol 9(1), 7-14.

Jafvert, C.T. and Kulkarni, P.P. (2008) Buckminsterfullerene's (C_{60}) octanol-water partition coefficient (Kow) and aqueous solubility. Environ Sci Technol 42(16), 5945-5950.

Jermann, D., Pronk, W. and Boller, M. (2008) Mutual influences between natural organic matter and inorganic particles and their combined effect on ultrafiltration membrane fouling. Environ Sci Technol 42(24), 9129-9136.

Jin, H., Heller, D.A. and Strano, M.S. (2008) Single-particle tracking of endocytosis and exocytosis of single-walled carbon nanotubes in NIH-3T3 cells. Nano Lett 8(6), 1577-1585.

Jonker, M.T. and Van der Heijden, S.A. (2007) Bioconcentration factor hydrophobicity cutoff: an artificial phenomenon reconstructed. Environ Sci Technol 41(21), 7363-7369.

Kaiser, S.M. and Escher, B.I. (2006) The evaluation of liposome-water partitioning of 8-hydroxyquinolines and their copper complexes. Environ Sci Technol 40(6), 1784-1791.

Kasermann, F. and Kempf, C. (1997) Photodynamic inactivation of enveloped viruses by buckminsterfullerene. Antiviral Res 34(1), 65-70.

Kroto, H.W., Heath, J.R., Obrien, S.C., Curl, R.F. and Smalley, R.E. (1985) C_{60}: Buckminsterfullerene. Nature 318(6042), 162-163.

Kuzmin, P.I., Akimov, S.A., Chizmadzhev, Y.A., Zimmerberg, J. and Cohen, F.S. (2005) Line tension and interaction energies of membrane rafts calculated from lipid splay and tilt. Biophys J 88(2), 1120-1133.

Kwon, J.H., Liljestrand, H.M. and Katz, L.E. (2006) Partitioning of moderately hydrophobic endocrine disruptors between water and synthetic membrane vesicles. Environ Toxicol Chem 25(8), 1984-1992.

Kwon, J.H., Liljestrand, H.M., Katz, L.E. and Yamamoto, H. (2007) Partitioning thermodynamics of selected endocrine disruptors between water and synthetic membrane vesicles: effects of membrane compositions. Environ Sci Technol 41(11), 4011-4018.

Kwon, J.H., Wuethrich, T., Mayer, P. and Escher, B.I. (2009) Development of a dynamic delivery method for in vitro bioassays. Chemosphere 76(1), 83-90.

Labille, J., Masion, A., Ziarelli, F., Rose, J., Brant, J., Villieras, F., Pelletier, M., Borschneck, D., Wiesner, M.R. and Bottero, J.Y. (2009) Hydration and dispersion of C_{60} in aqueous systems: the nature of water-fullerene interactions. Langmuir 25(19), 11232-11235.

Lesniak, A., Fenaroli, F., Monopoli, M.P., Aberg, C., Dawson, K.A. and Salvati, A. (2012) Effects of the presence or absence of a protein corona on silica nanoparticle uptake and impact on cells. ACS Nano 6(7), 5845-5857.

Li, Q., Xie, B., Hwang, Y.S. and Xu, Y. (2009) Kinetics of C_{60} fullerene dispersion in water enhanced by natural organic matter and sunlight. Environ Sci Technol 43(10), 3574-3579.

Li, W., Chen, C., Ye, C., Wei, T., Zhao, Y., Lao, F., Chen, Z., Meng, H., Gao, Y., Yuan, H., Xing, G., Zhao, F., Chai, Z., Zhang, X., Yang, F., Han, D., Tang, X. and Zhang, Y. (2008) The translocation of fullerenic nanoparticles into lysosome via the pathway of clathrin-mediated endocytosis. Nanotechnology 19(14), 145102.

Li, Y. and Gu, N. (2010) Thermodynamics of charged nanoparticle adsorption on charge-neutral membranes: a simulation study. J Phys Chem B 114(8), 2749-2754.

Limbach, L.K., Li, Y., Grass, R.N., Brunner, T.J., Hintermann, M.A., Muller, M., Gunther, D. and Stark, W.J. (2005) Oxide nanoparticle uptake in human lung fibroblasts: effects of particle size, agglomeration, and diffusion at low concentrations. Environ Sci Technol 39(23), 9370-9376.

Lin, I.C., Liang, M., Liu, T.Y., Monteiro, M.J. and Toth, I. (2012) Cellular transport pathways of polymer coated gold nanoparticles. Nanomedicine 8(1), 8-11.

Lovern, S.B. and Klaper, R. (2006) *Daphnia magna* mortality when exposed to titanium dioxide and fullerene (C_{60}) nanoparticles. Environ Toxicol Chem 25(4), 1132-1137.

Lynch, I. and Dawson, K.A. (2008) Protein-nanoparticle interactions. Nano Today 3(1-2), 40-47.

Lyon, D.Y., Adams, L.K., Falkner, J.C. and Alvarezt, P.J. (2006) Antibacterial activity of fullerene water suspensions: effects of preparation method and particle size. Environ Sci Technol 40(14), 4360-4366.

Ma, X. and Bouchard, D. (2009) Formation of aqueous suspensions of fullerenes. Environ Sci Technol 43(2), 330-336.

Ma, Z. and Lim, L.Y. (2003) Uptake of chitosan and associated insulin in Caco-2 cell monolayers: a comparison between chitosan molecules and chitosan nanoparticles. Pharm Res 20(11), 1812-1819.

Mao, S., Germershaus, O., Fischer, D., Linn, T., Schnepf, R. and Kissel, T. (2005) Uptake and transport of PEG-graft-trimethyl-chitosan copolymer-insulin nanocomplexes by epithelial cells. Pharm Res 22(12), 2058-2068.

Martin, D., Maran, U., Sild, S. and Karelson, M. (2007) QSPR modeling of solubility of polyaromatic hydrocarbons and fullerene in 1-octanol and n-heptane. J Phys Chem B 111(33), 9853-9857.

McMahon, D.P., Cheung, D.L. and Troisi, A. (2011) Why holes and electrons separate so Well in polymer/fullerene photovoltaic cells. Journal of Physical Chemistry Letters 2(21), 2737-2741.

Mornet, S., Lambert, O., Duguet, E. and Brisson, A. (2005) The formation of supported lipid bilayers on silica nanoparticles revealed by cryoelectron microscopy. Nano Lett 5(2), 281-285.

Oberdörster, E. (2004) Manufactured nanomaterials (fullerenes, C_{60}) induce oxidative stress in the brain of juvenile largemouth bass. Environ Health Perspect 112(10), 1058-1062.

Oberdörster, E., Zhu, S.Q., Blickley, T.M., McClellan-Green, P. and Haasch, M.L. (2006) Ecotoxicology of carbon-based engineered nanoparticles: Effects of fullerene (C_{60}) on aquatic organisms. Carbon 44(6), 1112-1120.

Oberdörster, E.Z., S.; Blickley, M.; Mcglellan-Green, P.; Haasch, M.L. (2006) Ecotoxicology of carbon-based engineered nanoparticles: Effects of fullerene (C_{60}) on aquatic organisms. Carbon 44, 1112-1120.

Opperhuizen, A., Serne, P. and Van der Steen, J.M. (1988) Thermodynamics of fish/water and octan-1-ol/water partitioning of some chlorinated benzenes. Environ Sci Technol 22(3), 286-292.

Pade, V. and Stavchansky, S. (1997) Estimation of the relative contribution of the transcellular and paracellular pathway to the transport of passively absorbed drugs in the Caco-2 cell culture model. Pharm Res 14(9), 1210-1215.

Panyam, J. and Labhasetwar, V. (2003) Biodegradable nanoparticles for drug and gene delivery to cells and tissue. Adv Drug Deliv Rev 55(3), 329-347.

Pérez, S.F., M.; Barceló, D (2009) Analysis, behavior and ecotoxicity of carbon-based nanomaterials in the aquatic environment. Trends in Analytical Chemistry 28(6), 820-832.

Petersen, E.J. and Henry, T.B. (2012) Methodological considerations for testing the ecotoxicity of carbon nanotubes and fullerenes: review. Environ Toxicol Chem 31(1), 60-72.

Petosa, A.R., Jaisi, D.P., Quevedo, I.R., Elimelech, M. and Tufenkji, N. (2010) Aggregation and deposition of engineered nanomaterials in aquatic environments: role of physicochemical interactions. Environ Sci Technol 44(17), 6532-6549.

Pizzarello, S., Huang, Y., Becker, L., Poreda, R.J., Nieman, R.A., Cooper, G. and Williams, M. (2001) The organic content of the Tagish Lake meteorite. Science 293(5538), 2236-2239.

Podolski, I.Y., Podlubnaya, Z.A., Kosenko, E.A., Mugantseva, E.A., Makarova, E.G., Marsagishvili, L.G., Shpagina, M.D., Kaminsky, Y.G., Andrievsky, G.V. and Klochkov, V.K. (2007) Effects of hydrated forms of C_{60} fullerene on amyloid 1-peptide fibrillization in vitro and performance of the cognitive task. J Nanosci Nanotechnol 7(4-5), 1479-1485.

Porter, A.E., Gass, M., Muller, K., Skepper, J.N., Midgley, P. and Welland, M. (2007) Visualizing the uptake of C_{60} to the cytoplasm and nucleus of human monocyte-derived macrophage cells using energy-filtered transmission electron microscopy and electron tomography. Environ Sci Technol 41(8), 3012-3017.

Porter, A.E., Muller, K., Skepper, J., Midgley, P. and Welland, M. (2006) Uptake of C_{60} by human monocyte macrophages, its localization and implications for toxicity: studied by high resolution electron microscopy and electron tomography. Acta Biomater 2(4), 409-419.

Pycke, B.F., Benn, T.M., Herckes, P., Westerhoff, P. and Halden, R.U. (2011) Strategies for quantifying C_{60} fullerenes in environmental and biological samples and implications for studies in environmental health and ecotoxicology. Trends Analyt Chem 30(1), 44-57.

Qiao, R., Roberts, A.P., Mount, A.S., Klaine, S.J. and Ke, P.C. (2007) Translocation of C60 and its derivatives across a lipid bilayer. Nano Lett 7(3), 614-619.

Rancan, F., Gao, Q., Graf, C., Troppens, S., Hadam, S., Hackbarth, S., Kembuan, C., Blume-Peytavi, U., Ruhl, E., Lademann, J. and Vogt, A. (2012) Skin penetration and cellular uptake of amorphous silica nanoparticles with variable size, surface functionalization, and colloidal stability. ACS Nano 6(8), 6829-6842.

Rejman, J., Oberle, V., Zuhorn, I.S. and Hoekstra, D. (2004) Size-dependent internalization of particles via the pathways of clathrin- and caveolae-mediated endocytosis. Biochem J 377(Pt 1), 159-169.

Roberts, J.E., Wielgus, A.R., Boyes, W.K., Andley, U. and Chignell, C.F. (2008) Phototoxicity and cytotoxicity of fullerol in human lens epithelial cells. Toxicol Appl Pharmacol 228(1), 49-58.

Rouse, J.G., Yang, J., Barron, A.R. and Monteiro-Riviere, N.A. (2006) Fullerene-based amino acid nanoparticle interactions with human epidermal keratinocytes. Toxicol In Vitro 20(8), 1313-1320.

Ruan, G., Agrawal, A., Marcus, A.I. and Nie, S. (2007) Imaging and tracking of tat peptide-conjugated quantum dots in living cells: new insights into nanoparticle uptake, intracellular transport, and vesicle shedding. J Am Chem Soc 129(47), 14759-14766.

Ruoff, R.S., Tse, D.S., Malhotra, R. and Lorents, D.C. (1993) Solubility of C_{60} in a Variety of Solvents. Journal of Physical Chemistry 97(13), 3379-3383.

Ryhanen, S.J., Saily, V.M. and Kinnunen, P.K. (2006) Cationic lipid membranes-specific interactions with counter-ions. J Phys Condens Matter 18(28), S1139-1150.

Saha, K., Agasti, S.S., Kim, C., Li, X. and Rotello, V.M. (2012) Gold nanoparticles in chemical and biological sensing. Chem Rev 112(5), 2739-2779.

Saleh, N.B., Pfefferle, L.D. and Elimelech, M. (2010) Influence of biomacromolecules and humic acid on the aggregation kinetics of single-walled carbon nanotubes. Environ Sci Technol 44(7), 2412-2418.

Santhosh, P.B., Velikonja, A., Perutkova, S., Gongadze, E., Kulkarni, M., Genova, J., Elersic, K., Iglic, A., Kralj-Iglic, V. and Ulrih, N.P. (2014) Influence of nanoparticle-membrane electrostatic interactions on membrane fluidity and bending elasticity. Chem Phys Lipids 178, 52-62.

Sayes, C.M., Gobin, A.M., Ausman, K.D., Mendez, J., West, J.L. and Colvin, V.L. (2005) Nano-C_{60} cytotoxicity is due to lipid peroxidation. Biomaterials 26(36), 7587-7595.

Sayes, C.M.F., J.D.; Guo, W.; Lyon, D.; Boyd, A.M.; Ausman, K.D.; Tao, Y.J.; Sitharaman, B.; Wilson, L.J.; Hughes, J.B.; West, J.L.; Colvin, V.L. (2004) The differential cytotoxicity of water-soluble fullerenes. Nano Lett 4, 1881-1887.

Schwarzenbach, R.P., Gschwend, P.M. and Imboden, D.M. (2003) Environmental organic chemistry, Wiley, Hoboken, N.J.

Seelig, J. and Ganz, P. (1991) Nonclassical hydrophobic effect in membrane binding equilibria. Biochemistry 30(38), 9354-9359.

Shang, L., Nienhaus, K. and Nienhaus, G.U. (2014) Engineered nanoparticles interacting with cells: size matters. J Nanobiotechnology 12, 5.

Shanker, B. and Applequist, J. (1994) Polarizabilities of fullerenes C_{20} through C_{240} from atom monopole-dipole interaction theory. Journal of Physical Chemistry 98(26), 6486-6489.

Singh, R. and Lillard, J.W., Jr. (2009) Nanoparticle-based targeted drug delivery. Exp Mol Pathol 86(3), 215-223.

Stottrup, B.L., Stevens, D.S. and Keller, S.L. (2005) Miscibility of ternary mixtures of phospholipids and cholesterol in monolayers, and application to bilayer systems. Biophys J 88(1), 269-276.

Strober, W. (2001) Trypan blue exclusion test of cell viability. Curr Protoc Immunol Appendix 3, Appedix 3B

Su, Y., Xu, J.Y., Shen, P., Li, J., Wang, L., Li, Q., Li, W., Xu, G.T., Fan, C. and Huang, Q. (2010) Cellular uptake and cytotoxic evaluation of fullerenol in different cell lines. Toxicology 269(2-3), 155-159.

Sugano, K., Kansy, M., Artursson, P., Avdeef, A., Bendels, S., Di, L., Ecker, G.F., Faller, B., Fischer, H., Gerebtzoff, G., Lennernaes, H. and Senner, F. (2010) Coexistence of passive and carrier-mediated processes in drug transport. Nat Rev Drug Discov 9(8), 597-614.

Sundara Rajan, S. and Vu, T.Q. (2006) Quantum dots monitor TrkA receptor dynamics in the interior of neural PC12 cells. Nano Lett 6(9), 2049-2059.

Tao, X., Fortner, J.D., Zhang, B., He, Y., Chen, Y. and Hughes, J.B. (2009) Effects of aqueous stable fullerene nanocrystals (nC_{60}) on Daphnia magna: evaluation of sub-lethal reproductive responses and accumulation. Chemosphere 77(11), 1482-1487.

Tervonen, K., Waissi, G., Petersen, E.J., Akkanen, J. and Kukkonen, J.V. (2010) Analysis of fullerene-C_{60} and kinetic measurements for its accumulation and depuration in Daphnia magna. Environ Toxicol Chem 29(5), 1072-1078.

Thio, B.J., Zhou, D. and Keller, A.A. (2011) Influence of natural organic matter on the aggregation and deposition of titanium dioxide nanoparticles. J Hazard Mater 189(1-2), 556-563.

Tokumasu, F., Jin, A.J., Feigenson, G.W. and Dvorak, J.A. (2003) Atomic force microscopy of nanometric liposome adsorption and nanoscopic membrane domain formation. Ultramicroscopy 97(1-4), 217-227.

Vasiluk, L., Pinto, L.J., Walji, Z.A., Tsang, W.S., Gobas, F.A., Eickhoff, C. and Moore, M.M. (2007) Benzo[a]pyrene bioavailability from pristine soil and contaminated sediment assessed using two in vitro models. Environ Toxicol Chem 26(3), 387-393.

Veatch, S.L. and Keller, S.L. (2003) Separation of liquid phases in giant vesicles of ternary mixtures of phospholipids and cholesterol. Biophys J 85(5), 3074-3083.

Verma, A. and Stellacci, F. (2010) Effect of surface properties on nanoparticle-cell interactions. Small 6(1), 12-21.

Wang, B., Zhang, L., Bae, S.C. and Granick, S. (2008) Nanoparticle-induced surface reconstruction of phospholipid membranes. Proc Natl Acad Sci U S A 105(47), 18171-18175.

Wang, H.B., DeSousa, R., Gasa, J., Tasaki, K., Stucky, G., Jousselme, B. and Wudl, F. (2007) Fabrication of new fullerene composite membranes and their application in proton exchange membrane fuel cells. Journal of Membrane Science 289(1-2), 277-283.

Wang, H.B., DeSousa, R., Gasa, J., Tasake, K., Stucky, G., Jousselme, B., Wudl, F. (2007) Fabrication of new fullerene composite membranes and their application in proton exchange membrane fuel cells. Jounal of membrane science 289(1-2), 277-283.

Wang, I.C., Tai, L.A., Lee, D.D., Kanakamma, P.P., Shen, C.K., Luh, T.Y., Cheng, C.H. and Hwang, K.C. (1999) C_{60} and water-soluble fullerene derivatives as antioxidants against radical-initiated lipid peroxidation. J Med Chem 42(22), 4614-4620.

Wang, Z., Tiruppathi, C., Minshall, R.D. and Malik, A.B. (2009) Size and dynamics of caveolae studied using nanoparticles in living endothelial cells. ACS Nano 3(12), 4110-4116.

Wenk, M.R., Fahr, A., Reszka, R. and Seelig, J. (1996) Paclitaxel partitioning into lipid bilayers. Journal of Pharmaceutical Sciences 85(2), 228-231.

Wiesner, M.R., Hotze, E.M., Brant, J.A. and Espinasse, B. (2008) Nanomaterials as possible contaminants: the fullerene example. Water Sci Technol 57(3), 305-310.

Wilhelm, C., Gazeau, F., Roger, J., Pons, J.N. and Bacri, J.C. (2002) Interaction of anionic superparamagnetic nanoparticles with cells: Kinetic analyses of membrane adsorption and subsequent internalization. Langmuir 18(21), 8148-8155.

Win, K.Y. and Feng, S.S. (2005) Effects of particle size and surface coating on cellular uptake of polymeric nanoparticles for oral delivery of anticancer drugs. Biomaterials 26(15), 2713-2722.

Wong-Ekkabut, J., Baoukina, S., Triampo, W., Tang, I.M., Tieleman, D.P. and Monticelli, L. (2008) Computer simulation study of fullerene translocation through lipid membranes. Nat Nanotechnol 3(6), 363-368.

Xia, T., Kovochich, M., Brant, J., Hotze, M., Sempf, J., Oberley, T., Sioutas, C., Yeh, J.I., Wiesner, M.R. and Nel, A.E. (2006a) Comparison of the abilities of ambient and manufactured nanoparticles to induce cellular toxicity according to an oxidative stress paradigm. Nano Lett 6(8), 1794-1807.

Xia, X.R., Monteiro-Riviere, N.A. and Riviere, J.E. (2006b) Trace analysis of fullerenes in biological samples by simplified liquid-liquid extraction and high-performance liquid chromatography. J Chromatogr A 1129(2), 216-222.

Xie, B., Xu, Z., Guo, W. and Li, Q. (2008) Impact of natural organic matter on the physicochemical properties of aqueous C_{60} nanoparticles. Environ Sci Technol 42(8), 2853-2859.

Yamamoto, H. and Liljestrand, H.M. (2004) Partitioning of selected estrogenic compounds between synthetic membrane vesicles and water: effects of lipid components. Environ Sci Technol 38(4), 1139-1147.

Yamamoto, H., Liljestrand, H.M. and Shimizu, Y. (2004) Effects of dissolved organic matter surrogates on the partitioning of 17beta-estradiol and p-nonylphenol between synthetic membrane vesicles and water. Environ Sci Technol 38(8), 2351-2358.

Yaron, P.N., Holt, B.D., Short, P.A., Losche, M., Islam, M.F. and Dahl, K.N. (2011) Single wall carbon nanotubes enter cells by endocytosis and not membrane penetration. J Nanobiotechnology 9, 45.

Zhang, B., Cho, M., Hughes, J.B. and Kim, J.H. (2009a) Translocation of C_{60} from aqueous stable colloidal aggregates into surfactant micelles. Environ Sci Technol 43(24), 9124-9129.

Zhang, X., Sun, H., Zhang, Z., Niu, Q., Chen, Y. and Crittenden, J.C. (2007) Enhanced bioaccumulation of cadmium in carp in the presence of titanium dioxide nanoparticles. Chemosphere 67(1), 160-166.

Zhang, Y., Chen, Y., Westerhoff, P. and Crittenden, J. (2009b) Impact of natural organic matter and divalent cations on the stability of aqueous nanoparticles. Water Res 43(17), 4249-4257.

Zhi, D., Zhang, S., Cui, S., Zhao, Y., Wang, Y. and Zhao, D. (2013) The headgroup evolution of cationic lipids for gene delivery. Bioconjug Chem 24(4), 487-519.

Zhu, Y., Li, W.X., Li, Q.N., Li, Y.G., Li, Y.F., Zhang, X.Y. and Huang, Q. (2009) Effects of serum proteins on intracellular uptake and cytotoxicity of carbon nanoparticles. Carbon 47(5), 1351-1358.

Vita

Yeonjeong Ha was born in Seoul, and lived in Cheong-ju, Korea as a child. After graduating Sang-dang high school, she entered Seoul National University in 2001. She received a Bachelor of Science in Chemistry in 2005. Yeonjeong worked in LG Chemistry Ltd. as a quality assurance engineer from 2005 to 2006. She entered graduate school at Seoul National University and received a Master of Science in Urban Planning in 2008. From March 2008 to February 2009, she worked in Seoul Dong Sung High School as a chemistry teacher, and from February 2009 to July 2009, Yeonjeong worked as a research scientist in Environmental Research Institute at Ajou University. She started her doctoral program in the Department of Civil, Architectural and Environmental Engineering at the University of Texas at Austin in August 2009.

Email address: gbhyjyh@gmail.com

This dissertation was typed by the author.